Prepared for:

RIKZ

Long-term Morphological Modeling of Marsdiep Basin in the Dutch Wadden Sea, the Netherlands

Report

April, 2007

Z4169.00

Prepared for:

RIKZ

Long-term Morphological Modeling of Marsdiep Basin in the Dutch Wadden Sea, the Netherlands

Ali Dastgheib

Report

April, 2007

Dedicated to whom I love

Preface

This document is presented as MSc. thesis for the partial fulfillment of requirements to obtain the Master of Science degree in Coastal Engineering and Port development from UNESCO-IHE in Delft, The Netherlands. This study is part of the project called "Interaction between the Long-term developments of Dutch Coast and the tidal basins Marsdiep and Westerschelde" carried out by Rijkswaterstaat (RIKZ) in WL|Delft Hydraulics.

This study was not possible without contribution of many people who helped me to push this work ahead. First, I want to thank my supervisor Prof. Dano Roelvink (UNESCO-IHE, WL|Delft Hydraulics) for his continuous encouragement and support, Dano was always there to listen to my questions and to show me the way to continue. Then I also want to thank the rest of my thesis committee, Dr. Ir. Zheng Bing Wang (WL|Delft Hydraulics, TU Delft), Ir. J. de Ronde (Rijkswaterstaat), and Ir. Mick van der Wegen (UNESCO-IHE), for their questions, comments and suggestions during this study, and their never-ending interest on this project. Furthermore, I am very grateful for the opportunity WL|Delft Hydraulics offered me to do my study there; also I should thank Rijkswaterstaat for financial support of this study.

I would like to thank the other employees at WL especially Edwin Elias, who did not mind to spend some of their time solving my problems, other MSc. students in so-called 'student island' of MCM department of WL|Delft Hydraulics with whom I had a great time not feeling far from home.

Let me say also "THANK YOU" to my friends in UNESCO-IHE, with whom I laughed, cried, celebrated, worried, or in one word, lived in past one and a half year.

I can never forget where my interest in coastal engineering originated, PTP Consultant Engineers Company in Tehran, I should thank my colleagues and friends there, who are doing the works which I was supposed to do.

Finally I want to thank my parents for giving me life in the first place, for educating me, for unconditional love, support, and encouragement to pursue my interests, even when my interests went against their will.

Ali Dastgheib
Delft, April 2007

Abstract

The equilibrium condition in tidal basins, especially in the Dutch Wadden Sea, which is a multi-basin tidal system, has been the subject of numerous studies in recent decades. This concept is more important when the tidal basin imports sediment from the adjacent coastline and its ebb-tidal delta. In the Dutch Wadden Sea the construction of the Afsluitdijk in 1932 affected the behavior of tidal basins, especially Marsdiep, to a large extent and disturbed its equilibrium condition. Nowadays, 75 years after the construction of Afsluitdijk, it seems that Marsdiep has not reached a new equilibrium condition and it imports large volumes of sand every year.

In this study a process-based model (Delft3D) with the state of the art morphological modeling technique of 'online approach' is used to simulate the morphological changes of the Western Wadden Sea for a duration of 2100 years. The main forcing which is included in the simulations is tidal forcing and different simulations with different initial conditions of the model are carried out.

The main parameters of tidal basins are calculated and checked with suggested empirical equilibrium relations in the literature. It is shown that such a process based model can simulate the morphological evolution of the tidal basins in the Western Dutch Wadden Sea and can model a stable (equilibrium) condition in these basins. This stable condition is however strongly dependent on the initial condition of the model as well as the forcing conditions.

On the other hand some simulations are carried out with initial real bathymetry and the impact of changing boundaries of tidal basins in the Western Dutch Wadden Sea is analyzed. The hypothesis that the basins are expanding towards the east, especially in the case of Marsdiep is also observed in this simulation.

Comparing all the results of the simulations in this study, it is concluded that the process - based model results show the morphological evolution towards empirical equilibrium equations suggested in literature, mainly in line with the relations rather than in terms of exact coefficients.

Contents

List of Figures

List of Tables

1 Introduction

Barrier islands, tidal inlets, and tidal basins are found in many places along the coastlines in the world. One of these areas which has attracted much attention is the Wadden Sea, situated at the south east of North Sea along the coastline of The Netherlands, Germany, and Denmark, consisting of 33 tidal inlet systems over approximately 500 km. The associated barrier islands of these inlets divide the nearly 10,000 km^2 tidal flat area from the North Sea (Elias, 2006). The part of the Wadden Sea which is located in the Dutch coastline is shown in the figure 1-1. Continuous sedimentation in the tidal basins is one of the characteristic features of Wadden Sea. This sediment demand is fed by sediment supply from the barrier coastline, ebb tidal deltas and adjacent North-Holland coastline. As it is stated in Elias (2006) , this problem is addressed by Stive and Eysink (1989); they note that the cause of structural large sand losses from the North-Holland coastline is mainly the demand of sand in Wadden Sea tidal basins. Therefore morphological developments, stability, and changes of tidal basins and tidal inlets in Dutch Wadden Sea have a huge influence on the Dutch coastline mainly in terms of extensive erosion (need for nourishment) of the barrier islands and adjacent coasts.

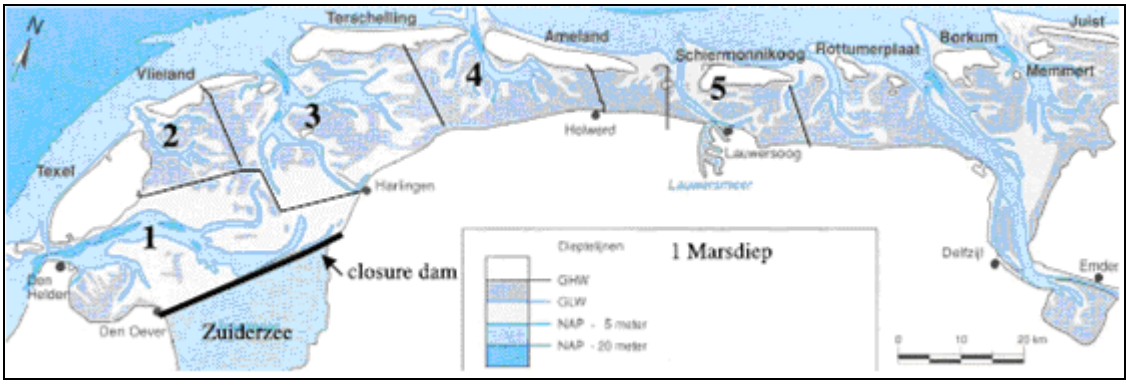

Figure 1-1:Overview tidal inlets Dutch Wadden Sea (with approximate tidal divides, Kragtwijk et al., 2004)

A tidal basin consists of three main morphological elements, which are tidal basin, tidal inlet, and ebb-tidal delta, these three elements under the effect of meteorological and hydrodynamic forces are interacting with each other to gain and maintain a (dynamic) equilibrium. Some times due to human intervention and/or natural phenomena, the effecting forces on the tidal basins change. These changes lead to morphological changes in different elements. First sediment is redistributed within the elements, and sand is exchanged between elements. But if these changes are larger, the sediment exchange may take place between the tidal basins and adjacent coastline. And in its turn it causes some morphological changes (and problems) in nearby coast lines.

The morphodynamic behavior of tidal basins compared to coastlines is less well understood, mainly because of a wide variety of spatial and temporal scales involved. The whole basin system (mega-scale), different morphological elements (macro-scale), and various morphological features inside each element (meso-scale) respond differently, temporally and spatially, to changes in forcing (Scale classification from De Vriend 1991). These

differences are to such an extent that the whole basin system may be in some equilibrium situation while there are large fluctuations within the elements.

The morphological stability of the tidal basins in Wadden Sea is disturbed by sea level rise and human influences, which is most pronounced in Marsdiep Basin after the closure of the Zuider Sea in 1932. After this closure large changes have been observed in the morphology of the basin and its channels and flat areas as well as in the ebb-tidal delta and adjacent coast line. Although the major effects of this closure have appeared in the first 40 years after the closure, the adjacent coastline is still eroding extensively. Also recent studies on the field data in the Marsdiep (e.g. Elias et, al, 2003), show that the sediment import to this basin is more than expected. Therefore it seems that this basin did not reach the stable morphological condition and the effect of construction of the Afsluitdijk and closure of the Zuider Sea is not dissipated yet. On the other hand the channel/shoal ratio in the Marsdiep and close-by basins suggests that this area is far from equilibrium and needs more sediment to reach its morphologically stable condition (Elias, 2006).

Thus there is a need to have a better understanding of long-term morphological development of Dutch Wadden Sea and especially Marsdiep basin by means of long-term mega-scale modeling to find the (quasi-) equilibrium of this basin.

Research Questions

The research questions in this study are formulated in 4 different questions which are addressed throughout the report and the conclusions of the report are based on these questions.

- Can a mega-scale stable situation of the Marsdiep Basin be predicted using a schematized long-term process-based morphological model and given constant boundary conditions?

- How much sand is needed to import to Marsdiep to reach this hypothetical stable morphological situation and is this amount of sediment available?

- What is the effect of near by basins in Wadden Sea, especially Vlie Basin, on the morphology of Marsdiep Basin?

- Is the result of schematized long-term morphological modeling of Marsdiep Basin in agreement with empirical models?

Methodology

Coastal engineers and geologists have made numerous efforts to model and understand morphodynamics and morphological equilibrium condition in tidal basins. these models were first distinguished by De Vriend et al (1993b) in two types of approaches: Behavior oriented modeling and Process based modeling.

The Behavior oriented modeling, which later is classified as data-based, empirical or semi-empirical by De Vriend (1996), is based on the analysis of measured data rather than the

underlying physical processes. Using these analyses, a range of equilibrium relations and conceptual models were developed to explain the variety in size, volumes, and distribution of channels and shoals in a tidal basin system. Well known relations are those of Escoffier (1940), O'Brien (1931; 1969), Hayes (1975; 1979), Oertel (1975; 1988), Walton and Adams (1976), Hubbard (1979) and FitzGerald (1988; 1996), but many more exist. Although the conceptual models and empirical relations significantly contributed to the understanding of tidal basin behavior, nowadays the process-based numerical models describing detailed physical processes are available. The previous studies such as Wang et al (1995), Cayocca (2001), Hibma et al. (2003), Lesser et al (2004), Hibma (2004), and Elias (2006) shows that the process-based models, describing the flow field , resulting sediment transport and bottom changes can be used to study complicated morphological situation in tidal basins. Different types of morphological modeling for both behavior oriented and process based approaches are described in chapters 2

To answer the research questions in this study, a process based model (Delft3D – FLOW and MOR modules) is used. In this study some schematized models of Wadden Sea with relatively coarse grid and short computational time are run and a sensitivity analyses on the parameters which may be responsible for the long-term evolution of the Marsdiep basin is carried out. After that a few long-term models (~2000 years) are setup with the selected parameters according to the above mentioned analyses.

After the problem identification, the research questions and the methodology of this research, this report continues with a short description of physics, modeling and equilibrium in morphodynamics of tidal basins (chapter 2) and the hydrodynamic and morphodynamic characteristics of the study area with their historical changes (chapter 3). Later, chapter 4 describes the model which is used, sensitivity analyses and setup of the different runs. This chapter is followed by analyzing the results and discussions (chapter 5). Finally chapter 6 concludes the report and gives some recommendations for future studies.

2 Tidal Basin Morphodynamics

By definition a tidal inlet is an opening in the coastline through which the water (and sediment) is exchanged between the sea and the tidal basin. The tidal inlet system can be analyzed by monitoring the behavior of its three main components: ebb-tidal delta, tidal inlet (inlet gorge) and tidal basin (back-barrier basin). In the following paragraphs these 3 components are introduced briefly.

Figure 2-1: Different components of Marsdiep Tidal inlet system in Dutch Wadden Sea: Ebb-tidal Delta (Yellow), Tidal inlet (Blue), Tidal Basin (Green)

2.1 Tidal basin components

The ebb-tidal delta is the accumulated mass of sediment at the seaward side of the tidal inlet. The ebb-tidal delta acts as a sediment storage and supply. In the case that the tidal inlet system needs sediment normally the ebb-tidal delta is the first supplier of the sediment and if there is not enough sediment available in the delta, the sediment will be provided by the adjacent coast line. On the other hand if there is extra sediment in the tidal basin it usually is dumped on the ebb-tidal delta.

Dean and Walton (1975) defined the volume of the ebb-tidal delta by comparing the no-inlet bathymetry with the current bathymetry. They assumed that the inlet does not disturb the no-inlet bathymetry of the coastal slope. Therefore the no-inlet bathymetry is assumed to be the same as the bathymetry at the adjacent coast line. The difference between the volume of sand in no-inlet bathymetry and the bathymetry of ebb-tidal delta is defined to be the volume of ebb-tidal delta.

The morphology of this delta is defined by the interaction between the tidal currents and waves. This delta is created by the sediment eroded from the inlet gorge while tide is deepening the tidal inlet. Since the tidal inlet is usually narrow, the current velocity and the corresponding sediment transport capacity is high in the inlet, so the sediment is eroded from the inlet. But as the distance from the inlet increases the current velocity decreases quickly. This drop in velocity leads to sedimentation in front of the inlet.

A number of empirical relations have been developed to explain the variety in size, volume, and distribution of the channels and shoals on the ebb-tidal delta. Most of the studies agree that the main parameter which determines the shape of ebb-tidal delta is the relation between tidal forces and wave energy flux. Sha and Van den Berg (1993) showed that the ebb-tidal delta tends to have an asymmetry against the direction of tidal wave propagation. Also waves try to push the main ebb channel in the direction of the main wave at the deep water. According to Sha (1990), in the Wadden Sea the shape of the ebb-tidal delta is mainly determined by the magnitude of the tidal prism. Inlets with a large tidal prism show up-drift asymmetrical ebb-tidal deltas, while the ones with small tidal prism show down-drift asymmetrical ebb-tidal deltas. Different geometry of ebb-tidal delta under the effect of combination of different forces is shown in the figure 2-2.

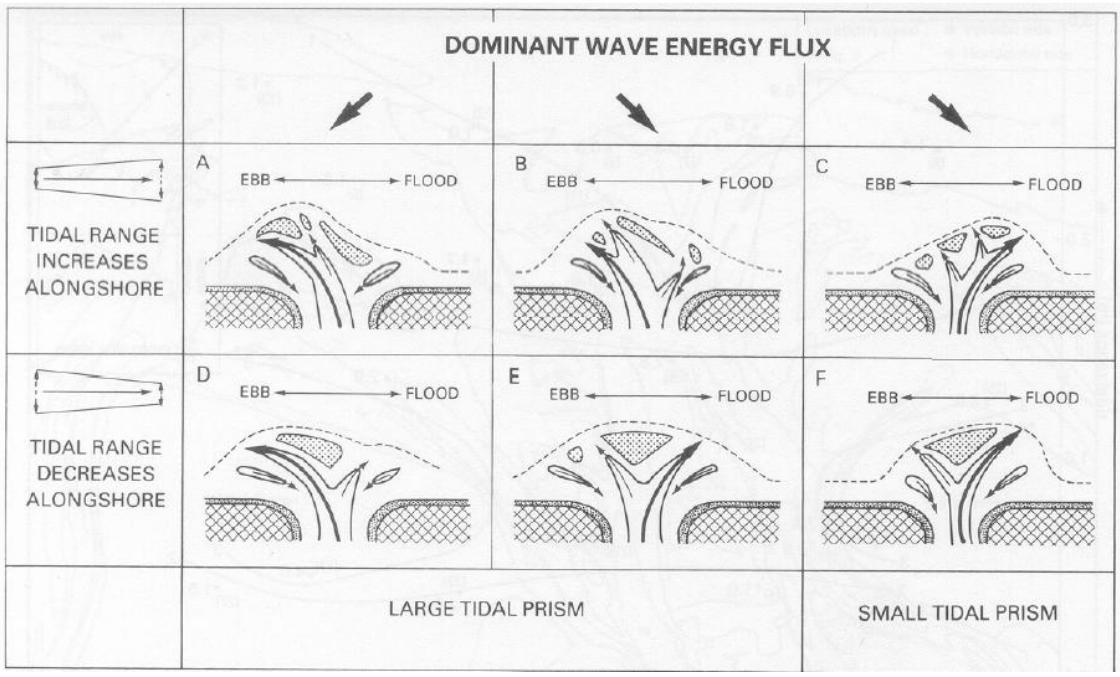

Figure 2-2: Development of the ebb-tidal delta under different forcing condition (Sha and Van den Berg, 1993)

Bruun and Gerritsen (1959) were among the first to recognize the importance of sediment by-passing. In tidal inlet systems sediment by-passing can be defined as the sediment exchange from the up-drift coast to down-drift coast over the ebb-tidal delta. They interpreted the effect of wave and tide to different sediment by-passing mechanisms. They categorized the natural sediment by-passing mechanism with the ratio between longshore sediment transport, by waves and tidal inlet currents.

If the ratio between longshore sediment transport by waves and tidal inlet currents is high or in other words, the wave action dominates, the mechanism of sediment by-passing is called 'Bar by-passing'. In this mechanism a sand bar is formed in front of the inlet. The wave generated longshore sediment transport occurs over the bar in the direction of the down-drift island. If the total longshore sediment transport capacity remains constant, the dimension of the submerged bar can be estimated. The depth of the submerged bar is restricted by the breaker depth of the waves. If the longshore sediment transport increases the submerged bar will get shallower and wider. On the other hand if the ratio between longshore sediment transport by waves and tidal inlet currents is low, the by-passing occurs by the tidal flow action. In this mechanism which is called 'Tidal flow by-passing' sediment transport through the channels and migration of tidal channels and bars dominates. Since the material is deposited on the up-drift bank of the channels, tidal channels migrate to down-drift. The bars between the channels may also follow this migration and join the down-drift barrier coast.

The most recent conceptual model for sediment by-passing are the models proposed by FitzGerlad et al. (2000) to explain the sediment by-passing in mixed-energy tidal inlets. Later these models shown to be valid in a wide range of mixed-energy tidal dominated inlets (Elias 2006). These models are illustrated by Elias (2006) in figure 2-3.

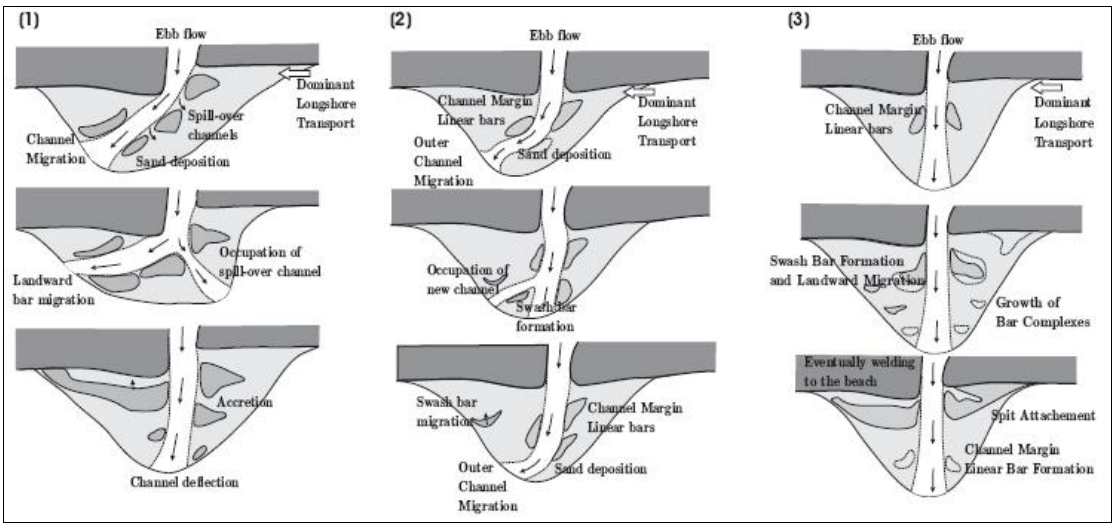

Figure 2-3: Models of sediment by-passing (1) Cyclic ebb-tidal delta breaching, (2) Outer channel shifting, (3) Stable inlet processes, (Elias (2006), Redrawn after FitzGerald et al. (2000)).

(1) cyclic ebb-tidal delta breaching; The main ebb channels periodically migrate down-drift due to sediment accumulation at the up-drift side of the ebb-delta. These shoals deflect the main ebb-channel in down-drift direction. The curved channel is hydraulically less efficient and a more competent, seaward-directed pathway through the ebb-tidal delta forms.
(2) outer channel shifting; Similar to cyclic ebb-tidal delta breaching, but the channel migration is limited to the distal part of the channel while the proximal part remains stable.
(3) stable inlet processes; The main ebb channel remains stable in position often related to the presence of erosion resistant layers. Bar complexes, formed by stacking and coalescence of swash bars on the delta platform, migrate onshore due to the dominance of landward flow created by wave swash.

The other component of the tidal inlet system is the tidal basin. Tidal basin is located between the barrier islands and the main land. The tidal basin usually consists of the channels and shoals with inter-tidal sand and/or mud flats and marshes.

Considering the channel shoal patterns, the tidal basins are divided in two groups: The tidal basins with branching (Fractal) channels and the ones with braided channel patterns. In branching patterns, the large inlet channel branches in to smaller ones and, which branch in turns, length of these channels decreases logarithmically and they are related to the prism and draining area (Hibma et al. 2004). These basins are normally short. Dutch Wadden Sea tidal basins are the examples of such tidal basins. In Wadden Sea the branching continues in 3 or 4 stages and the minimum scale of branching is 500m (Cleveringa and Oost, 1999), while the geological nature defined the upper limit (Rinaldo et al., 2001). Figure 2-4 shows an example of the fractal channels in Dutch Wadden Sea.

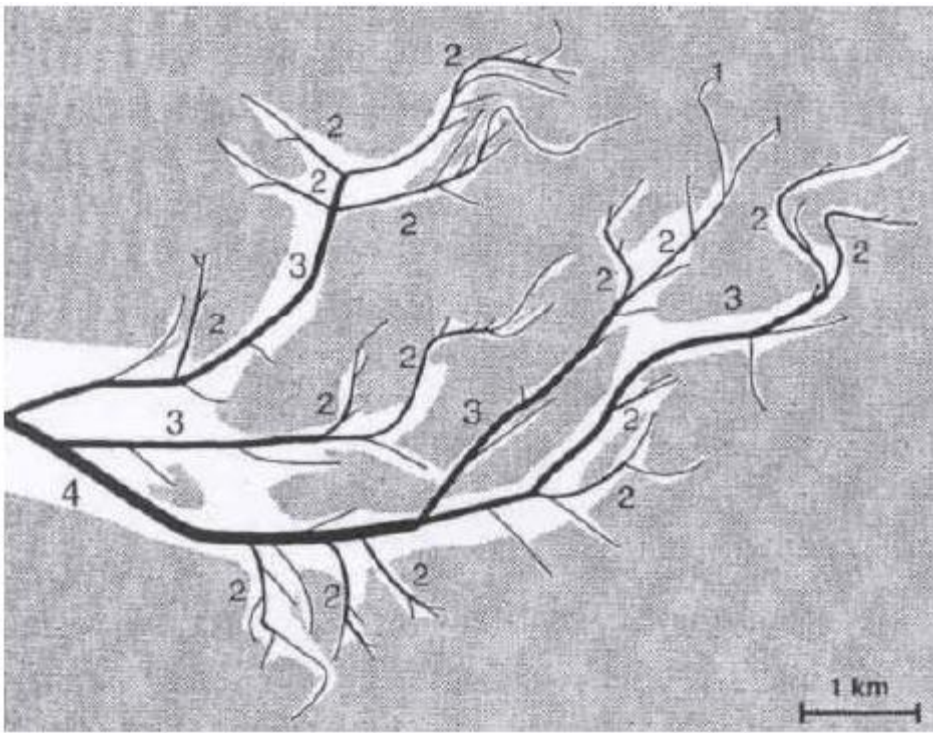

Figure 2-4: Branching channel pattern. The smallest channels are assigned to the first order. Two first order channels merge into a second order channel and so on (Cleveringa and Oost, 1999).

The other channel-shoal pattern which usually is the case in long tidal basins is the braided pattern. This kind of pattern is observed by Van Veen (1950 Dutch, translated to English in 2001) in Western Scheldt in the Netherlands. Ahnert (1960) describe the characteristics of this pattern in a sketch (figure 2-5) based on the morphology of Patuxent River. As it is shown in the figure 2-5, the braided pattern consists of braided ebb and flood-dominated meanders with a shoal in between. The Western Scheldt Estuary also shows the same braided pattern in the middle stretch. Van Veen (1950 Dutch, translated to English in 2001) sketches the same pattern in Western Scheldt (figure 2-6).

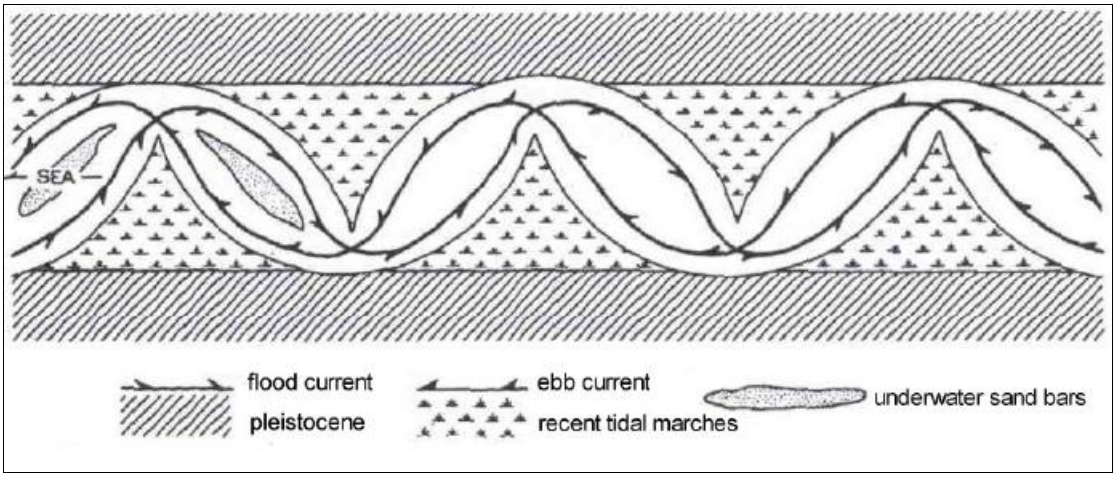

Figure 2-5: Sketch of meandering tidal channel system (Ahnert, 1960).

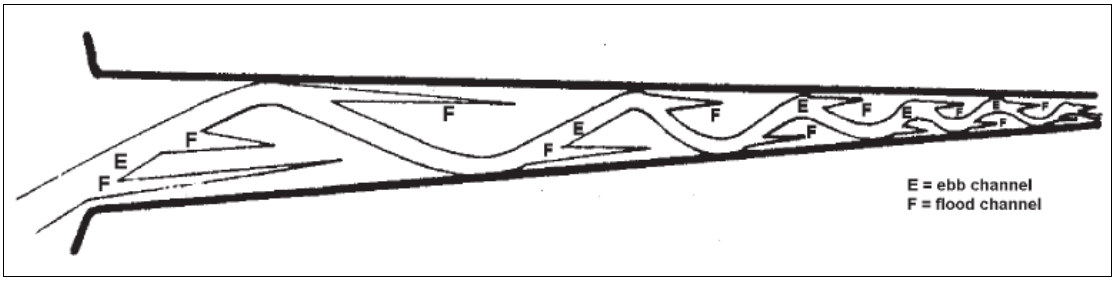

Figure 2-6: Sketch of ebb (E) and flood (F) channel system (Van Veen, 1950).

2.2 Classification of tidal basins

As it was mentioned in the previous section the ratio between longshore sediment transport by waves and tidal currents is one of the governing parameters in tidal inlet system morphology. Therefore the tidal inlets can be classified on this basis. Hayes (1979) used this principle to classify the tidal basins. With respect to tidal condition he introduced the following categories:

Micro-tidal	Tidal range <1.0 m
Low Meso-tidal	1.0 m < Tidal range <2.0 m
High Meso-tidal	2.0 m < Tidal range <3.5 m
Low Macro-tidal	3.5 m < Tidal range <5.5 m
High Marco-tidal	5.5 m < Tidal range

The effect of the waves on tidal inlets, which is mainly limiting the area of ebb-tidal delta, is categorized in 3 different classes by means of average annual significant wave height:

Low wave energy	$H_S < 0.6$ m
Medium wave energy	0.6 m $< H_S < 1.5$ m
High wave energy	1.5 m $< H_S$

The actual classification of the tidal inlets based on both wave height and tidal range is done by Hayes (1979) as follows (as well as in figure 2-7):

Wave dominated inlets
Mixed energy – wave dominant
Mixed energy – tide dominant
Tide dominant – low
Tide dominant – high

Clearly, different forcing condition leads to different morphology. So each class in the above mentioned classification can be described by morphological features as follows:
Wave dominated inlets have long continuous barriers, with only few tidal inlets and a lot of washovers.
Mixed energy – wave dominant inlets have a larger number of inlets and a small number of washovers. The size of the ebb-tidal delta is larger than the wave dominated inlets.
Mixed energy – tide dominant inlets have abundant tidal inlets, larger ebb-tidal deltas, and usually drumstick barriers.
Tide dominant – low inlets occasionally show wave built bars and transitional forms can be recognized.
Tide dominant – high inlets have predominant tidal current ridges, extensive salt marshes, and tidal flats. Often they have large ebb-tidal deltas and very deep inlet gorges.

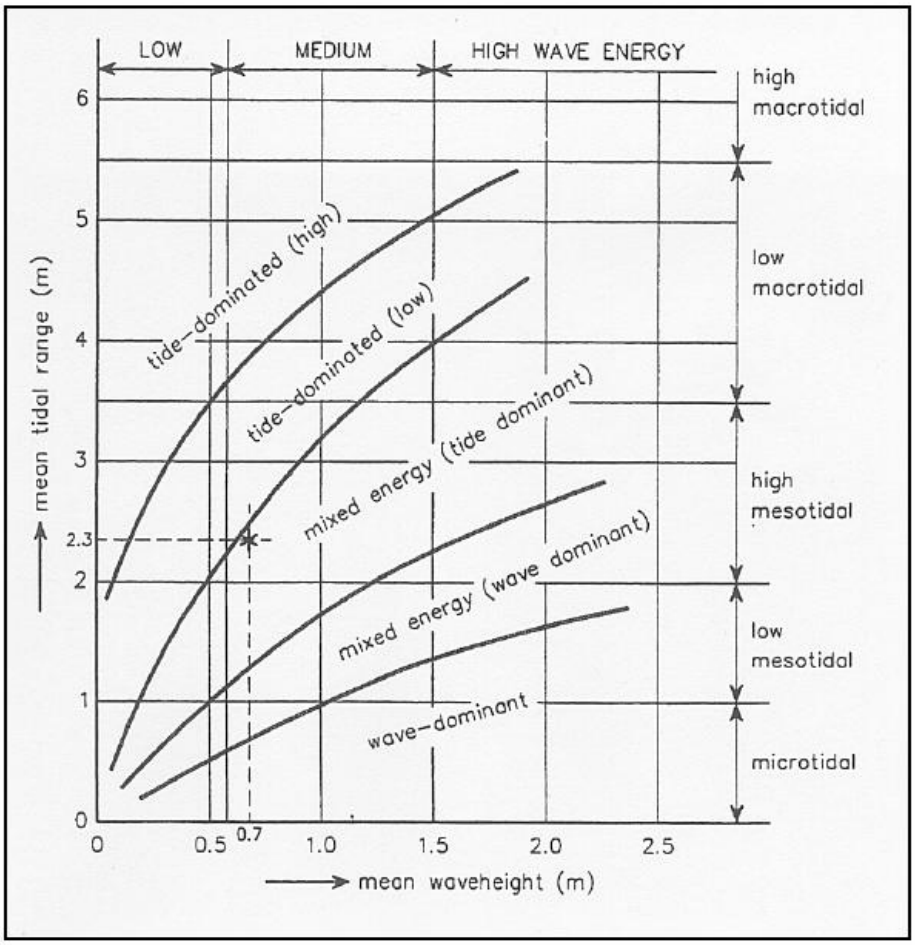

Figure 2-7: Hydrodynamic classification of tidal inlet (Based on Hayes (1979))

2.3 Different Scales in tidal basin morphodynamics

Morphodynamics of the tidal basins is more complicated than the normal coastlines. In a tidal basin morphodynamics a wide variety of spatial and temporal scales are involved. The whole basin system, different morphological elements, and various morphological features inside each element respond differently, temporally and spatially, to changes in forcing. These differences are to such an extent that the whole basin system may be in some equilibrium situation while there are large fluctuations within the elements. Therefore to analyze the morphodynamic behavior of the tidal inlets different scales should be considered. These scales are defined by De Vriend (1991); this classification in scales is the reference of almost all the studies since then. He defined the scales in four different scales, How ever these scales can not be separated by rigid borders:

The Micro-Scale level: the smallest scale morphological phenomena such as ripples and dunes formation; the principle forces are the diurnal tide and the weather condition.

The Meso-Scale level : the level of the principal morphological features, such as channels and shoals(hundred meters in space and years in terms), the principal forces are seasonal and inter annual changes in tide and weather conditions, and human interventions such as sand mining.

The Macro-Scale level: the level that these features interact, the ebb-tidal delta in space and decades in time, the principle forces are the long-term cycles in tide, decadal variations in wave climate, and repeating human activities.

The Mega-Scale level: the level at which the principal elements of the entire system (ebb-tidal delta, inlet and the basin) interact, so generally many kilometers in space and centuries in time. the principal forces are mean sea level rise, climate change, and long term tidal variations.

These scales are summarized in figure 2-8.

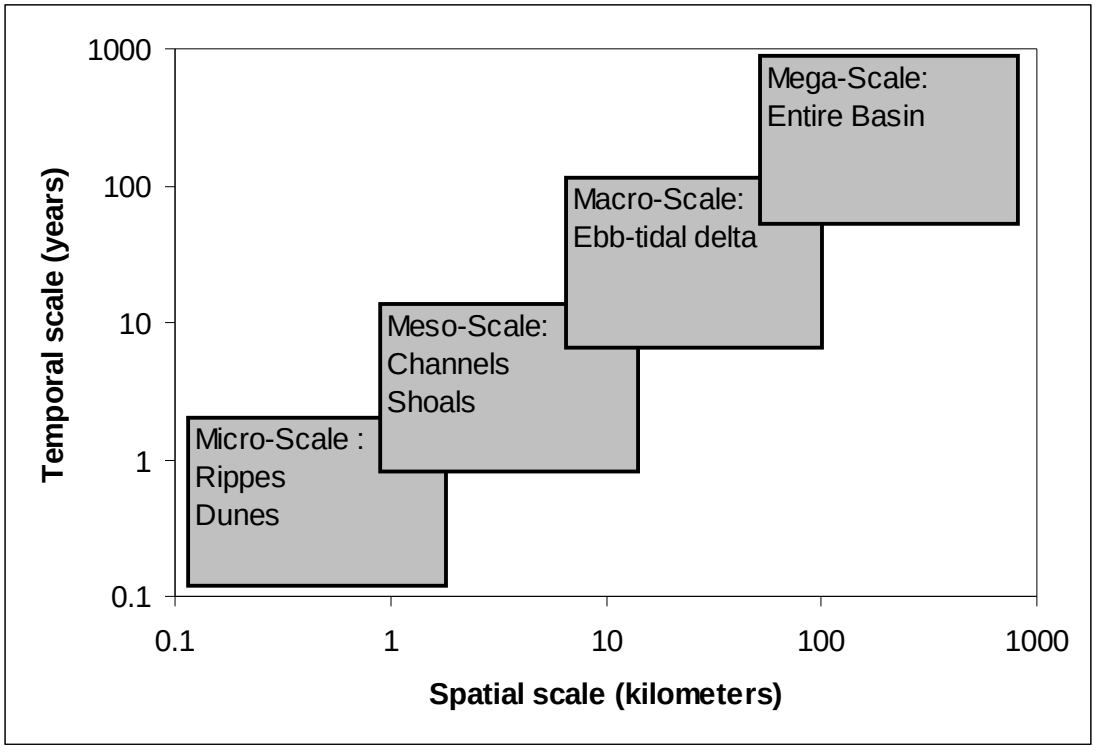

Figure 2-8: Different Morphodynamic scale of tidal basins (Based on De Vriend 1991)

The main approach of this study is to model the Mega-Scale evolution of the tidal inlet system in Dutch Wadden Sea.

2.4 Long-term morphological modeling of tidal basins

As it was mentioned before there are lots of different phenomena effecting on the morphological evolution of a tidal basin. These effects are varying in wide range of temporal and spatial scales. Therefore one model type can not provide the necessary morphological information to fulfill all kind of needs. It is claimed by De Vriend (1996) that "*the all purpose model for tidal inlet morphodynamics does not exist and is not likely to emerge in near future*". To the knowledge of the author such a model is not developed in recent years either. The models which can perform well in small-scale phenomena do not necessarily perform the same in larger scales and vise versa. So, the morphological models also should be classified according to the morphodynamic scale of phenomena of interest. Since the long-term modeling is the main approach in this study, different type of long-term models are described briefly in this section.

In morphological modeling of the coastal zones, including the tidal basins, there are two main approaches distinguished by De Vriend et. al. (1993b): 'behavior oriented models' and 'process-based models'. He also introduced a combination of these two approaches called 'formally integrated, long term models' later. (De Vriend, 1996).

2.4.1 Behavior based models

In behavior based models the underlying processes of morphology phenomena are neglected and modeling is based on the empirical relation between different coastal parameters (Van der Wegen, 2005). These kinds of models rely on the available measured data of coastal parameters. Different behavior based models have been developed for long-term morphological modeling including the specific models for tidal basins. Behavior based models by its turn categorized in different classes by De Vriend (1996).

2.4.1.1 Data-based models

The main assumption in this type of model is that the processes which govern the trend of the evolutions in coastal region remain constant during the time; or in other words in this models it is assumed that the coastal parameters continue their past evolution with the same trend. The simplest form of this model is the extrapolation of a parameter in time using a linear regression. the more sophisticated model of this type using a multi-scale nonlinear system is also developed and has been used in tidal basin systems. Using the relations resulted from the regressions the behavior of the parameters can be predicted.

Another type of the data-based model called 'translation' in literature is to predict the behavior of a coastal system by using the data and evolution history of a well monitored similar system. In this type of model it is assumed that both systems respond to the interferences similarly.

The data based models have been used in predicting the behavior of the tidal basins. However in such a complex model there are a large number of inputs and parameters to be taken into account. So it is difficult to find the relation between the mechanisms and different aspects of evolution. Therefore using the data-based models in tidal basins requires a good understanding of the physical mechanisms. (De Vriend, 1996).

2.4.1.2 Empirical models

The empirical models belong to two different categories: the equilibrium state models (relationships) and the transit empirical models.

In the equilibrium state relations, it is assumed that there is a coastal system (e.g. tidal basin) which is already in its (dynamic-) equilibrium and it can be chosen as a model of other systems with similar conditions. Relations between different parameters of such a system are determined by analyzing the measured data; these relations are assumed to be valid for similar systems. This type of relations has been used in tidal basin morphology extensively. However, In most of the available equilibrium state relations, some of data, which have been used in the analyses, are not the data from equilibrium conditions. In this report these relations are described in a specific section.

Transit empirical models describe the evolution of a morphological parameter between a given actual state and its equilibrium state as an exponential decay process which can be translated in mathematical form as follows. (De Vriend, 1996)

$$\frac{dA}{dt} = \frac{A_e - A}{\tau}$$

In which:

A : morphological parameter
t : time
A_e : equilibrium state value of A
τ : characteristic time scale of the process

The solutions of this equation are:

For constant A_e:

$$A(t) = A_e - [A_e - A(0)]\exp(-\frac{t}{\tau})$$

For slow linear varying A_e:

$$A(t) = A_e(t) - \tau\frac{dA_e}{dt} - [A_e(0) - \tau\frac{dA_e}{dt} - A(0)]\exp(-\frac{t}{\tau})$$

One example of such a model is shown in figure 2-9. It shows that the actual state of the parameters keeps lagging behind the linear varying equilibrium state.

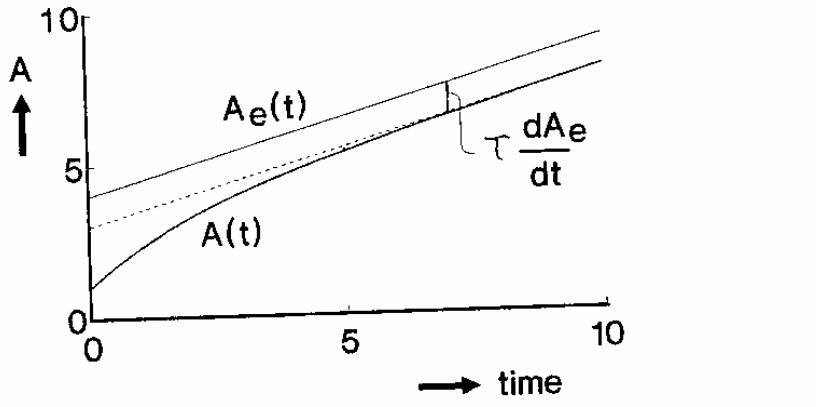

Figure 2-9: Example of the evolution of a morphological parameter in a transit empirical model. (De Vriend ,1996)

Transit empirical models are based on this assumption that each element of the system behaves independently. This assumption is not always true for a tidal basin system, in which there are sediment exchange between basin, ebb-tidal delta, and adjacent coast line. In other words this kind of model can be used in a tidal basin system only if the sufficient sediment is available inside the modeled element.

2.4.1.3 Semi-empirical models

In semi-empirical models, the approach is to use all kind of available information, such as measured data in the field, equilibrium state equations, and large scale balance equations in relation with the available theory. Due to lack of enough detailed empirical information, these models can not be used in detail scaled. In the case of a tidal basin, these models are developed for the scale of basin, ebb-tidal delta, etc.
A large number of models with this approach have been developed for different elements of a tidal basin system, some of them are : Di Silvio's basin model (Di Silvio, 1989), Van Dongeren's basin model (Van Dongeren, 1994), Karssen's basin model (Karssen, 1994a, 1994b), De Vriend et al's delta model (De Vriend et al, 1994), Steetzel's model of the entire Wadden Sea coast (Steetzel, 1995)- all described by De Vriend (1996). More recent models of this type, which are still developing are ESMORPH and ASMITA. (Stive et al. 1998)

2.4.2 Process based models

Process based models are based on the description of underlying physical processes. This type of models consists of a number of modules which describe hydrodynamic field (wave and current) and sediment transport respectively. These modules interact dynamically with bathymetry changes and lead to a morphology evolution.

These models need a careful selection of the processes to be modeled. Each of the relevant processes should be modeled adequately, not only in the sense of process description, but

also, the combination of the modules, which forms the model as a whole (De Vriend. 1996). On the other hand the input to the model should be schematized. In this regard another distinction is made on the process based models. Some models simulate the long-term effects, by modeling the full description of the of small scale processes, but with the schematized inputs. Using the morphological tide to represent the full neap spring tidal cycle is an example of such approach. This type of approaches is referred as 'Input reduction' in literature. Some other models only use the modules to describe the most important physical processes. This approach is called 'Model reduction' (Van der Wegen, 2005). However in most cases both input reduction and model reduction concepts are applied.

Another issue in the process based (long-term) morphological modeling is how to couple the basic modules of different processes in a model, to reach the result with desired accuracy in a reasonable computational time. Some different techniques are developed in this regard, which are described in the next section.

2.4.3 Long-term morphological process based modeling techniques

The hydrodynamic changes and corresponding sediment transport usually occurs in time scale of hours to days, while the morphological changes take place over a very longer time. Therefore the main challenge in process based morphological models, especially when a long-term model is needed, is to link the short-term hydrodynamic and sediment transport processes to the long-term morphological changes.

To tackle this problem deferent strategies have been developed and used in practice. Roelvink (2006) reviews these approaches in four categories that were developed more or less in historical sequence:

- Tide averaging (with continuity correction)
- Rapid assessment of morphology (RAM)
- Online approach
- Parallel online approach

2.4.3.1 Tide averaging approach

In this approach it is assumed that small morphological changes in a single tidal cycle do not affect the hydrodynamic and sediment transport pattern much. Therefore in one tidal cycle, the hydrodynamics and sediment transport modules can be run on a rigid boundary. Then rate of bed level changes is computed from the average tidal sediment transport. Usually an explicit scheme is used to update the bathymetry based on the calculated rate of bed level changes and new bathymetry is fed back to the hydrodynamic and sediment modules for the next step.

In this approach the morphological time step is limited both numerically and practically. Numerically this time step is limited by the bed courant number:

$$CFL = \frac{c\Delta t}{\Delta s}$$

In which:

t : time
s : computational direction
c : bed celerity

The bed celerity can be estimated by:

$$c = \frac{\partial S}{\partial z_b} \approx \frac{bS}{h}$$

In which:

b : power of the transport relation
S : tide average transport in s direction
h : tide average water depth

On the other hand the morphological time step is also limited by the accuracy of time integration. Therefore it is necessary to update the transport regularly.

The sediment transport field, which should be updated, is based on the changes of velocities in hydrodynamic field, mainly flow velocity and orbital velocity. An efficient way to adjust the flow field after small changes in bathymetry is the concept of 'continuity correction'. In this concept, it is assumed that the flow and wave patterns (flow rate, wave height, wave period and wave direction) do not change for small bathymetry changes. Therefore the flow velocity and orbital velocity will be a function of only water depth and can be adjusted easily. Then updating the sediment transport field is only a matter of re-computing the sediment transport based on the adjusted hydrodynamic field. The main limitation of this concept is the assumption that the flow pattern is constant in time. This may lead to some unrealistic high flow velocities in shallow areas while they are getting shallower.

Some examples of application of this method are presented in Roelvink et al. (1994), Stijn et al (1998), and Cayocca (2001)
The flow diagram of this approach is presented in figure 2-10.

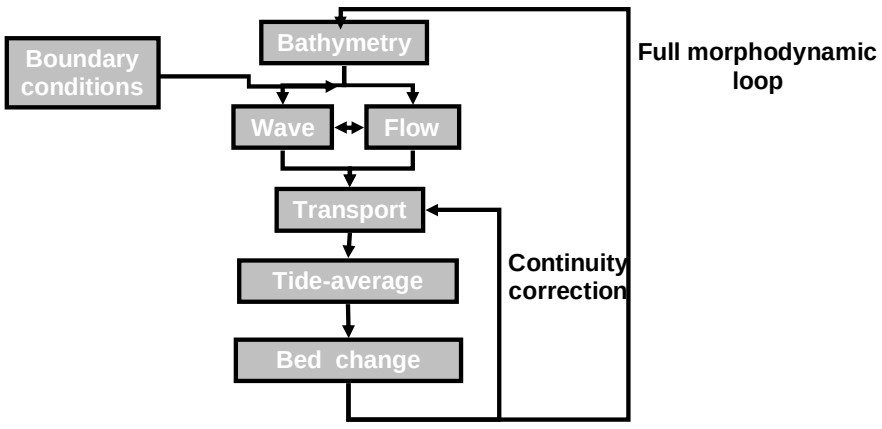

Figure 2-10: Flow diagram of tide-averaging morphodynamic model setup (Roelvink, 2006)

2.4.3.2 Rapid assessment of morphology (RAM) approach

In some projects there is a need to avoid a full morphodynamic simulation and interpret the outcome of initial transport computations. In this case if only the sediment/erosion rate is taken to account, the results may not be accurate enough. The RAM approach is developed to overcome this problem.

In this approach the same assumption which is used in 'continuity correction' is made. It means that for any set of current and wave patterns, the transport at each point is only a function of water depth.

This method is described with two simple equations. First the sediment balance, which relates, bed changes to sediment transport gradients:

$$\frac{\partial z_b}{\partial t} + \frac{\partial S_x}{\partial x} + \frac{\partial S_y}{\partial y} = 0$$

and sediment vector, describing the response of sediment changes to the bed level changes:

$$\vec{S} = \frac{\vec{S}_{t=0}}{\left|\vec{S}_{t=0}\right|} f(z_b)$$

In which:

z_b : bed level
S_x, Sy : sediment transport components
$\vec{S}$: sediment transport vector

Considering the transport usually is proportional to the velocity to the power of b:

$$\left|\vec{S}\right| \propto |u|^b \propto \left(\frac{|\vec{q}|}{h}\right)^b \propto |\vec{q}|^b \, h^{-b}$$

With similar consideration for orbital velocity, a suitable function for $f(z_b)$ is:

$$\left|\vec{S}\right| = A(x,y)h^{-b(x,y)}$$

Where h is water depth with respect to the high water. If b is constant in the field, the value of A can be calculated from the local water depth and the initial sediment transport.

These two relations can be solved with the same bathymetry update scheme as in a full morphodynamic model in a short computational time.

The diagram of flow in Ram method is shown in the figure 2-11.

If the area to be modeled is complicated, the RAM model can still be used and as soon as the changes in bathymetry become large, the full model of the hydrodynamic and sediment transport is needed. This model is carried out for a number of input conditions. The weighted average of the sediment transport is the basis for the next RAM computation. The updated bathymetry is fed back to the hydrodynamic and sediment transport model again.

Some practical case of this approach is presented in Roelvink et al. (1998, 2001)

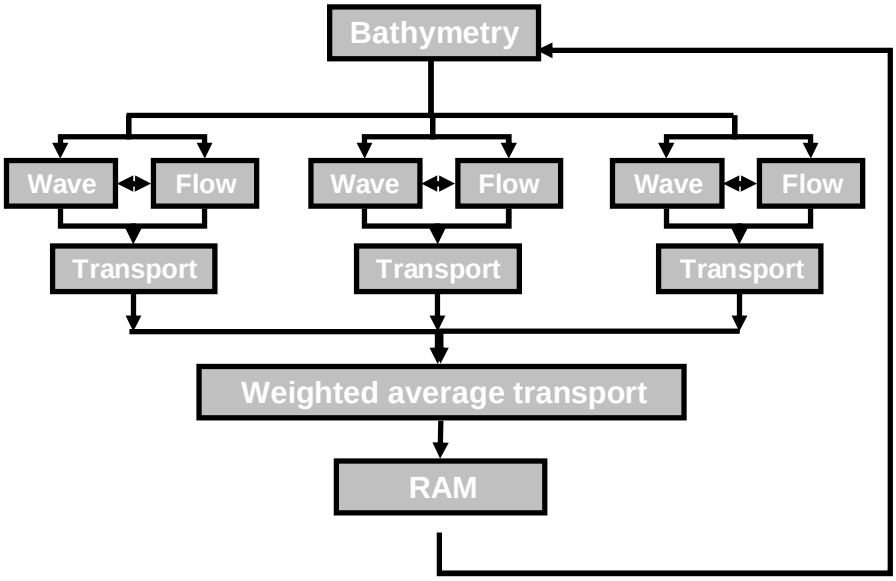

Figure 2-11: Flow diagram of RAM approach (Roelvink, 2006)

2.4.3.3 Online approach

A completely different approach for morphological modeling is recently integrated in Delft3D software. In this approach the flow, sediment transport and bed-level changing run with the same (small) time steps (Lesser et al., 2004, Roelvink, 2006). Since the morphologic changes are calculated simultaneously with the other modules the coupling errors are minimized. However, as described in Lesser et al. (2004), because this approach does not consider the difference between the flow and morphological time step, a 'morphological factor' to increase the depth changes rate by a constant factor (n) should be applied (Roelvink, 2006). So after a simulation of one tidal cycle in fact the morphological changes in n tidal cycle are modeled. In this model even if a large value is chosen for n, the bed level changes is computed in much smaller time steps than the other models. Another advantage of 'online' approach is that since all the processes are coupled in the same time scale, it is easy to include different interaction between flow, sediment, and morphology. Also from the computational point of view, in this approach there is no need to store a large amount of data for different processes. The drying and wetting areas are also treated more straightforward in this approach. Examples of the practical usage of this approach can be

found in Lesser et al. (2003, 2004). This method has been used for detail event-scale modeling also (Roelvink et al, 2003) for a case of breaching of a sand dam or narrow barrier island. The flow chart of this approach which is called 'online' approach is shown in the figure 2-12.

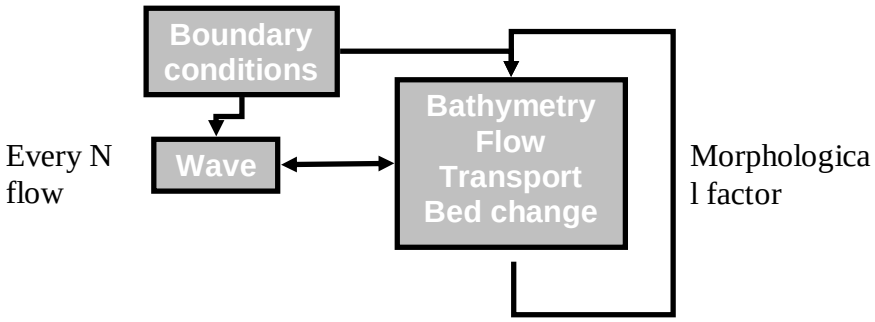

Figure 2-12: Flow diagram of 'online approach' (Roelvink, 2006)

2.4.3.4 Parallel online approach

The base of this approach is the difference between the time-scale of hydrodynamic changes and morphology changes. The hydrodynamic conditions vary much faster than the morphology. If all the hydrodynamic conditions may occur in a small time interval compare to the morphological time-scale, they may occur simultaneously also. Therefore if these conditions share the same bathymetry, they can be modeled in parallel in the morphological model. The bathymetry should be updated according to the weighted average of the changes in the bottom level in all the conditions. The flow diagram of this approach is shown in the figure 2-13.

In this approach the different conditions are processed in parallel, then the resulting bed level change of all the conditions, is merged by weighted averaging, to one new bathymetry for the next step. In this approach a series of PC's or a Linux cluster should be used to model the parallel processes.

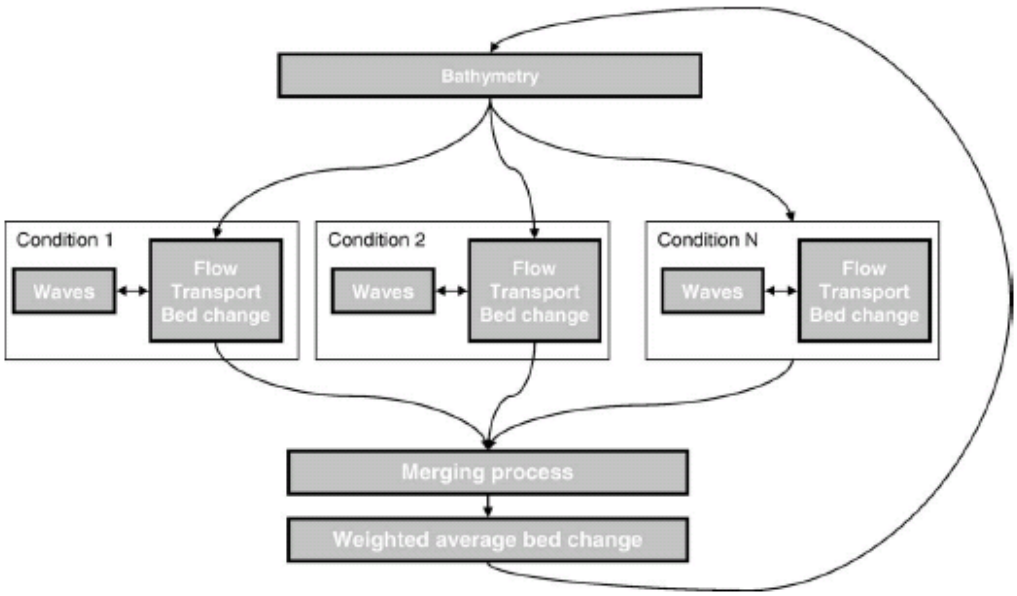

Figure 2-13: Flow diagram of the 'online parallel approach' (Roelvink, 2006)

2.4.3.5 Comparison of the approaches

Roelvink (2006) shows that 'online' and especially 'parallel online' approaches are more accurate than the tide-averaging methods for the similar morphological factor (n) in 'online' approaches and morphological time-scale (nT) in tide-averaging approach. Figure 2-14 shows the comparison of online approach and tide-averaging with continuity correction.

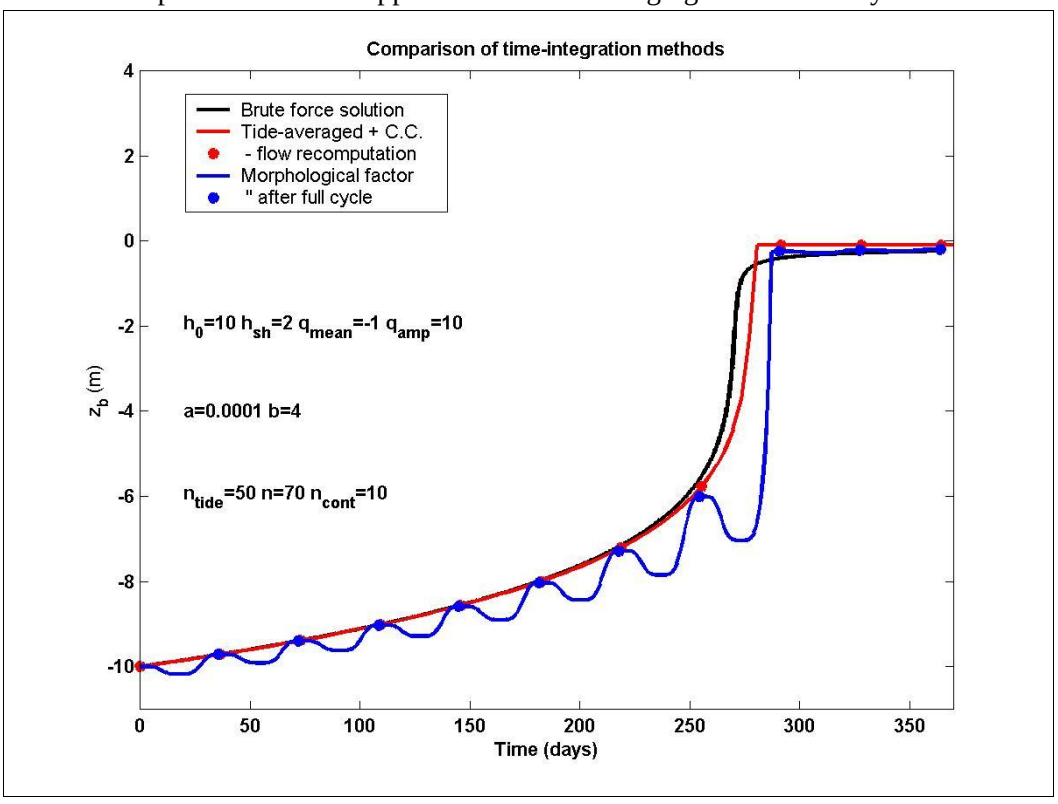

Figure 2-14: Comparison of online approach and tide-averaging with continuity correction (Roelvink 2004)

The efficiency of different approaches is investigated by Roelvink (2006), in terms of numerical stability, accuracy, and coping with variable inputs. Table 2-1 describes the difference in the efficiency of different approaches. The parameter n is the number of tidal cycles of morphological changes, through which a whole tidal cycle has to be run. The n_{RAM} is the number of RAM steps between the full hydrodynamic updates. n_{Cond} is the number of conditions with equal probability of occurrence that should be represented in one year (700 tides) of morphological changes.

Table 2-1: Over view of efficiency of different approaches for morphological modeling (Roelvink, 2006)

Method	Numerical stability	Accuracy	Coping with variable input
Tide-averaging	$n < \frac{h\Delta x}{b < S > T}$	$\varepsilon_{rel} = \frac{1}{2}\frac{b\Delta z_b}{h}$	$n<700/n_{cond}$
RAM	$n < \frac{h\Delta x}{b < S > T} n_{RAM}$	$\varepsilon_{rel} = \frac{1}{2}\frac{b\Delta z_b}{h}$	No restriction
Online	$n < \frac{h\Delta x}{bS_{max} dt_{flow}}$	$\varepsilon_{rel} = \frac{1}{2}\frac{b}{h}\left(\Delta z_{b,t+nT} - n\Delta z_{b,t+T}\right)$	$n<700/n_{cond}$
Parallel online	$n < \frac{h\Delta x}{b < S >_{max} dt_{flow}}$	$\varepsilon_{rel} = \frac{1}{2}\frac{b}{h}\left(\Delta z_{b,t+nT} - n\Delta z_{b,t+T}\right)$	No restriction

Since in this study very long-term simulations should be carried out, therefore the ‘online’ or ‘parallel online’ methods with large morphological factor are the best choice. But for the ‘parallel online’ some parallel processors are needed, therefore the ‘online’ approach is used.

2.4.4 Formally integrated, long term models

One way to model the long-term evolution of a tidal basin is to formally integrate the mathematical equation of physical processes over the time and space domain. Since these equations are normally nonlinear, the closure terms should be involved. The closure terms have to be modeled in terms of large-scale dependent variables, empirically or based on a theoretical analysis of the relevant interaction processes (De Vriend 1996).

This approach is used by Krol (1990) to integrate a simple 1D morphological model of a tidal estuary. Later Fokkink (1992), Schuttelaars and De Swart (1994) followed the same approach. (All stated in De Vriend (1996)).

2.5 Definition of tidal basin parameters

Inside a tidal basin, two different morphological features are present ‘Channels and Flats’. These two features are normally defined as it is shown in the figure 2-15.

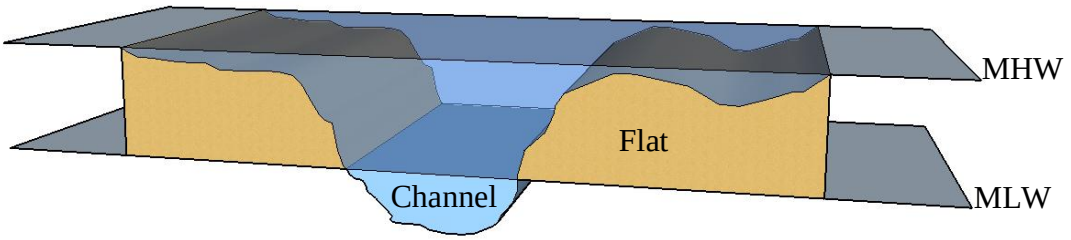

Figure 2-15: Illustration of Channel and Flat areas in an arbitrary tidal basin (Van Geer, 2007)

The characteristics of these two morphological features together with the hydrodynamic parameters are widely used in the literature to analyze the behavior of the tidal basins. The definitions of these parameters in the literature are not rigid and they are subjected to some changes in different sources, in this study all the relations are based on the following definitions:

Area of the basin (A_b):
Area of the Basin is defined as the wet area of the basin at the mean high water.

Tidal prism (P):
Tidal prism is the volume of water which is exchanged during each tidal cycle between the basin and sea. It is defined as the volume of water inside the basin between mean high water and mean low water.

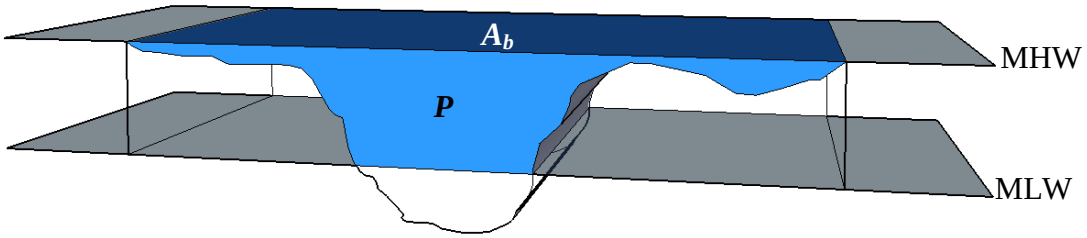

Figure 2-16: Illustration of Area of the basin and Tidal Prism in a tidal basin (Van Geer, 2007)

The inter-tidal flat area (A_f):
The inter-tidal flat area (flat area) is defined as the area of the between MLW and MHW

The inter-tidal flat volume (V_f):
The inter-tidal flat volume or in short term, flat volume, is the amount of sediment inside the basin between the mean low water and mean high water.

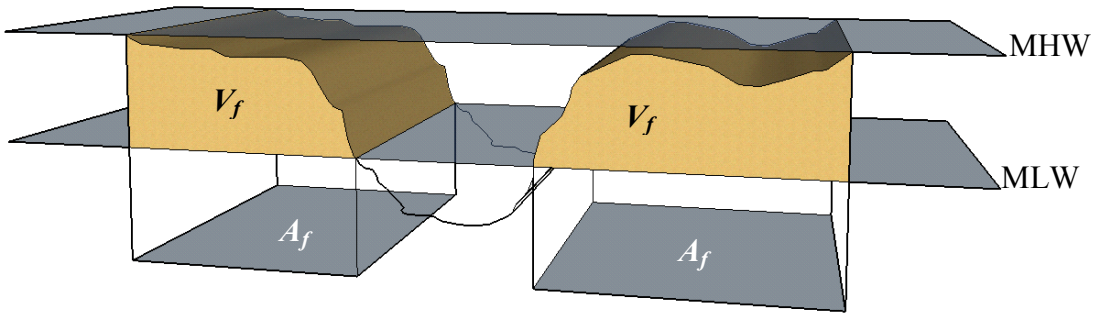

Figure 2-17: Illustration of Inter-tidal flat volume and area in a tidal basin (Van Geer, 2007)

Channel area (A_c):
Channel area is defined as the wet area of the basin at mean low water.

Channel volume (V_c):
Channel volume is the volume of water in a tidal basin under the mean low water.

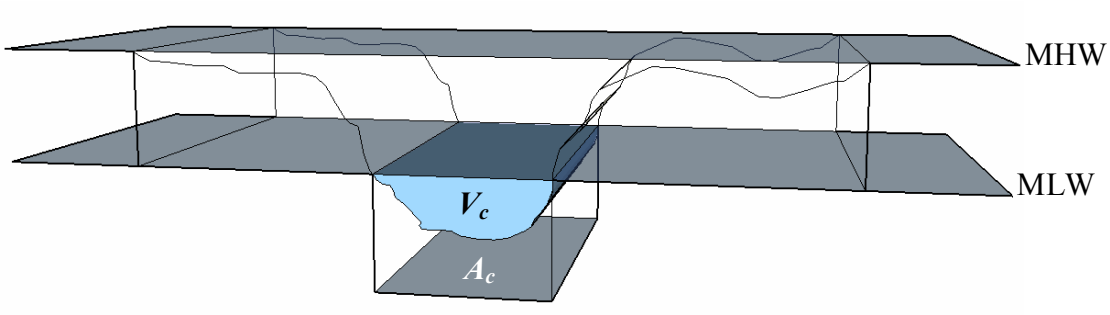

Figure 2-18:Illustration of channel volume and area in a tidal basin (Van Geer, 2007)

In the literature, in some equations the channel volume is defined differently. Since that equation (Diagram of Friedrichs and Aubrey, 1988) is used in this report, that definition with its corresponding channel depth is also introduced here.

Channel volume, channel depth – Alternative definition ($V_{c\text{-}F.A.}$, h):
In this definition the channel volume and channel depth are defined as follows:

$$V_{c-F,A} = V_c + A_c.a$$

and

$$h = \frac{V_{c-F,A}}{A_c} = \frac{V_c}{A_c} + a$$

in which 'a' is the tidal amplitude.

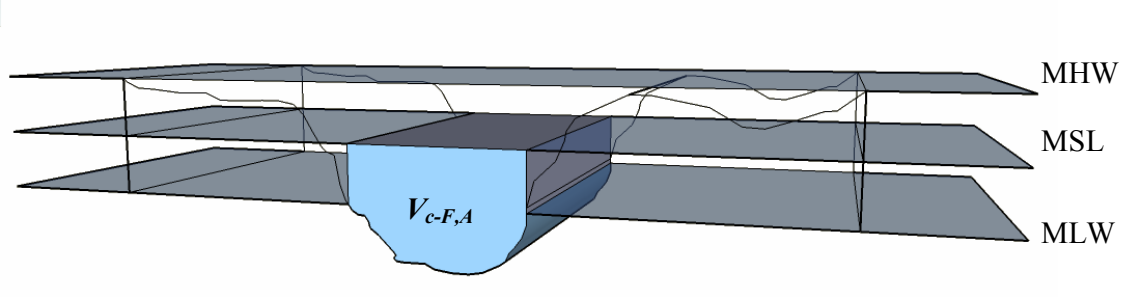

Figure 2-19: Illustration of alternative channel volume in a tidal basin

Volume of inter-tidal storage (V_s):
Volume of inter-tidal storage is the volume of water on the flats between the mean high water and mean low water.

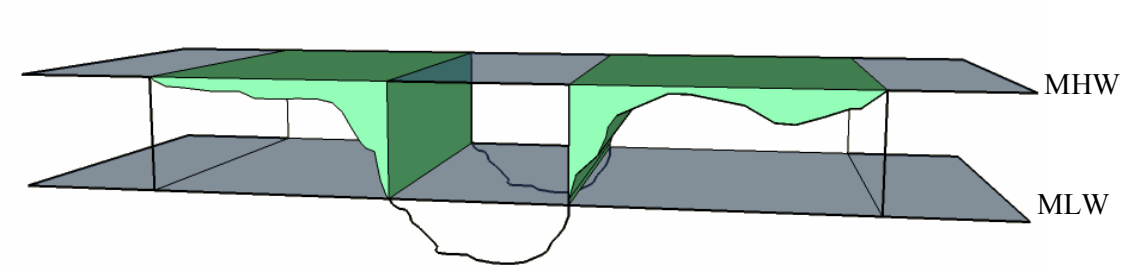

Figure 2-20: Illustration of inter-tidal storage volume in a tidal basin

Height of flats (h_f):
Height of flats, which is usually used in the equilibrium situation, is defined as the average height of the flat areas calculated by the following relation:

$$h_f = \frac{V_f}{A_f}$$

Other definitions, which are normally used in literature, are:

Hypsometry of a basin:
Hypsometry, or hypsography, of the basin is defined as the vertical distribution of basin surface area to height. A tidal basin can have large inter-tidal area and shallow channels, but also it can have small inter-tidal area and deep channels. In reality a tidal basin can be any where between these two extreme conditions. Figure 2-21 shows these two examples of tidal basins and their hypsometry curves.

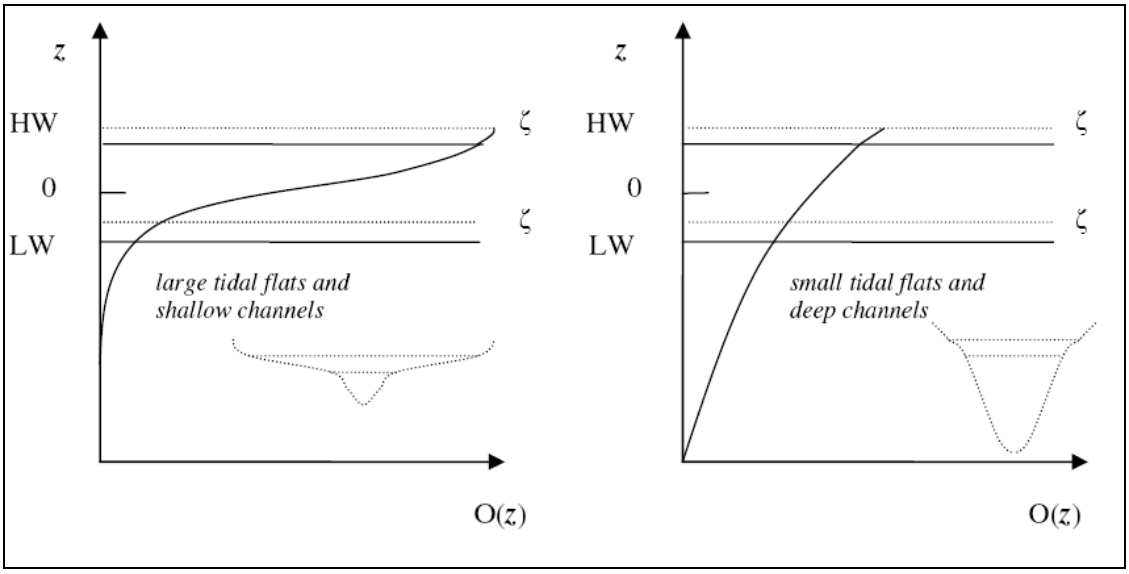

Figure 2-21: Examples of hypsometry curves (TU delft lecture note no. CT-5303)

Area of the inlet cross section (A_C):
Area of the inlet cross section is defined with respect to the mean water level.

Volume of the ebb-tidal delta (V_0):
Volume of the ebb-tidal delta is the volume of sand which is stored in the ebb-tidal delta, defined by Dean and Walton (1975) (see section 2.1)

Most of the abovementioned parameters can be determined from the hypsometry data of the basin. Clearly these parameters are in relation with each other. These relations are as follows:

$$P = 2a \cdot A_b - V_f$$

$$A_f = A_b - A_c$$

$$V_{c-F,A} = V_c + A_c.a$$

$$V_s = P - A_c.2a$$

$$h = \frac{V_{c-F,A}}{A_c} = \frac{V_c}{A_c} + a$$

$$h_f = \frac{V_f}{A_f}$$

$$V_f = A_f.2a - V_s$$

2.6 Equilibrium equations and indicators in tidal basins

During the long-term simulation of the tidal basins, there should be some relations and indicators, to compare the result of the process based model with them and determine the condition of the basins in the model with respect to the equilibrium condition. Although as it was mentioned before, due to data used in finding the equilibrium equations, these relations are subjected to some distortion, they are still a proper indicator of the stability in a tidal basin at least in their forms, rather than the coefficients.

In this section the parameters and relations which are checked to analyze the model output while seeking an equilibrium condition are introduced.

Sediment exchange:
If a tidal basin system is in some sort of (dynamic-) equilibrium the average net sediment exchange between the back barrier basin, ebb-tidal delta and adjacent coast lines should be negligible. This sediment exchange can be translated as the changes of the sediment volume inside the back barrier basin. In the current study this volume is chosen as an equilibrium indicator.

Channel Volumes:
A famous relation which can be found in the literature is the relation between the tidal prism and the channel volume (Eysink, 1990). According to Eysink (1992) the relation is:

$$V_c = \alpha_c \cdot P^{\beta_c}$$

in Which
V_c [m^3] : Channel volume below MLW
P [m^3] : Tidal prism
β_c [-] : 1, 55
α_c [-β_c] : 16e-6 for the Dutch Wadden Sea

Flat Area:
In the literature there are some suggestions for the flat area in equilibrium condition, De Vriend et al. (1989) showed a general relation between the flat area and the total area of the basin:

$$A_f = A_b - \beta \frac{2a}{h_c} A_b^{\frac{2}{3}}$$

in Which
A_f [m^2] : Flat Area at MLW
A_b [m^2] : Total Area of basin
β [-] : Constant
h_c [-] : Characteristic channel depth
a [m] : Tidal amplitude

Renger and Partenscky (1974) worked on the same form of relation for inlets in the German Bight. Later Eysink (1991) re-wrote their relation as:

$$\frac{A_f}{A_b} = 1 - 0.025 \cdot A_b^{0.5}$$

A_f [Km^2] : Flat Area at MLW
A_b [Km^2] : Total Area of basin

Eysink (1991) use the same form of relation ($\left(\frac{A_f}{A_b}\right)$ as a function of A_b) to analyze the available data in tidal inlets and estuaries in The Netherlands. He summarized his result in the following figure.

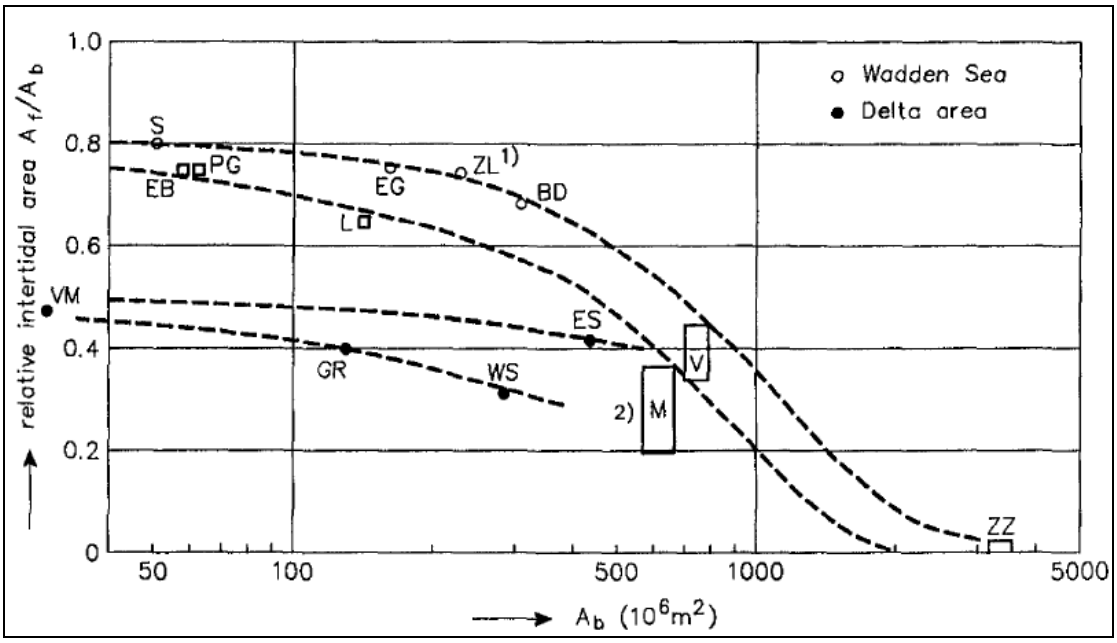

Figure 2-22: Relative flat area in Dutch Wadden Sea and Delta Area (Eysink, 1991)

In this study the relative flat area $\left(\frac{A_f}{A_b}\right)$ is chosen as one of the equilibrium indicators. Also the evolution of the flat area is monitored in the model.

Flat Height:
Eysink (1990) claims that flats tend to reach an equilibrium height related to the tidal range:

$$h_f = \alpha_{fe} \cdot 2a$$

$$\alpha_{fe} = \alpha_f - 0.24 \cdot 10^{-9} \cdot A_b$$

In which

h_f [m] : Height of flat
A_b [m^2] : Total Area of basin
a [m] : Tidal amplitude
α_f [-] : 0.41 according to Eysink (1990)
: 0.38 – 0.5 according to Van Goor (2001) for Dutch Wadden Sea

Flat Volume:
From the relations for an equilibrium flat height and an equilibrium flat area, a relation for flat volume in equilibrium is derived as follows:

$$V_f = (\alpha_f - 0.24 \cdot 10^{-9} \cdot A_b) \cdot \left(\frac{A_f}{A_b} \right) \cdot A_b \cdot 2a$$

In which

V_f [m3]: Flat Volume
A_f [m^2] : Flat Area
A_b [m^2] : Total Area of basin
a [m] : Tidal amplitude
α_f [-] : 0.41 according to Eysink (1990)
: 0.38 – 0.5 according to Van Goor (2001) for Dutch Wadden Sea

Area of Cross Section:
As it is stated in De Vriend (1996), O'Brien (1969) was the first to suggest a linear relation between the cross section area of the inlet and tidal prism. Later Eysink et al. (1990) showed the similar relation:

$$A_c = \alpha_A . P$$

In which

A_c [m^2]: Area of inlet cross section
P [m^3]: Tidal Prism
α_A [m^{-1}] : 7e-5 according to Eysink (1990)

Volume of ebb-tidal delta:
Other important equation is the relation between stored sand in the ebb-tidal delta and the tidal prism (Dean and Walton, 1975):

$$V_0 = \alpha_0 . P^{\beta_0}$$

In which

V_0 [m^3]: Volume of ebb-tidal delta
P [m^3] : Tidal Prism
β_0 [-] : 1.23
α_0 [1.23^{-1}] : 65.7e-3 for Dutch Wadden Sea, according to Eysink (1990)

Friedrischs & Aubrey Diagram:
Friedrischs & Aubrey (1988) used a 1-D numerical model to study the influence of geometry and bathymetry of short, friction dominated and well-mixed estuaries. They suggested that two non-dimensional parameters can be used to characterize the tidal basins. These parameters are responsible for different types of asymmetries. The first one is a/h, tidal amplitude over the depth of the channel with respect to MSL, which shows the relative shallowness of the estuary. The second parameter is V_S/V_C where V_S is the Volume of inter-tidal storage and V_C is the *alternative* definition of the channel volume noted in this report as $V_{C\text{-}F,A}$. Speer et al. (1991) translated the Friedrischs & Aubrey (1988) result to a graph (figure 2-23) which distinguishes the flood or ebb-dominant tidal basins. Later it is suggested that the border between these two regions can represent the equilibrium condition of the basins.

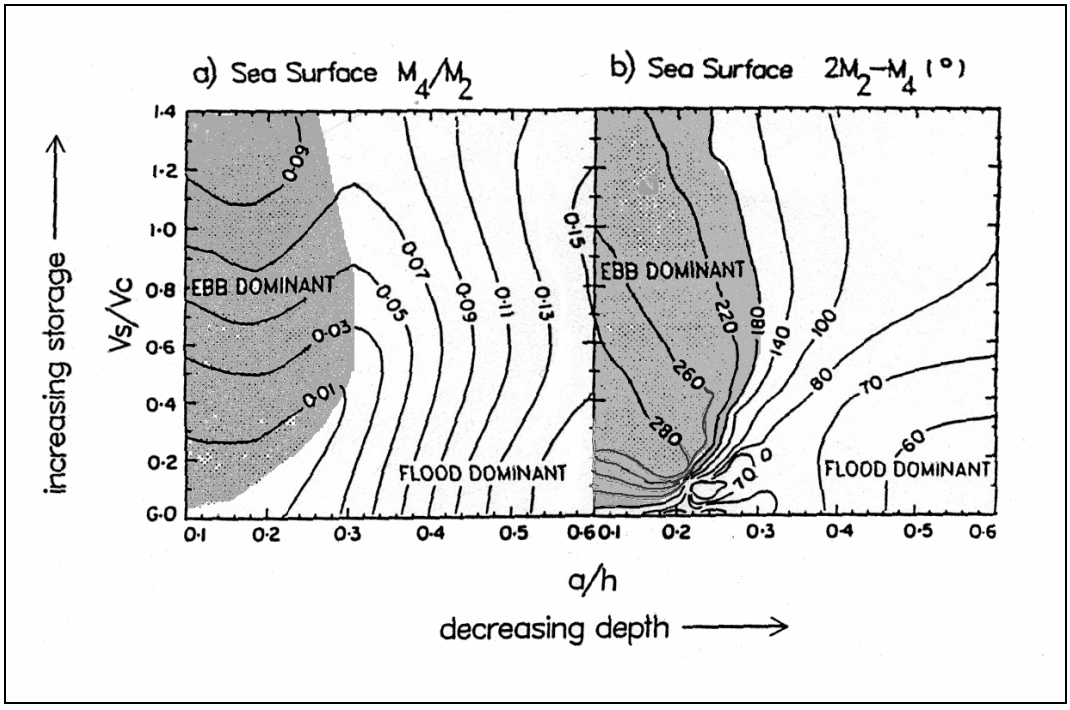

Figure 2-23: Diagram Based on Friedrischs & Aubrey models (Speer et al., 1991)

3 Study Area

The Wadden Sea located at the south east side of the North Sea, consists of 33 tidal inlets system along the approximately 500 km of The Netherlands, Germany and Denmark coastlines. The barrier islands of these tidal basin systems separated the largest tidal flat area from the North Sea (Elias 2006). The part of the Wadden Sea which is along The Netherlands coastline (Dutch Wadden Sea) is shown in figure 3-1. The ebb-tidal delta shoals in Dutch Wadden Sea are relatively large while they are associated with relatively narrow and deep channels, the back barrier basins of these tidal inlet systems consist of extensive systems of branching channels, tidal flats, and salt marshes.

The tidal basins in the east and west of Dutch Wadden Sea differ in different aspects : in the eastern part (Ameland and Frisian) the back barrier area is shallower including large flat areas and small channels, while in the Western part, mainly in Marsdiep and Vlie, channels are much deeper and flat areas are relatively small (Elias 2006).

Figure 3-1: Satellite image of Dutch Wadden Sea: 1- Texel-Marsdiep 2- Eierlandse Gat 3- Vlie 4- Ameland 5- Frisian

The main area of interest in the current study is the Western part of Dutch Wadden Sea, especially the Marsdiep basin. In this chapter first the historical evolution of the Wadden Sea is discussed and then some characteristics of different basins are mentioned.

3.1 Formation of Wadden Sea

From a geological point of view the Wadden Sea is a very young formation. The Wadden Sea with the shape of today was not formed till the early Holocene period.

During the ice age of the Pleistocene, the level of the sea was 100 to 135 m below the present sea level, the south part of the current North Sea was dry, and the United Kingdom and Ireland were connected to west Europe. The ice layers from the different ice ages had resulted in a thick layer of highly irregular surface. During the Holocene these irregularities either have been filled up by fluvial sediment or have been used by rivers , The orientation of the later form Texel as well as where the Marsdiep came through are determined roughly by the lower part of the Pleistocene layers.

During the Boreal geological period (10000-9000 before present), due to melting of the ices the sea level rose with the rate of about 1 m/century. Because of this rapid sea level rise the shelf between the United Kingdome and Western Europe flooded.

This sea level rise also retreated the coastlines and rivers near the coastlines developed the lagoons and estuaries. At this time (beginning of Atlanticum-around 9000 years ago), the Dutch coastline was located about 25 km seaward from its current position. Despite the sea level rise at that time, due to changes in wave and tidal condition in the North Sea, a sand bar was created at the west of the Dutch coast. This sand bar trapped the water behind it and formed a lagoon between the main land and the sea. Large quantities of peat were formed in this lagoon.

In the late Atlanticum (5500 before present.), the coastlines were not closed any more and most probably were subjected to a large tidal range. So the sand bar interrupted by inlets and the enclosed lagoon changed to a tidal lagoon, on the other hand the Pleistocene high near the Texel and Vlieland were under the effect of the barrier islands along the Dutch coastlines.

When the rate of sea level rise decreased, the available sediment from sea and rivers was enough to cope with the sea level rise. So the barrier coastline at the west side closed again and made the tidal lagoon to be a fresh water environment. In this lake the formation of peat layer was much easier, but on the north part some of the tidal inlets remain the same or even became larger.

During the Sub-Atlanticum period (began 2500 years ago), in the area of current Wadden Sea new inlets formed and especially in the west part of current Wadden Sea, newly formed inlet ended the formation of peat layers and made place for marine sediments.

At the Roman time, a fresh lake called Flevo was situated at the same place as current IJssel Lake. This lake at this time had no connection with the sea. But due to continuous erosion finally a connection took place between the sea and the former Flevo Lake. From this time on Flevo is not a lake any more but a sea called Zuider Sea.

The first connection between Zuider Sea and North Sea happened in the place of current Vlie inlet. Then during 800 to 1300 A.D and due to a series of storms in the 12^{th} century another inlet was developed in the western part of the Wadden Sea, which is called Marsdiep

now. The strong current coming through the Marsdiep caused the continuous erosion of peat layers and Marsdiep channel got deeper and deeper, and the tidal volume of Marsdiep increased. The Zuider Sea reached its largest size at this time and since then due to sedimentation of the tidal flats the Wadden sea decreases in size. (Elias 2006 , Ubbink, 2004) this procedure showed in the figure 3-2.

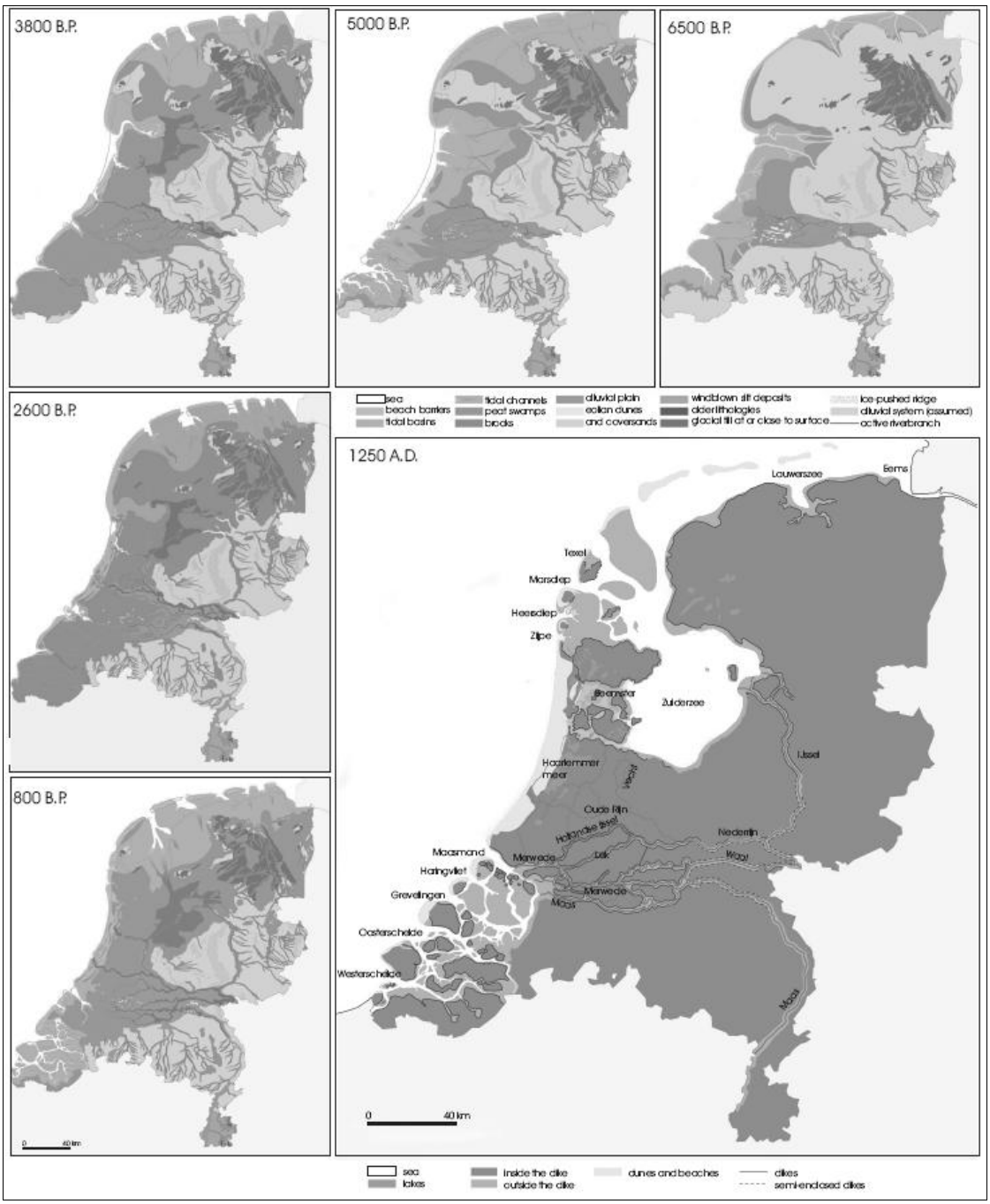

Figure 3-2:Geological evolution of the Netherlands 6500 Before Present (B.P) - 1250 A.D. (Elias, 2006 after De Mulder et al. 2003).

3.2 Human intervention

From many years ago the developments in the Dutch coast are not only because of the natural forces but also due to human interventions. These interventions primarily were to protect the shorelines from eroding and flooding, to prevent the salt-intrusion, and also to facilitate the navigation. Before the flooding disaster of 1916 these interventions were limited to the levees and small dikes. But after this disaster and also due to lack of agricultural lands and accommodation areas, in 1932 the Afsluitdijk was constructed, which closed the Zuider Sea from the Wadden Sea and turned it back to a fresh water lake. (Ubbink, 2004)

This construction had a huge effect on the hydrodynamic and morphodynamics of the Wadden Sea. Before the closure, the Marsdiep and Vlie inlets shared the Zuider Sea basin at the southern part of the Wadden sea. In total these two basins covered an area of 4000 km^2 with a basin length of 130 km. But after the construction of Afsluitdijk in 1932 this basin reduced to around 700 km^2 and length of about 30 km. Also this closure divided basins of Marsdiep and Vlie in two separate basins with a minor residual transport of sediment between the two basins (Elias et. al., 2003b)

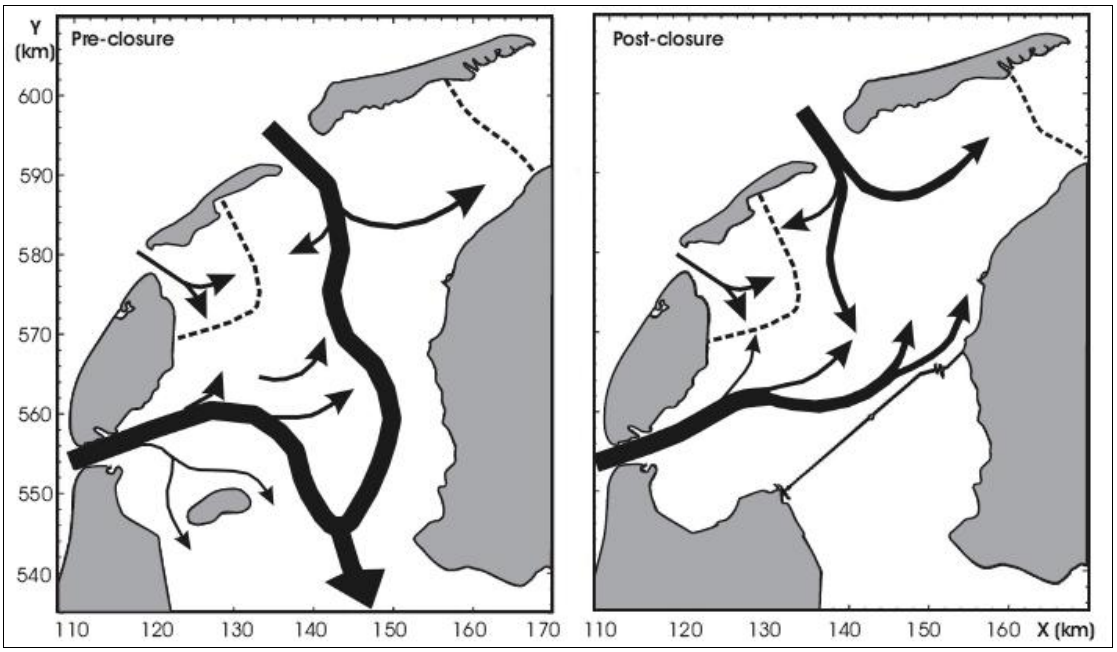

Figure 3-3: Impression of the tidal wave propagation prior (left) and after closure (right); (Elias et. al, 2003b, redrawn after Thijsse (1972))

Elias et. al (2003b) summarized the hydrodynamic and morphodynamic changes of Wadden Sea as follows:

"The closure of the Zuider Sea has decreased the Texel Inlet basin area substantially, whereas the tidal prism increased about 20%. This apparent contradiction mainly results from the changed characteristics of the tidal wave in the basin. Preceding the closure, the tidal wave in the Zuider Sea consisted of the combined tidal waves of the Texel and Vlie inlets. These two tidal waves propagated separately through the Wadden Sea and merged into one tidal wave in the Zuider Sea area (as illustrated in figure 3-3, left - panel). The tidal

wave reflected at the southern boundary of the Zuider Sea basin, about 130 km inland from the Texel inlet. The basin length (L) equals about half the tidal wave length (λ) and, in a hypothetical situation without bottom friction and the wave propagating at an oblique angle to the shore, a standing wave would form in the basin. In such case, at the location $L \approx 0.5\lambda$ from the southern boundary an anti-node in water level occurs at which discharges are zero and all exchange of water south of this boundary takes places in the basin.

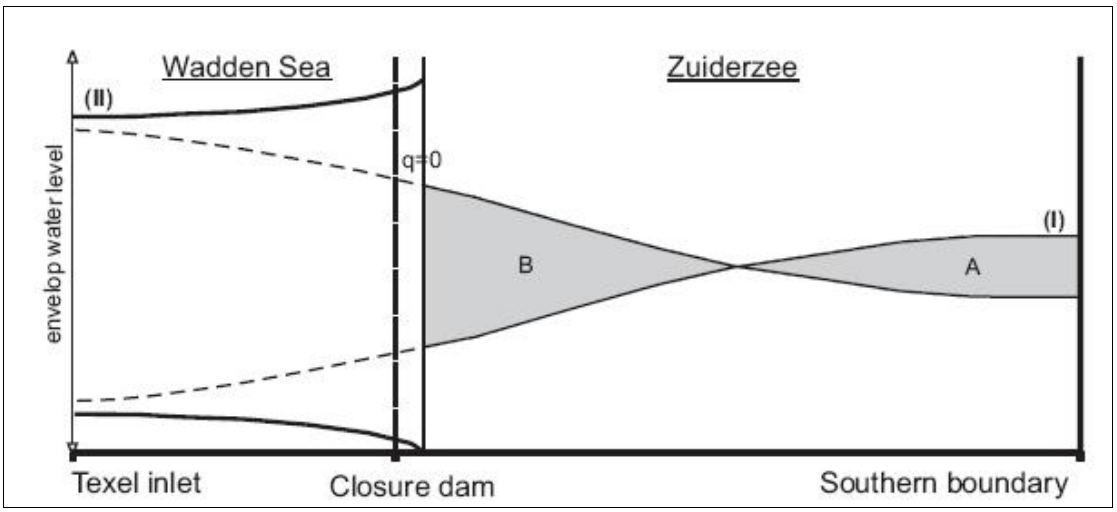

Figure 3-4: Schematization tidal wave envelop prior (I) and after the closure (II). (Elias et. al, 2003b)

In reality, the tidal wave propagating through the Zuider Sea, that is limited in depth, decreased and deformed by bottom friction. The reflected tidal wave is considerably smaller in amplitude than the incoming tidal wave. The interference of the two waves results in the formation of a damped tidal wave with a propagating character at the inlet and a standing character near the southern boundary. A schematization of the resulting tidal wave envelope is indicated by (I) in figure 3-4 (after Kragtwijk, 2001).

The no-exchange boundary (indicated by q = 0 in figure 3-4) is no longer located at $L \approx 0.5\lambda$, but is formed at the location where the areas indicated by (A) and (B) balance. This location is closer to the southern boundary. The actual location of the closure dam is north of the no-exchange line because the tidal ranges in the basin were predicted to increase substantially. Due to the closure dam the basin length reduced to about 30 km(figure 3-3, right panel) that is small compared to the tidal wave length ($L \approx 0.2\lambda$), and a tidal wave is formed with a standing wave character. This strong decrease in basin length reduced the damping of the tidal wave due to friction and with more reflection at the closure dam the tidal ranges increased drastically (tidal wave envelope after the closure indicated by (II) in Fig. 3-4). This is the reason that the location of the closure dam was chosen seaward of the no-exchange location, i.e. to minimize the changes in flow velocities through the inlets (Lorentz, 1926).

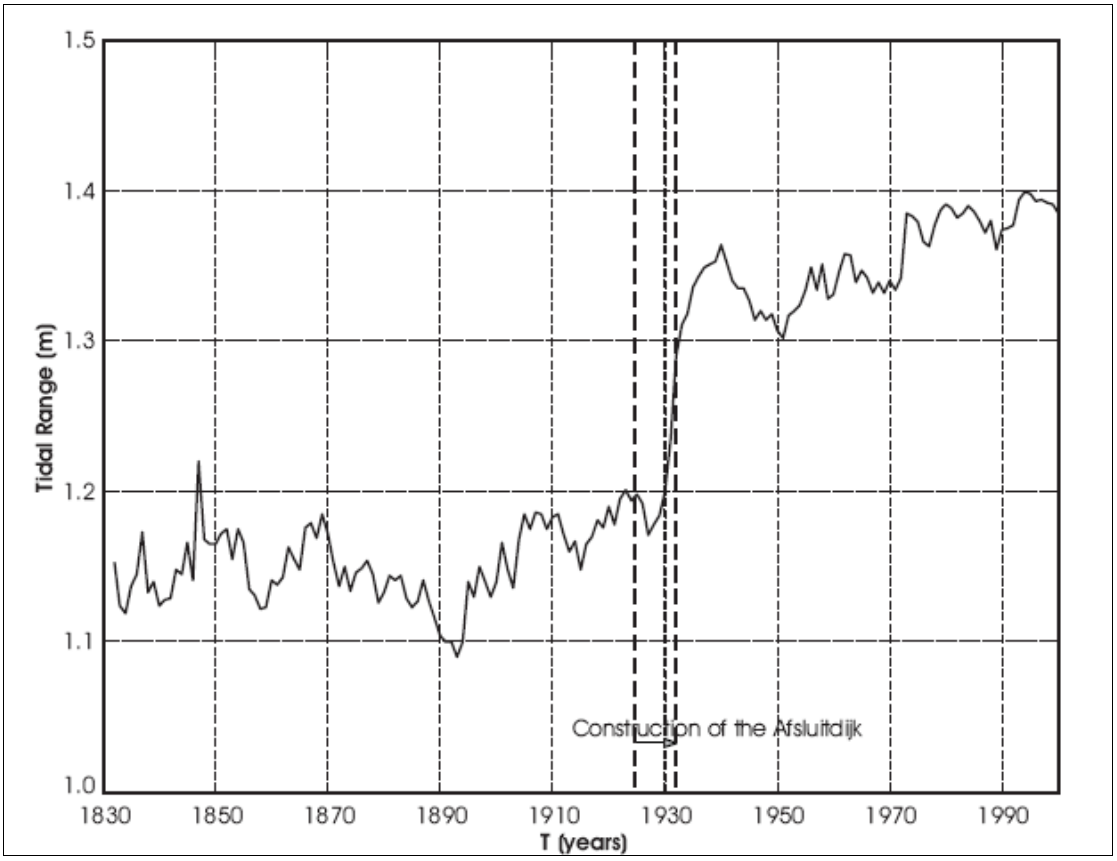

Figure 3-5: Tidal range station Den Helder measured over the period 1830 - 2000. (Elias et. al, 2003b)

Alterations in tidal range and tidal volumes were predicted and have occurred. The increase in tidal range is clearly reflected in figure 3-5 by the water level observations of the measuring station Den Helder, located in the Texel inlet gorge. The tidal ranges increased nearly instantaneously with approximately 15%. This corresponds reasonably with the 21% increase predicted by Lorentz et al. (1926). At the location of the Afsluitdijk in Den Oever, the increase in tidal range was even more dramatic as an increase of nearly 100% was observed and predicted (Thijsse, 1972).

In addition to this increase in tidal range, the changed flow patterns in the basin must have contributed to the large changes in hydrodynamics and morphodynamics of the basin. The closure resulted in closing of the southward flow channels. Consequently, these channels lost their effective function, while flow through eastward channels increased. This latter flow was further enhanced by the eastward deflection of the tidal wave at the closure dam (figure 3-3, right panel). The two tidal waves originating from Texel and Vlie inlet now meet east of the original meeting point, at the location of Harlingen, forming a tidal divide. This eastward extension resulted in an actual drainage area that is slightly larger than the active part of the drainage area prior to the closure (Klok and Schalkers, 1980).

The analysis shows that most of the former Zuider Sea did not actively take part in the water exchange with the Wadden Sea. The basin area after the closure is at least comparable with the active basin area prior to closure. Combined with the enlargement of the tidal range an increase in tidal prism of about 26% was observed (and predicted).

With these large changes in hydrodynamics and particularly in geometry, pronounced changes in basin morphology have occurred. This cause and effect can be deducted from empirical relations. Prior to the closure, it is plausible that the basin was in an equilibrium state and the size of the inter-tidal shoal area was related to the drainage area (Eysink et al., 1992; Louters and Gerritsen, 1994). With the closure, the back part of the basin (Zuider Sea) that contained a relative large portion of shoals was separated from the basin. The remaining shoal area was too small relative to the area of the channels; therefore, a morphologic adjustment of the basin was to be expected during the initial stage of non-equilibrium after the closure.

The basin forms part of a coherent morphological system (De Vriend, 1996). The changes in hydrodynamics and morphodynamics of the basin must have had effects on the other parts of this system (e.g. the ebb-tidal delta and adjacent coastlines). For instance, Walton and Adams (1976) showed the direct correspondence between an inlets tidal prism and the volume of sand comprising the ebb delta shoals. The observed changes in tidal prism must have influenced the ebb-tidal delta. The morphological system can also be described as a sand-sharing system. By definition, all parts of such a system are coupled, and in dynamic equilibrium with each other under constant forcing. Changes in forcing or geometry of any part of the system result in sediment transport to or from other parts of the system (Oost, 1995)."

3.3 Equilibrium in Wadden See

Elias et. al. (2003b) based on theoretical knowledge and analysis of bathymetry data, introduce a conceptual model for development of Wadden Sea tidal basins after the large scale human intervention, basically the closure of Zuider Sea. This model is shown in the following figure.

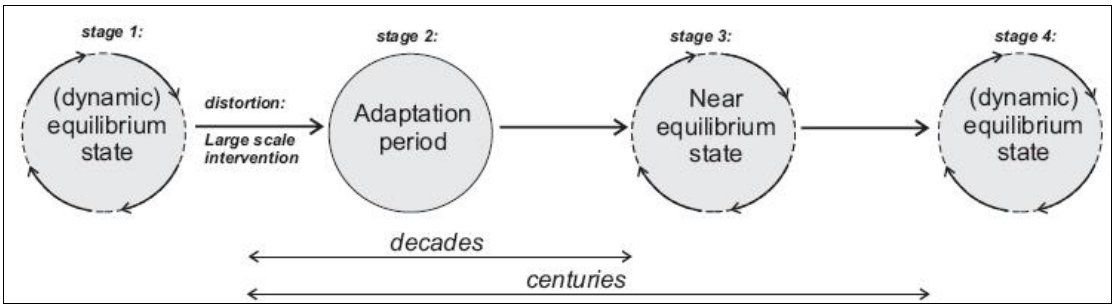

Figure 3-6: Conceptual model for Wadden Sea tidal basins. (Elias, 2006)

This model describes the morphological development of Wadden Sea in four different stages. In stage one, which is before the human intervention, it is assumed that the whole system of Wadden Sea is in a dynamic equilibrium. In this stage the characteristics of morphological elements of tidal basins can be described with empirical relations (e.g. Walton and Adams, 1976; De Vriend and Ribberink, 1996; Buonaiuto and Kraus, 2003; Gerritsen, 1990; Eysink et al., 1992; Louters and Gerritsen, 1994). This dynamic equilibrium, disturbed with the effects of closure of Zuider Sea. Since the part of Zuider Sea, which was closed by the Afsluitdijk, was part of basin of tidal system, the closure must be manifested in other parts of the system. Stage two is the period of large changes. In this

stage the natural behavior of the tidal basin systems is dominated by the human intervention. Therefore the empirical relations of equilibrium can not describe the morphological development of the tidal basin systems. This stage called ‘adaptation period’ has the time scale in the order of several decades, and leads the system to reach a stage of ‘Near Equilibrium state’. In this stage (stage 3), the adaptation continues but on a long-term time-scale. It means that although the yearly changes are small but they have potentially large impacts on long-term changes. Finally after centuries the whole system will gain its new dynamic equilibrium state, clearly different from its original one (Stage 4).

It seems that the current condition of the Dutch Wadden Sea is somewhere at the end of stage 2 and beginning of stage 3.

3.4 Western Dutch Wadden Sea

In the western part of the Wadden Sea (study area of this research) there are three tidal inlets. These three tidal basins, from west to east, are Marsdiep, Eierlandse gat and Vlie. The tidal inlet of the Marsdiep basin and its ebb-tidal delta is called Texel inlet. In this section some characteristics of these inlets are discussed.

3.4.1 Tides in Wadden Sea

The vertical tidal motion along the coast of The Netherlands as well as in the Wadden Sea is generated from the tidal wave from the Atlantic Ocean, entering the North-Sea from North (between the Norway and Scotland) and from the south west (through the Calais Straight). These two waves interfere with each other and under the effect of Coriolis force and bottom friction, generate a complicated tidal flow pattern in the south of North-Sea. As it is shown in the figure 3-7 tides in south of North Sea propagates from west to east rotating counter-clock wise around the amphidromic points.

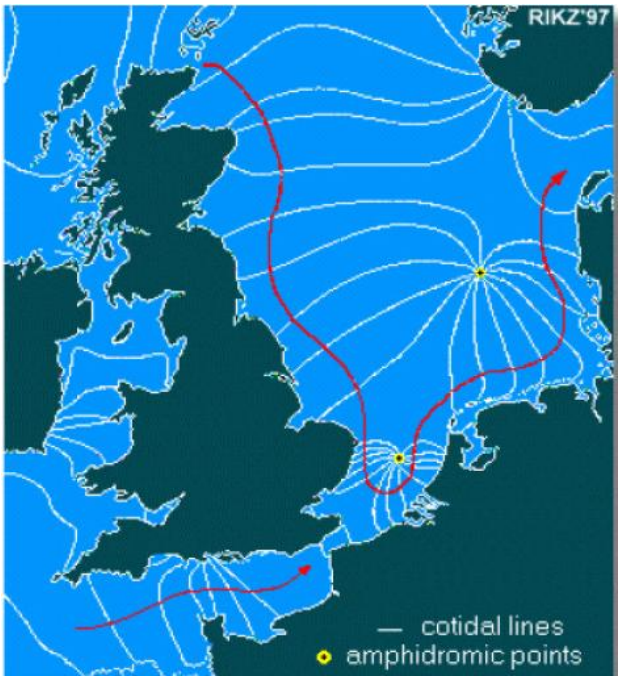

Figure 3-7: Propagation of tide in North-Sea (www.gtij.nl)

Along the Dutch coast the tide is a composition of standing and progressive wave, propagating from south to north, with the tidal current velocity of 0.5-1.0 m/sec (Elias, 2006) this wave meets the second tidal wave near Marsdiep inlet (Texel). The merged tidal wave moves to the east along the islands of the Wadden Sea. The amplitude of the tide decreases along the Dutch coast until its minimum at Den Helder (the tidal observation point at the Marsdiep inlet) and then increases again along the Wadden Sea (figure 3-8). The tidal wave enters the Wadden Sea through the tidal inlets and damps there.

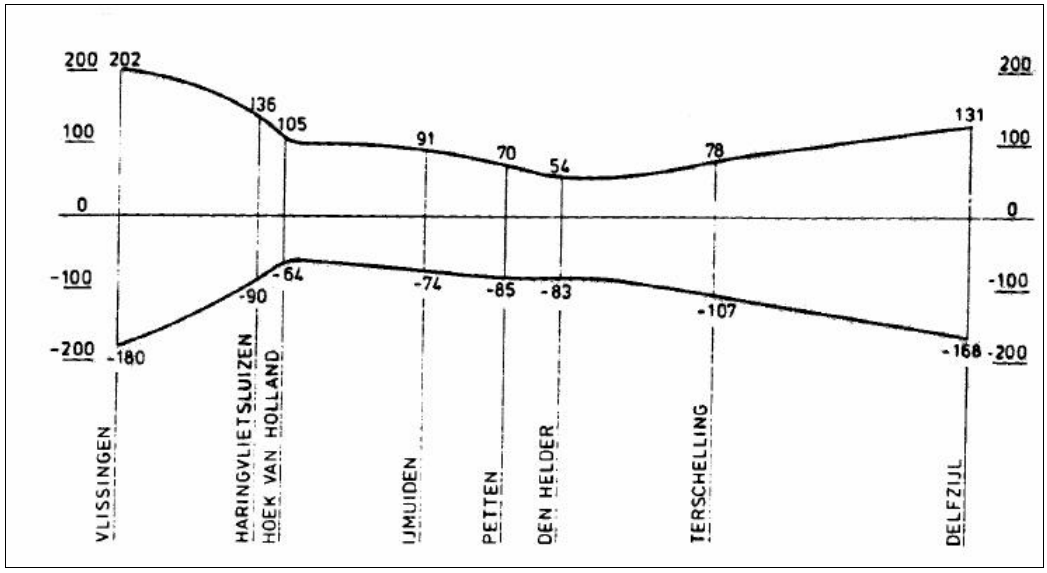

Figure 3-8:Variation of the tidal range along the Dutch coast (Van Der Spek and Noorbergen, 1992)

At the Marsdiep inlet the main dominant tidal component is M_2 and the maximum tidal current velocity in the Marsdiep is between 1.0 to 2.0 m/sec. The tidal asymmetry in Marsdiep is mainly due to distortion of the M_2 curve by M_4. The tidal range varies between 1.0 to 2.0 m with the mean value of 1.38m in Den Helder. (Elias, 2006). The tidal range increases to the mean value of about 2.0m in Vlie inlet.

3.4.2 Classification of tidal inlets in Wadden Sea

According to the classification of Hayes (1979) these inlets are classified as mixed-energy wave-dominated inlets, even under spring tide conditions. However, because of the large tidal prism and the relatively low wave energy, the morphology of the inlet shows tide-dominated characteristics such as a large ebb-tidal delta. (Davis and Hayes, 1984). Therefore it seems that the main force influencing the morphological changes of these basins is tide.

With respect to the channel and shoal patterns, these tidal basins in their new shape after the closure of the Zuider Sea are categorized as short basins and should have branching channel patterns but Marsdiep still hold its former shape of braided meandering channels.

3.4.3 Morphological characteristics of the basins and recent changes

The Dutch Wadden Sea is one of the best monitored coastal regions in the world. There are some depth measurements especially in Marsdiep from 16th centuries. Since 1987 Rijkswaterstaat (Directorate-General of Public Works and Water Management of The Netherlands) frequently measures the bed level in Wadden Sea. The ebb-tidal deltas are measured each 3 years, while the basins are measured each 6 years. RIKZ defined the borders between different basins and the data for each basin is stored in a 20 x 20 m resolution data base called 'Vaklodingen'. The available data before that time are less frequent and also less accurate; those data are stored in a 250 x 250 m grid. Also there are lots of water level measurements over the whole Wadden Sea. These data was/is being analyzed from morphological point of view (most recently, Elias, 2006, Wang et al., 2006 and Van Geer, 2007).

3.4.3.1 Sediment balance

It is found that in the Dutch Wadden Sea the trend of sediment transport is mainly from the ebb-tidal delta and coastlines into the basins. Wang et al. (2006) found that the Marsdiep and Vlie inlets show a decrease in ebb-tidal delta volume and an increase in the sand volume inside the basins. It is claimed in the literature that in a tidal basin system, the ebb-tidal delta and the basin are coupled sediment-sharing systems. It means that the sediment losses from the ebb-tidal delta should be deposited somewhere in the corresponding tidal basin. But Wang et al. (2006) showed that in the case of Dutch Wadden Sea it is valid for all the inlets together rather than the inlets individually. For example in the period of 1986-1997, total sediment loss from the ebb-tidal deltas is 95 Mm^3 while 105 Mm^3 of sediments is deposited in the basins. But if the individual inlets are considered, the sand volume in the ebb-tidal delta of Marsdiep is decreasing extensively, while the sediment volume inside the basin does not change remarkably. On the other hand in the Vlie the volume of ebb-tidal delta remains almost constant after 1990 but the volume of sand inside the Vlie basin increases more than 100 Mm^3(Wang et al. 2006). So it seems that tidal basins are exchanging sediment. . It is suggested that unlike two other basins Eierlandse Gat basin is more or less in an equilibrium condition. Figure 3-9 shows the changes in the sediment volumes inside the basins and ebb-tidal deltas.

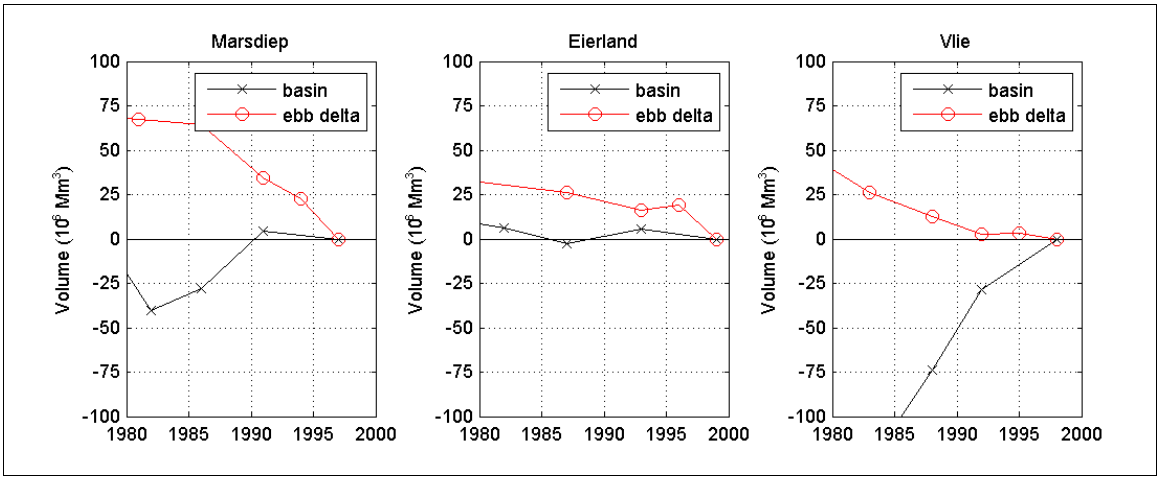

Figure 3-9:Detail of the recent changes in sediment volume of the Western Wadden Sea inlets (Wang et al. 2006)

3.4.3.2 Morphology changes

The morphological changes of the Wadden Sea due to the changes of sediment volumes in the basins and ebb-tidal delta after the closure of Zuider Sea are shown in the figure 3-10.

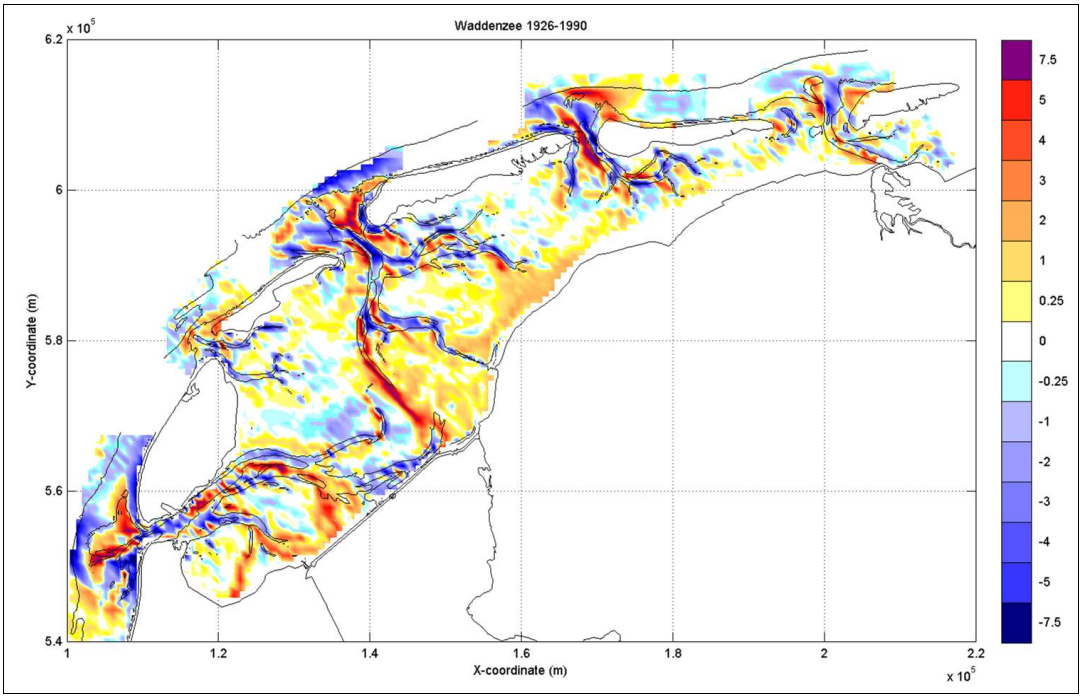

Figure 3-10:Sedimentation-erosion patterns in Wadden Sea in the period of 1926-1999 (Wang et al. 2006)

The changes in the Wadden Sea after the closure of the Zuider Sea are more pronounced in the western part of the Sea. The terminal parts of the channels are accreted very fast and some shoals have became shallower (Wang et al. 2006).

Although there is sedimentation in the basins, the main pattern of channels and shoals did not change a lot in recent decades. The main channel of Marsdiep basin (Texelstroom-Doove Balg) keeps its eastward direction and becomes deeper. But there are some patches of sedimentation and erosion, which indicate lateral channel migration.(Wang et al. 2006)

At the boundary of Vlie basin there are some sedimentation patches related to the infilling of the channels going to the former Zuider Sea. Wang et al. (2006) Also the main channel of Vlie seems to migration laterally to the west.

3.4.3.3 Main characteristics of the basins

The data derived from the hypsometry of different basins based on the work of Wang et al. (2006) is shown in Table 3-1.

Table 3-1: Major parameters derived from the hypsometric data for Marsdiep, Eierlandse Gat, and Vlie

Basin	Marsdiep	Eierlandse Gat	Vlie
Area of Basin (km2)	688.63	149.34	656.80
Area of channels (km2)	579.57	57.73	335.89
Volume of water under fixed HW (M m3)	3344.58	326.89	2217.34
Volume of water under fixed LW (M m3)	2249.13	123.72	1132.87
Tidal Prism (M m3)	1095.45	203.17	1084.47

Wang et al. (2006) also compared the current condition of the basins with the proposed equilibrium relations. For example the comparison with the Friedrichs and Aubrey graph is presented in the following figure.

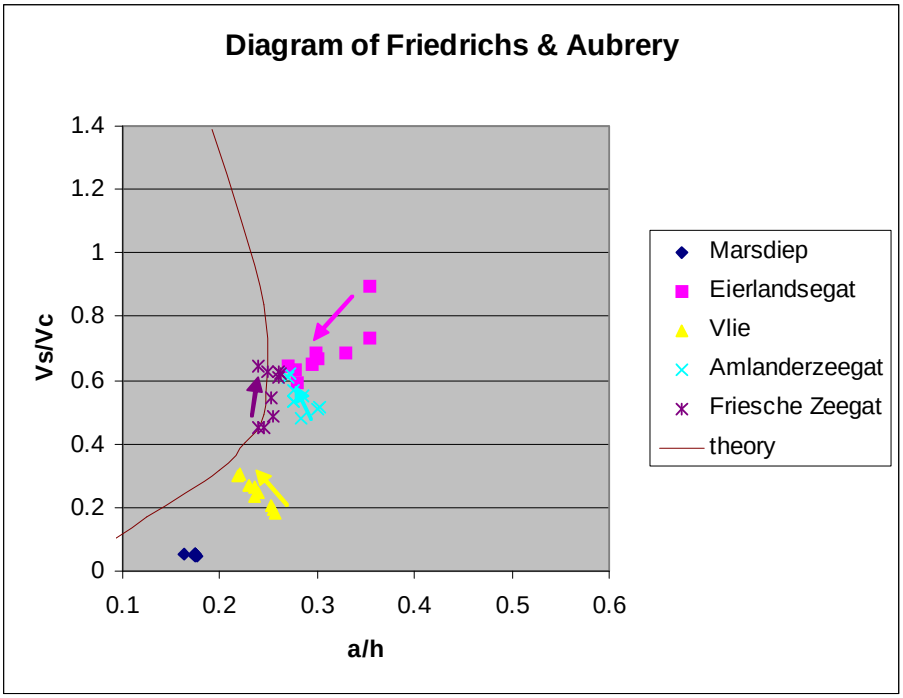

Figure 3-11: Current condition of the tidal basins in Wadden Sea on Friedrichs and Aubrey graph (Wang et al. 2006)

4 Model Setup

4.1 Model description

In order to fulfill the main goal of this study, to model the long-term morphological changes of Marsdiep and other tidal basins in the Western Wadden Sea, the Delft3D model is chosen as the main tool.

Delft3D is a finite-difference model, which simulates different processes on a curvilinear staggered grid. Different components of water level, water depth, and velocity are defined on different locations on the grid cells.

Delft3D model has been widely used in simulations of the wave propagation, currents, sediment transport, morphological development, and water quality in different locations in the world. (www.delftsoftware.wldelft.nl). Each process is simulated with a different module in the model and these modules can communicate with each other whenever it is needed.

The main processes to be modeled in this study are tidal current, sediment transport and bottom changes (morphological changes) . The flow chart of the modeling is presented in the figure 4-1.

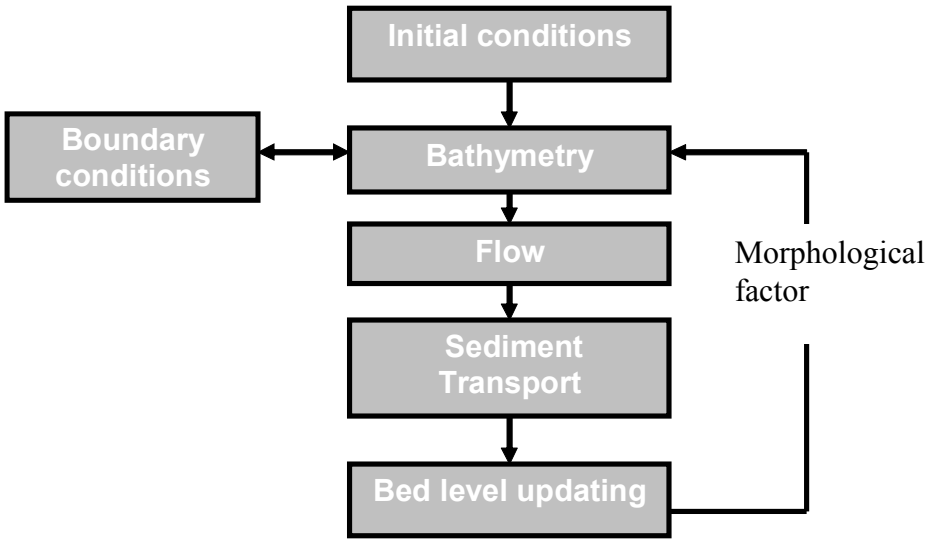

Figure 4-1: Flow chart of the modeling

The modules that solve the equation for these processes are described in this section briefly.

4.1.1 Flow

Delft3D flow module can model different type of currents such as tide and wind-driven flows (i.e. storm surges), stratified and density driven flows, river flows etc. In the case of tidal current the module computes unsteady flow from the tidal forcing based on the shallow water equations. If the simulation is depth-averaged (Introduced by 2DH in the figure 4-2, Delft 3D user manual, 2006), the depth-average equation of conservation of momentum will be as follows :

X- Direction :

$$\frac{\partial \bar{u}}{\partial t} + \bar{u}\frac{\partial \bar{u}}{\partial x} + \bar{v}\frac{\partial \bar{u}}{\partial y} + g\frac{\partial \zeta}{\partial x} + c_f \frac{\bar{u}\left|\sqrt{\bar{u}^2 + \bar{v}^2}\right|}{h} - \nu\left(\frac{\partial^2 \bar{u}}{\partial x^2} + \frac{\partial^2 \bar{u}}{\partial y^2}\right) - fv = 0$$

Y-Direction :

$$\frac{\partial \bar{v}}{\partial t} + \bar{v}\frac{\partial \bar{v}}{\partial y} + \bar{u}\frac{\partial \bar{v}}{\partial x} + g\frac{\partial \zeta}{\partial y} + c_f \frac{\bar{v}\left|\sqrt{\bar{u}^2 + \bar{v}^2}\right|}{h} - \nu\left(\frac{\partial^2 \bar{v}}{\partial x^2} + \frac{\partial^2 \bar{v}}{\partial y^2}\right) + fu = 0$$

and the depth-averaged continuity equation is given by:

$$\frac{\partial \zeta}{\partial t} + \frac{\partial h\bar{u}}{\partial x} + \frac{\partial h\bar{v}}{\partial y} = 0$$

These relations are solved simultaneously with a finite-difference scheme.

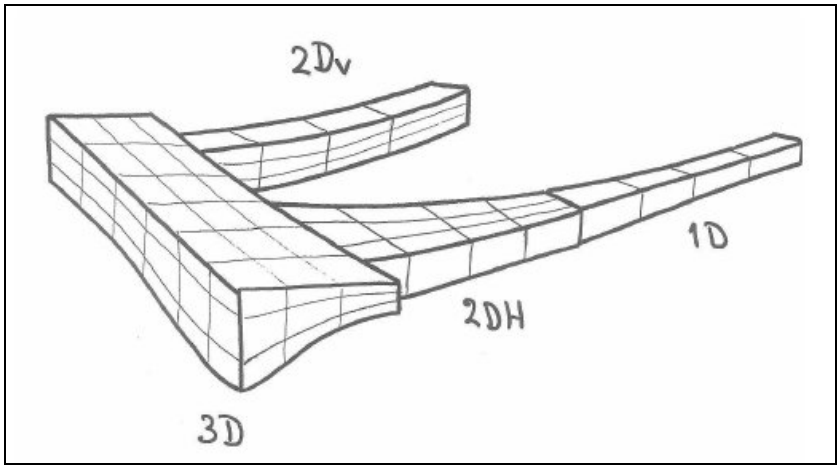

Figure 4-2: Different types of model in terms of dimension (Delft hydraulics, Delft-3D user manual, 2006)

4.1.2 Drying and flooding

One of the most important phenomena that should be taken into account in the modeling of tides especially in tidal basins with shallow flats is the drying and flooding of the flats. In Delft3D model, the process of drying and flooding is simulated by deactivating the 'dry' grid points from the flow domain when the tide falls and by reactivating them when they become 'wet' in the rise of tide. A dry point is defined by a threshold water depth (e.g. 0.1 m). If the water depth in a velocity point is less than this threshold that point is considered to be dry and the velocity is set to zero. If the water level in this point rises to twice the threshold value the grid node at this point will be reactivated in the flow domain. (Delft 3D user manual, 2006)

4.1.3 Sediment transport

In order to calculate the sediment transport, Delft3D can use a large variety of empirical sediment transport relation for bed load, suspended load and total load for both cohesive and non-cohesive sediments such as Engelund-Hansen, Meyer-Peter-Muller, Van Rijn (1984), Ribberink-Van Rijn, Van Rijn (2003), etc. (Delft 3D user manual, 2006).

In the current study there are no wave forces involved and the sediment is mainly sandy so the Engelund-Hansen sediment transport relation for total bed load is applicable. This relation is as follows :

$$S = S_b + S_s = \frac{0.05\alpha U^5}{\sqrt{g}C^3\Delta^2 D_{50}}$$

In which

U [m/sec] : Magnitude of flow velocity
Δ [-] : Relative density
C [$m^{0,5}$ /sec] : Chézy friction Coefficient
D_{50} [m] : Median grain size
α [-] : Calibration coefficient (*O(1)*)

4.1.4 Effect of bed slope on sediment transport

Bed-load transport is affected by bed level gradients. There are two different slope directions. First the bed slope in the initial direction of transport (longitudinal bed slope) and second the bed slop in the direction perpendicular to that (transverse bed slope).
The 'longitudinal bed slope effect' changes the magnitude of the sediment transport vector in the same direction of initial sediment transport while the 'transverse bed slope effect' changes the transport towards the direction of slope by either a rotation of the transport vector or by adding a transverse transport component (Delft 3D user manual, 2006).

For adjustment of the sediment transport rate due to longitudinal bed slope effect Bagnold (1966) suggested the following relations:

$$\vec{S'} = \alpha_s \vec{S} .$$

with:

$$\alpha_s = 1 + \alpha_{bs} \left[\frac{\tan(\phi)}{\cos\left(\tan^{-1}\left(\frac{\partial z_b}{\partial s} \right) \right)\left(\tan(\phi) - \frac{\partial z_b}{\partial s} \right)} - 1 \right]$$

In which:

S : Initial sediment transport vector
S' : Adjusted sediment transport vector for longitudinal bed slope effect
Φ : Initial angel of friction of bed material
α_{bs} : User defined tuning parameter.
$\frac{\partial z_b}{\partial s}$: Bed slope in the direction of initial sediment transport

The transverse bed slope effect is taken into account by implementing the Ikeda (1982, 1988) suggestion:

$$S_n = \left| S' \right| \alpha_{bn} \frac{u_{b,cr}}{\left| \vec{u_b} \right|} \frac{\partial z_b}{\partial n}$$

In which:

S_n : Additional sediment transport vector in the direction perpendicular to the initial direction of sediment transport. (Figure 4-3)
S' : Adjusted sediment transport vector for longitudinal bed slope effect
α_{bn} : User defined tuning parameter.
$U_{b,cr}$: Critical current velocity near bed
$\frac{\partial z_b}{\partial n}$: Bed slope perpendicular to the direction of initial sediment transport

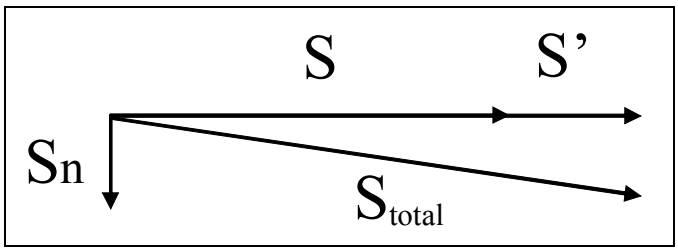

Figure 4-3: Effect of bed slop on sediment transport

4.1.5 Bed level update

In each time step after determining the sediment transport, bed level variation is determined based on the sediment transport fields using a sediment conservation model, which solves bed level continuity equation:

$$(1-\varepsilon)\frac{\partial z_b}{\partial t}+\frac{\partial S_x}{\partial x}+\frac{\partial S_y}{\partial y}=T_d$$

In which:

(S_x,S_y)	: Sediment transport components
z_b	: Bed level
ϵ_{por}	: Bed porosity, generally equal to 0.4
T_d	: Deposition or erosion rate (of suspended sediment/silt)= 0 in the current study

4.1.6 Morphological modeling approach

The approaches which are employed in Delft3D software to model the morphology changes are the 'online' and 'parallel online' approaches, described in section 2.4.3. The morphological factor should be defined by user. In this study the 'online' approach with the morphological factor of 300 is used.

Another feature which is used in morphological modeling is 'Erosion of dry cell'. The conventional schemes to solve the flow and sediment transport processes do not let dry cells close to the flow to be eroded, even if a deep score hole develops close by. In the flow module of Delft3D a new algorithm is implemented that can distribute the erosion volume over the wet cells and adjacent cry cells according to a pre-defined percentage, till the dry cell is eroded enough to considered as wet cell. In the current study this switch is ON with the value of 1.0. It means that in the case of erosion of a wet cell adjacent to dry cells all the erosion is assigned to the adjacent dry cell (Delft 3D user manual, 2006). This is shown in the figure 4-4.

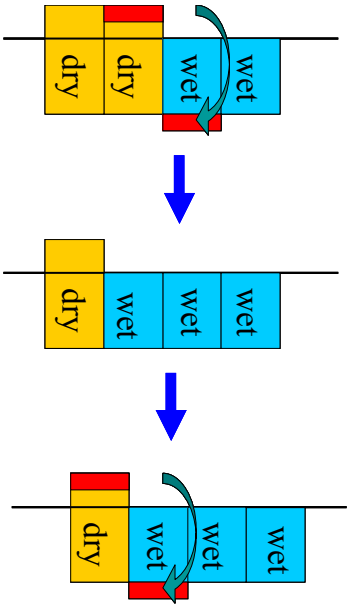

Figure 4-4: Visualization of dry cell erosion

4.2 Grids

A local model for the Western Dutch Wadden Sea should be set up. Although the main area of interest is Marsdiep, Eierlandse Gat and Vlie, to avoid the effect of boundaries, the model is extended to tidal divide between Ameland and Frisen basins. In this study it was necessary to set up a model with a reasonable computational time that can simulate long-term (~ 2000 years) morphological changes. So the grid sizes should be as large as possible. On the other hand the grid size should not distort the results. The validity of the results is more important at the tidal inlets. In the inlets there should be enough grids to avoid the effect of the land boundaries on the results. In this study the average spacing between grid lines is about 500 m. The grid cells are inside the basins and they are much bigger at the offshore boundary. The grid mesh covers only the area under the high water and the other parts of the barrier islands are excluded from the model. Based on these considerations two different grid meshes are made: Grids A and B (Figure 4-5 and 4-6)

Grid A is a numerically developed grid with the same rate of increasing in grid size through out the model with almost the same size of grid in all the inlets and without any refinement of grids.
Grid B is based on the coastlines of the islands and the grid lines are smoothed along the islands and inlets the main characteristics of both grids are compared in Table 4-1.

Table 4-1: Grids characteristics

Grid name	No. of nodes in M direction	No. of nodes in N direction	No. of Grid cells
A	78	161	9130
B	70	127	6876

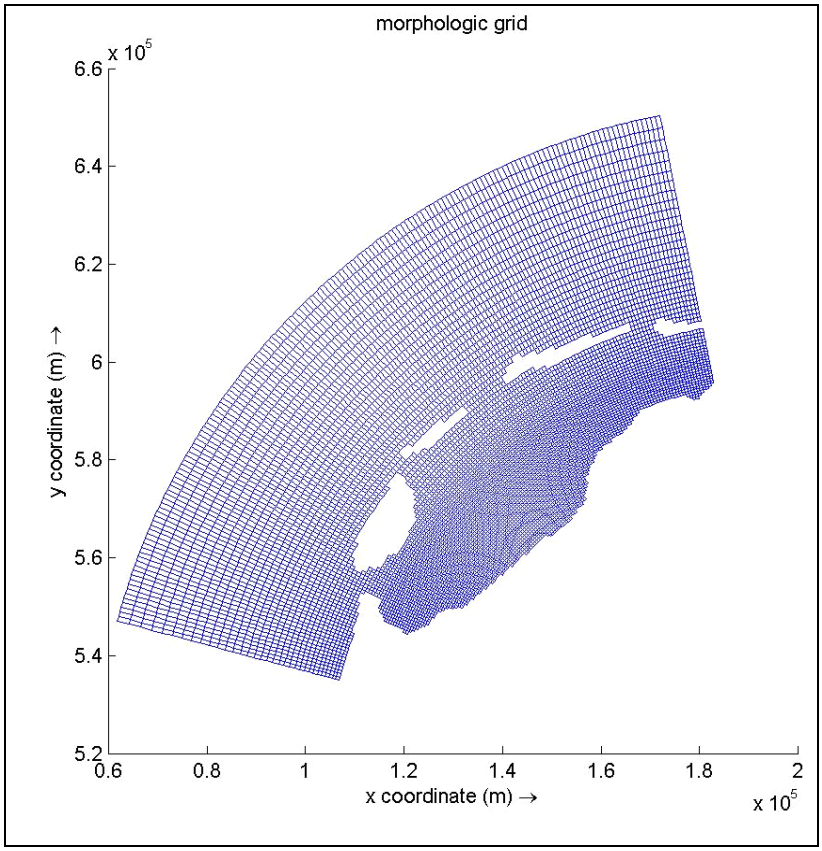

Figure 4-5: Hydro-Morphological grid A

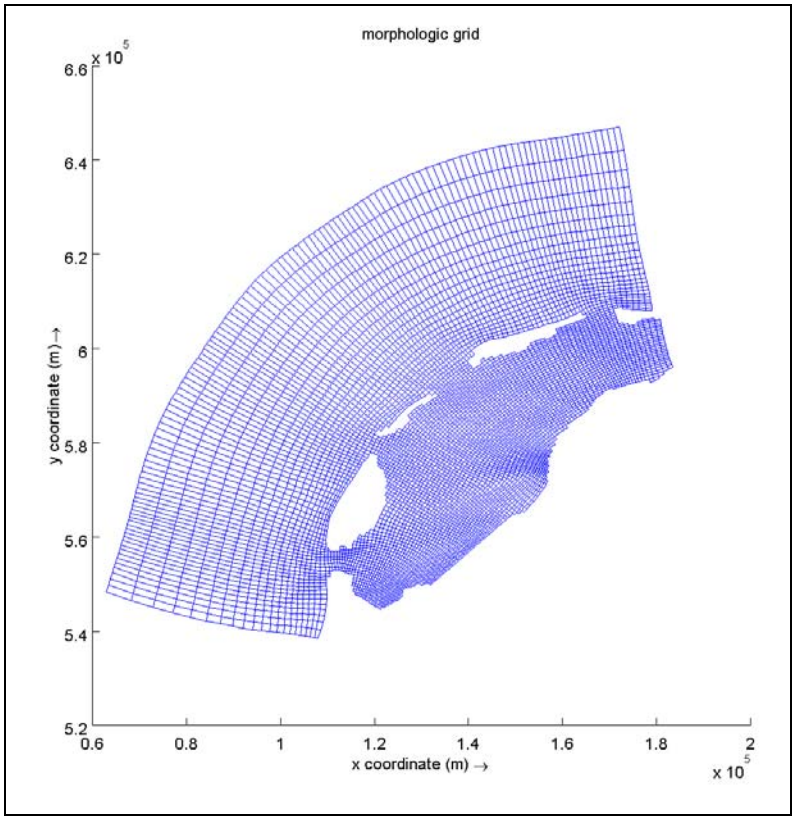

Figure 4-6: Hydro-Morphological grid B

The main difference of these two grids is shown in figure 4-7 for the modeled Texel inlet. As it is clear in Grid A the grid lines are not perpendicular to the inlet entrance and the deviation of grid lines from the coastline is obvious.

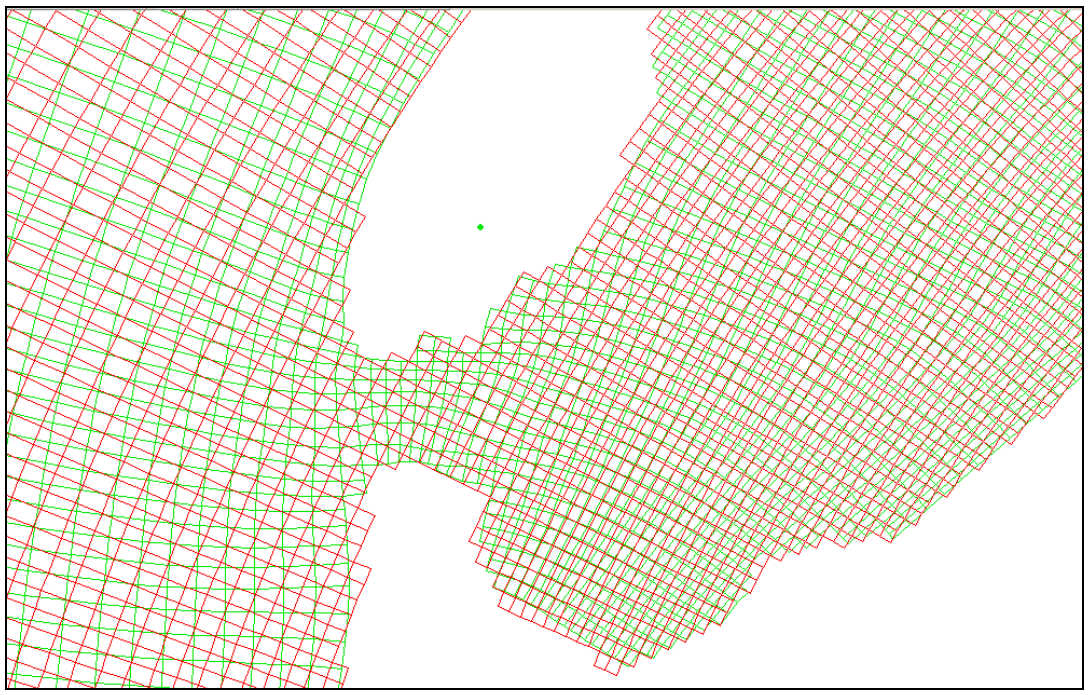

Figure 4-7: The grid lines at the Texel inlet A in red and B in green

To check the effect of the grids on the results, two relatively short models (60 years of morphological time) are carried out with an imaginary flat bathymetry inside the basins. The morphology of the Texel inlet at the end of 60 years is shown in the figures 4-8 and 4-9.

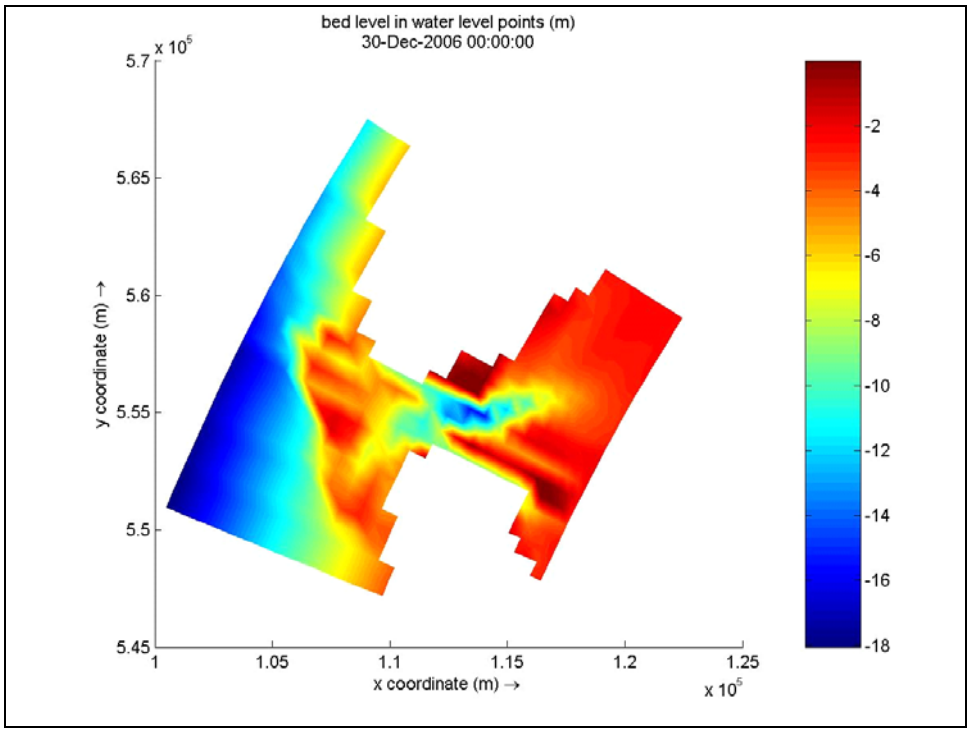

Figure 4-8: The Texel inlet after 60 years of morphological modeling with grid A

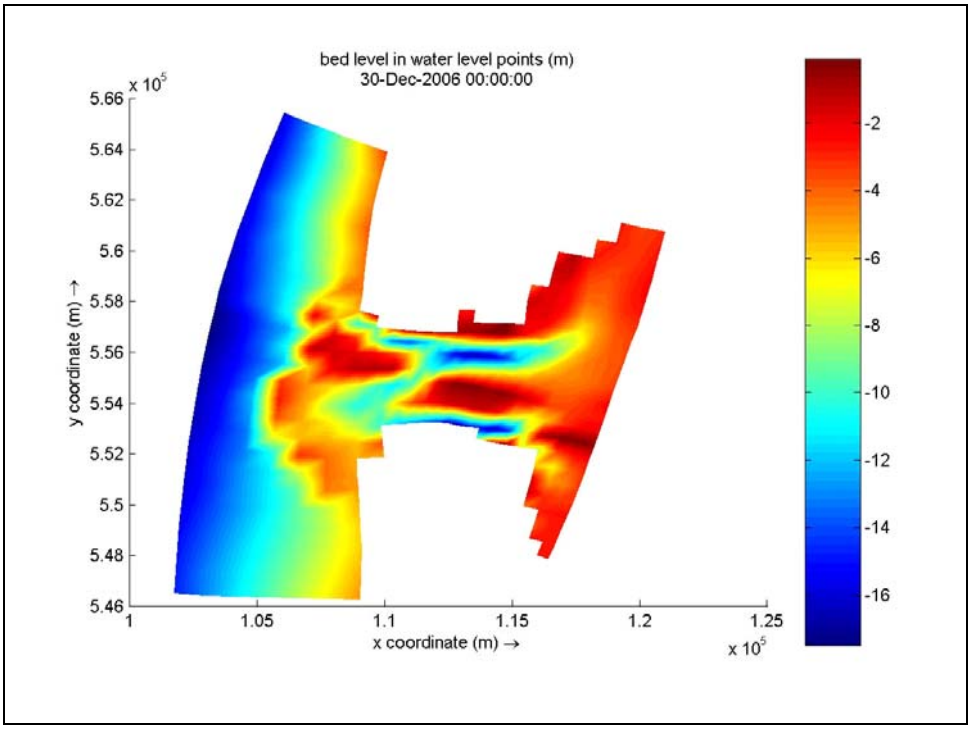

Figure 4-9: The Texel inlet after 60 years of morphological modeling with grid B

It is clearly observed that the orientation of the grid lines with respect to tidal inlet has an effect on the result of the model, so grid B is used for this study.

4.3 Forcing

The main forces acting on a hydro-morphological model for coastal regions are tides, wind, waves and wind and wave setups. But in the long – term morphological evolution of the tidal basins the tidal asymmetry has the main role, so in this study only the tidal forces are modeled.

In order to determine the values for the boundary condition of this local model, a calibrated model for the vertical tide in North Sea, called 'ZUNO', is used.

The 'ZUNO' model is based on the 'Zuidelijke Noordzee model' from the Dutch Ministry of Public Works and constructed by WL Delft Hydraulics. A detailed description of the calibration and validation of the model can be found in Roelvink et al. (2001).

The 'ZUNO' model has approximately 20,000 computational grids. In the coastal zone the grid sizes are approximately 1.5 km alongshore and 400m cross-shore. The model is forced by the boundary conditions on two open boundaries. The Southern boundary situated south of the straight of Dover and the northern boundary between Scotland and the north of Denmark. At these boundaries water levels are specified as astronomic components by tidal constants, amplitudes and phases of tidal constituents. The calibration of the model was based on the comparing the water level resulted from the model and the reality. The ZUNO model is shown in the figure 4-10.

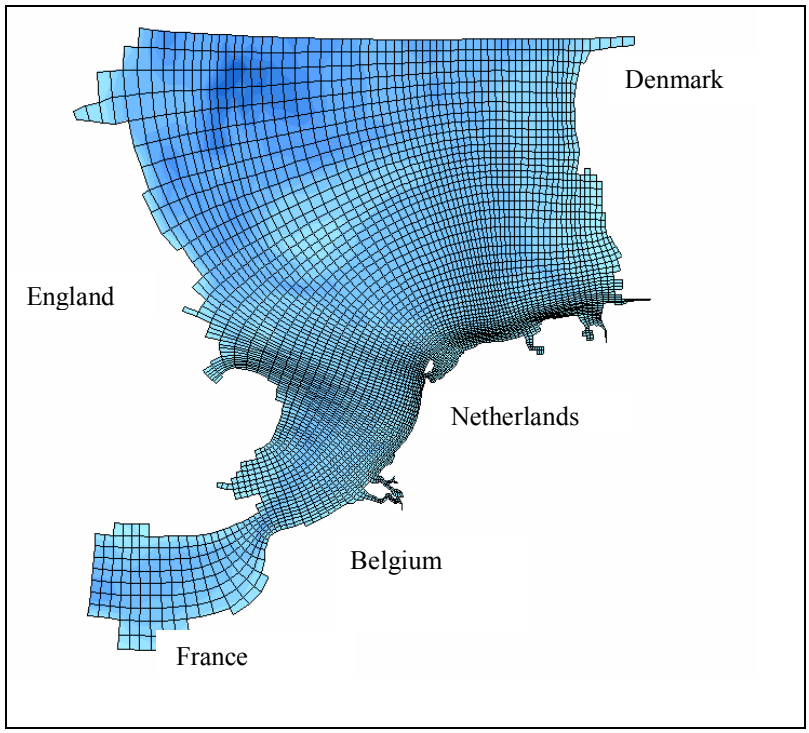

Figure 4-10: ZUNO model

Since the main tidal components to be taken into account are M components and most importantly M_2, in this study, Zuno model is run with the forcing boundary conditions of only M_2 and once with M_2, M_4 and M_6 for one year. During these runs the tidal level variations at the boundaries of local model are observed. The position of the local grid on the ZUNO grid is shown in the figure 4-11.

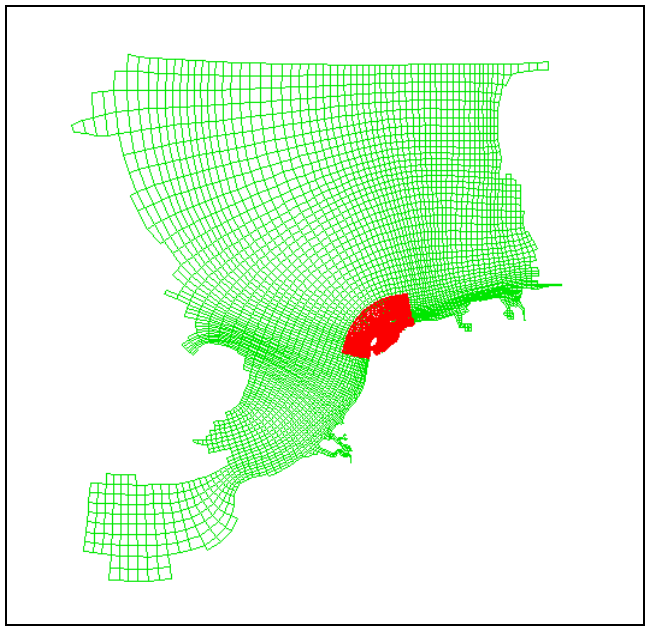

Figure 4-11: Position of the grid of local model on the ZUNO grid

Since the North Sea near the Dutch coast is relatively shallow it is expected that even in the ZUNO run with only M_2 component, some M_4 and M_6 generated as well. For both runs of

ZUNO model the recorded tidal variations at local model boundaries are analyzed and M_2, M_4 and M_6 are extracted for these boundaries. These components are used to form boundary conditions for the local model.

The boundaries for the local model consist of 3 boundaries: one boundary at the sea side and two other lateral boundaries. The sea side boundary is chosen to be a harmonic boundary, while the lateral boundaries are Neumann (water level gradient) boundary. Figure 4-12 shows the local model configuration.

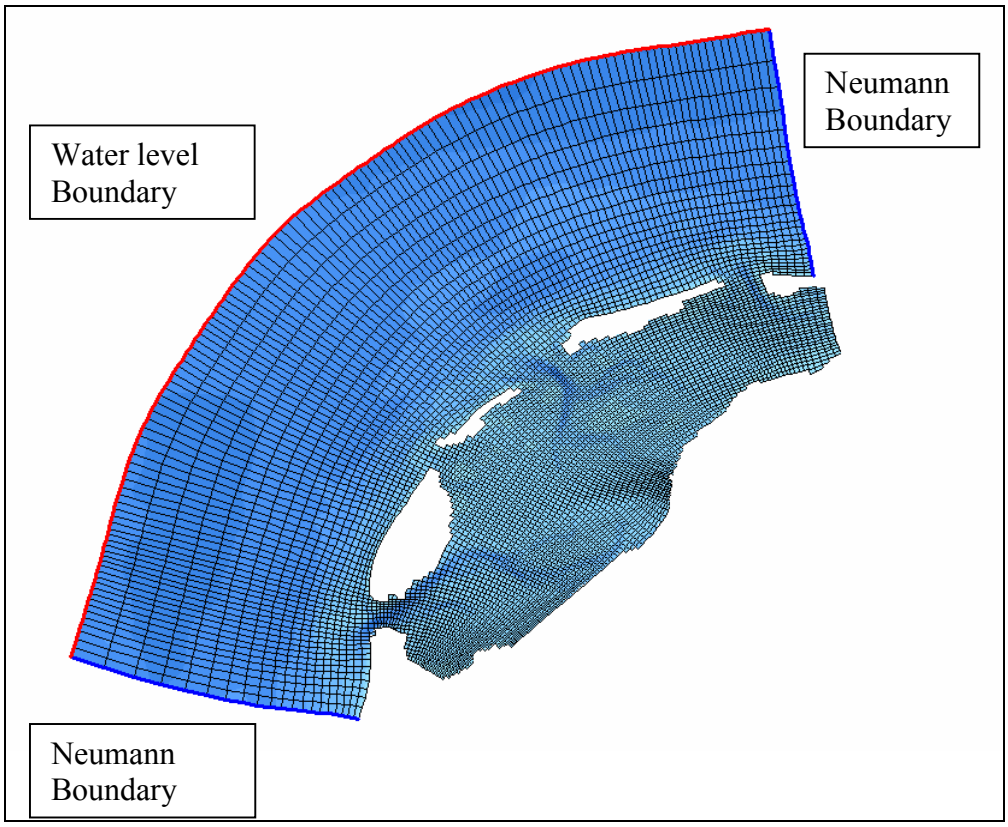

Figure 4-12: Local model boundaries

In order to choose the best forcing condition, the local model was carried out with 3 different boundary conditions and the real bathymetry of Wadden Sea in 1998. These boundary conditions are summarized in the following table.

Table 4-2: Tidal components used in different boundary conditions

Boundary condition name	ZUNO Model forcing	Local model forcing
ZM2-M2M4M6	M_2	M_2,M_4,M_6
ZM2-M2	M_2	M_2
ZM2M4M6-M2M4M6	M_2,M_4,M_6	M_2,M_4,M_6

In these runs the water level variation is observed in south of the Texel inlet (at the position of Den Helder) the tidal signals at this location are shown in the figure 4-13.

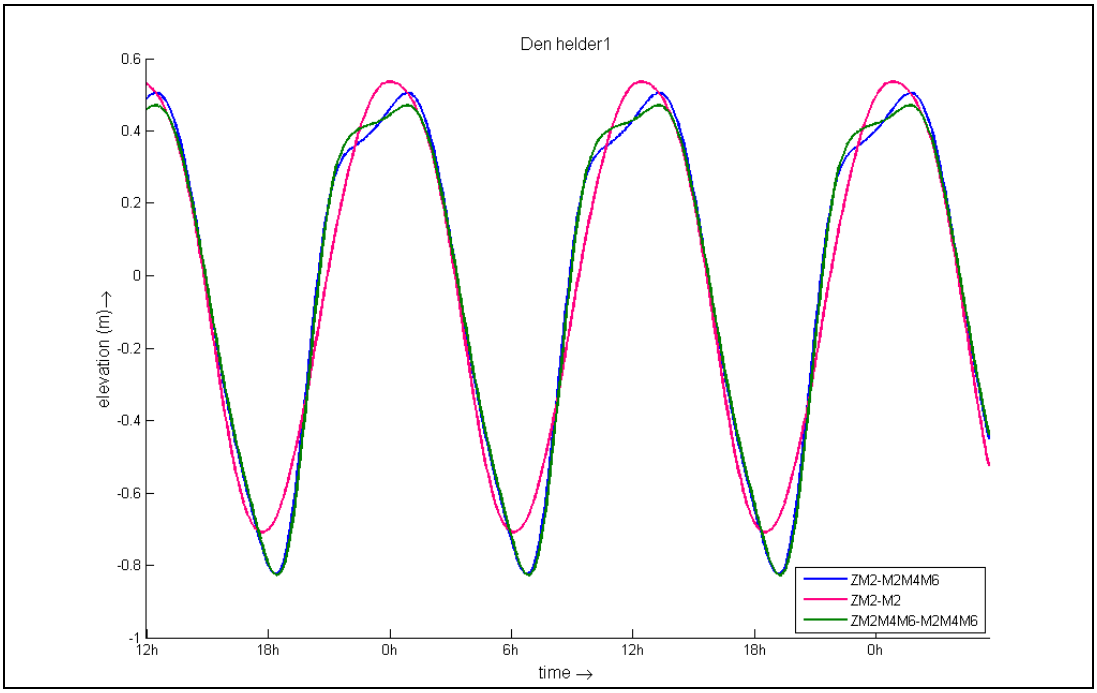

Figure 4-13: Tidal signal in south of Texel inlet (Den Helder) in local model for different forcing conditions

The observed tide in Den Helder in the local model is analyzed and compared with the result of ZUNO model and the measurements at the same station in table 4-3.

Table 4-3: Amplitude of tidal components in models compared to the measurements in Cm

Model	ZUNO Model		Local Model			Measurement
Forcing / Component	**M_2**	**M_2,M_4,M_6**	**ZM_2-M_2**	**ZM_2-$M_2M_4M_6$**	**$ZM_2M_4M_6$-$M_2M_4M_6$**	
M2	71.13	71.02	60.98	61.36	61.23	65.568
M4	15.12	15.85	4.89	12.86	13.42	10.885
M6	8.83	8.84	1.12	6.77	6.43	5.819

From the figure 4-13 and table 4-3, it is clear that the ZM_2-M_2 forcing condition can not represent the tide in front of the Texel inlet. Since the M_4 and M_6 component should be used in Zuno model forcing, it was decided to use these components in the local model too. Therefore $ZM_2M_4M_6$-$M_2M_4M_6$ forcing condition is used in most of the long simulations, however to show the effect of different forcing on the morphological changes one long-term simulation with ZM_2-M_2 is also carried out.

4.4 Sediment properties

In this study only one fraction of sediment is used. The sediment in the model is sand with D_{50} of 200 µm. This simplification prevents the channel bottoms from armoring and leads to some unrealistic deepening of channels. The effect of lack of armoring is decreased by limiting the available sediment in the model to the maximum expected depth of channels (45 m).

4.5 Bathymetry

The other parameter that can affect the hypothetical equilibrium condition of a tidal basin in a process-based model is the initial bathymetry. In this study beside the real bathymetry, two other types of schematized bathymetries also are modeled. The most important point in the choosing the bathymetries is the available sediment in the model. The amount of available sediment in all the bathymetries should be reasonably similar to the available sediment in real bathymetry.

4.5.1 Real bathymetry

For runs with real bathymetry, the bathymetry data for 1998 from RIKZ is used, this data is projected on the grid using triangulate interpolation. This bathymetry is shown in figure 4-14.

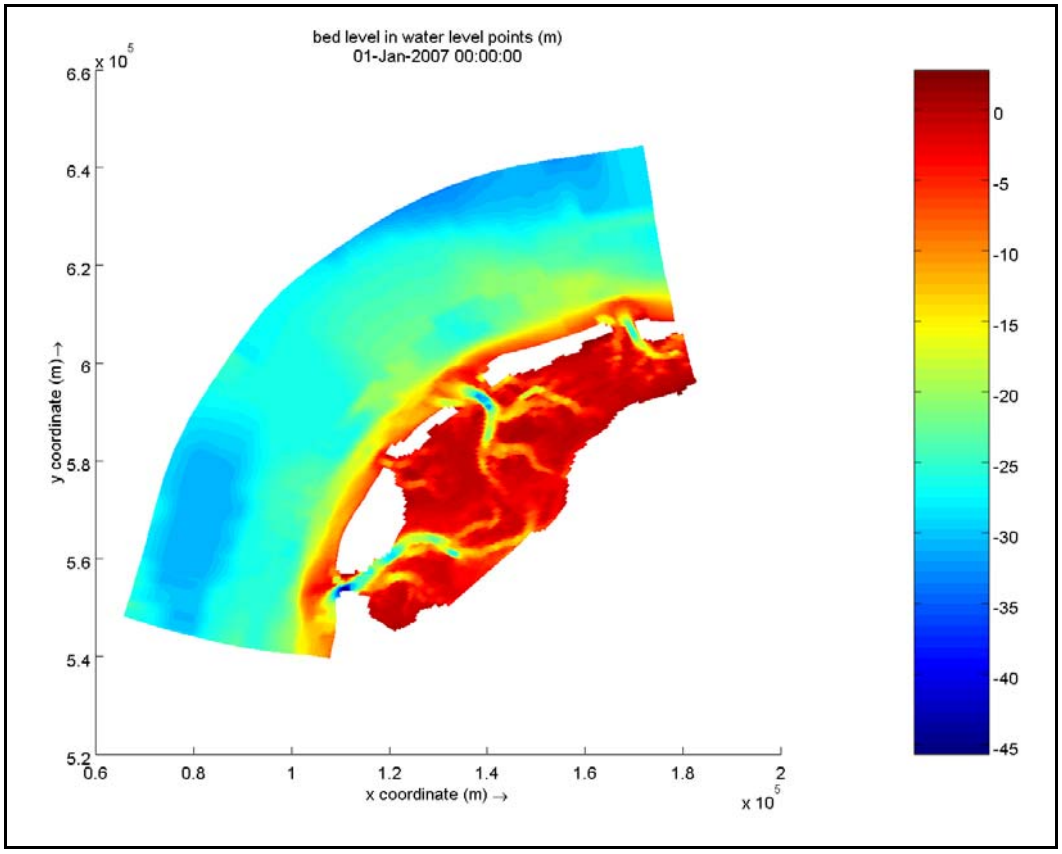

Figure 4-14: Bathymetry of 1998 projected on the grids

4.5.2 Flat bathymetry

An other interesting way to model a tidal basin is to use a flat bathymetry inside the basin without any kind of ebb-tidal delta outside the inlet and let the model to show the mechanism of building and changing the ebb-tidal delta out-side the basin and channel and shoal patterns inside. So it is decided to make some schematized bathymetries with flat bed inside the Wadden Sea. Following steps are taken to make such a bathymetry:

- Inside the Wadden Sea assumed to be flat
- The effects of tidal basins on the sea side such as ebb tidal deltas are omitted

- The slope of coastal shelf is made uniform
- The offshore side of the model is made flat

A sample of this bathymetry with the same depth scale of figure 4-14 is shown in figure 4-15.

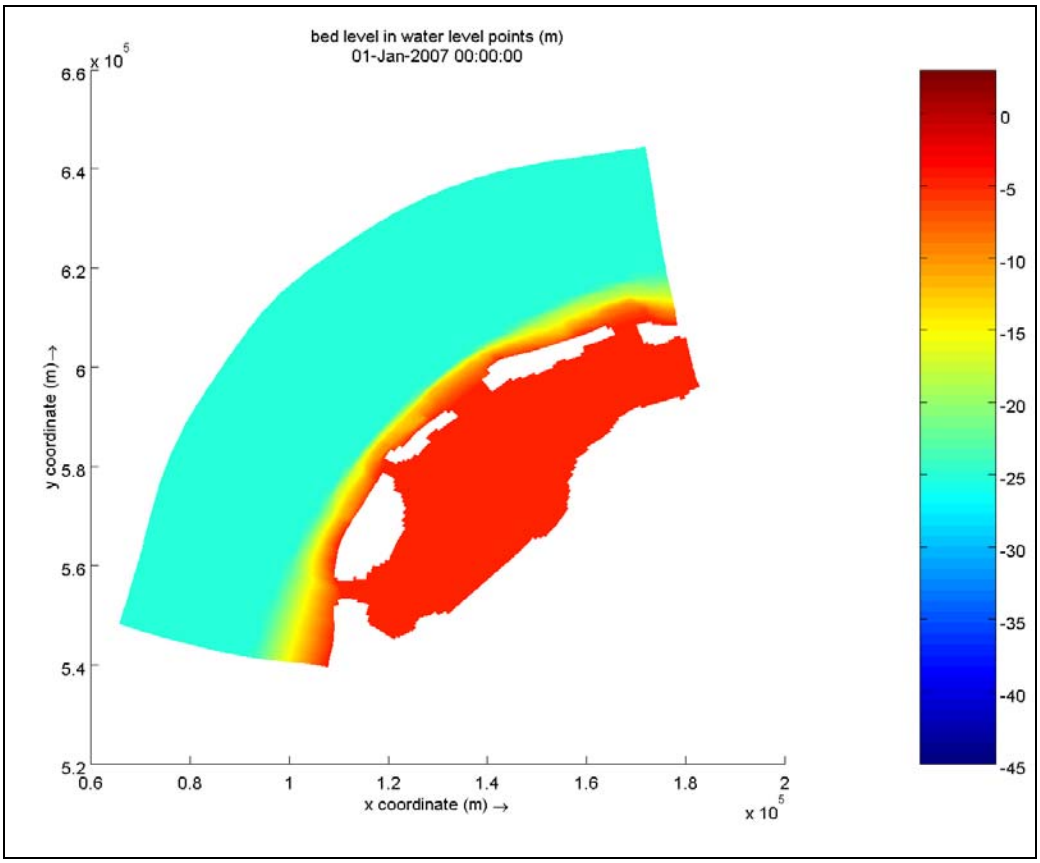

Figure 4-15: A sample of schematized bathymetry with flat bed level inside the Wadden Sea

To determine the depth of the flat Wadden Sea some analysis on available and distribution of the sediment inside the model has been done and based on different criteria, different depths are chosen:

- Depth = 3.62 : The volume of sediment inside the basins is equal to the real bathymetry plus the available sediment in the ebb-tidal deltas.

- Depth = 4.54 : The volume of sediment inside the basins is equal to the real bathymetry

- Depth = 5.02 : The volume of sediment inside the Marsdiep basins is equal to the real bathymetry plus the available sediment in its own ebb-tidal deltas (Texel island)

- Depth = 8.00 : The volume of sediment inside the basins is far less than the real bathymetry

4.5.3 Sloping bathymetry

During the attempts to model the morphological evolution of the tidal basins with a process based models in recent studies some times a sloping bathymetry toward the inlet is used as the initial bathymetry. In this study also, a schematized sloping bathymetry is made for the Wadden Sea. The procedure of this schematization is as follows.

- The tidal basins are separated based on the borders defined by RIKZ in 'Vaklodingen' data base.
- In each basin the depth of each grid point is plotted versus the distance from the middle point of the inlet.
- The depth of grid points are classified and averaged according to the distance from the inlet in 2.5 km groups.
- Using the average values, the depth of each point is defined as a function of the distance from the inlet.
- The available sediment of each ebb-tidal delta is distributed uniformly inside the corresponding basin.
- The slope of the coastal shelf is made uniform
- The offshore side of the model is made flat

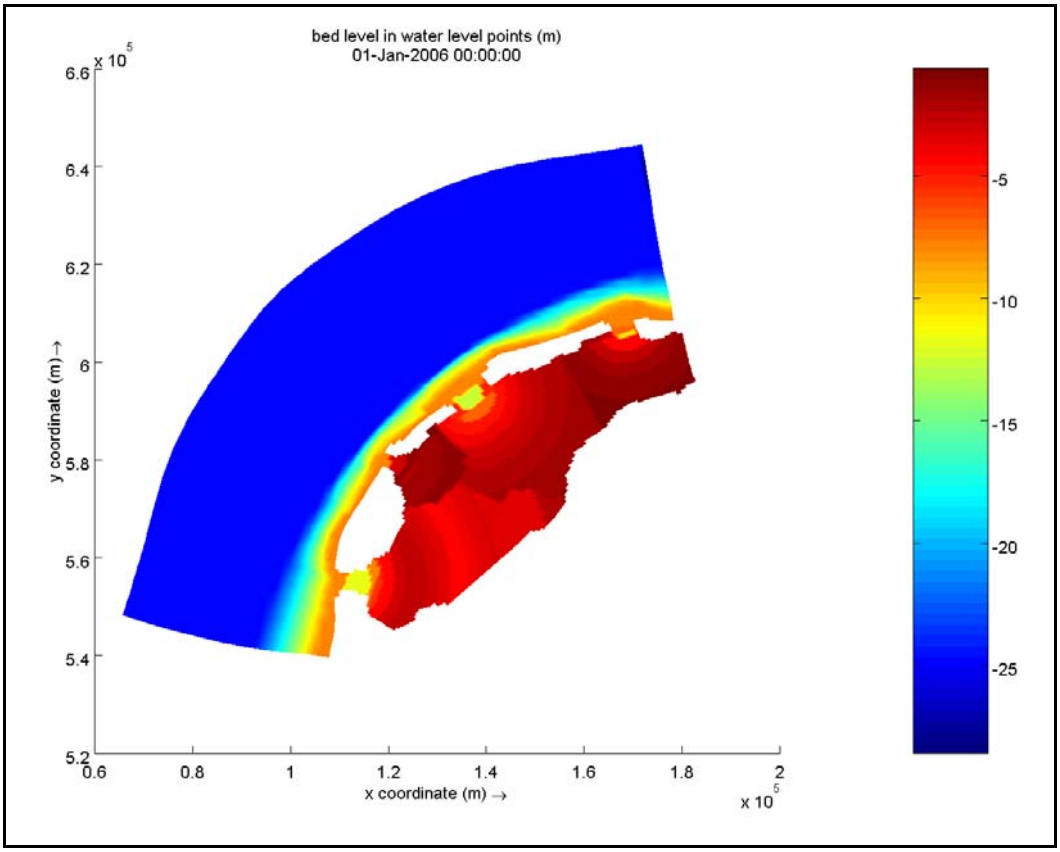

Figure 4-16: Sloping bathymetry

4.6 Sensitivity analyses on the transverse bed slope effect

One of the coefficients, which is shown to have an effect on the morphological modeling of tidal basins using Delft3D, is the tuning parameter of transverse bed slope effect (α_{bn}). It is shown that the default value of α_{bn} (=1.5) is not appropriate for the long-term simulations with large morphological factors (Thanh, 2006). Thanh (2006) suggested the value of 5 for α_{bn} in the modeling of morphological changes in an estuary by comparing the width of embayment in the model and an empirical relation. The initial simulations in the current study show that in this case even the value of 5 is not large enough yet. Therefore a sensitivity analyses is done for a model with the flat bathymetry as initial condition.

4 different values of α_{bn} are used for the model (5,10,20,50) and the simulations for 300 years of morphological time are carried out. Initial bathymetry for this runs are the flat bathymetry in Wadden Sea with the depth of 3.62.

Figure 4-17 shows that the final hypsometry of the Marsdiep basin does not change with changing the α_{bn} , so other characteristics of the basin should be taken into account to choose the appropriate value for α_{bn} .

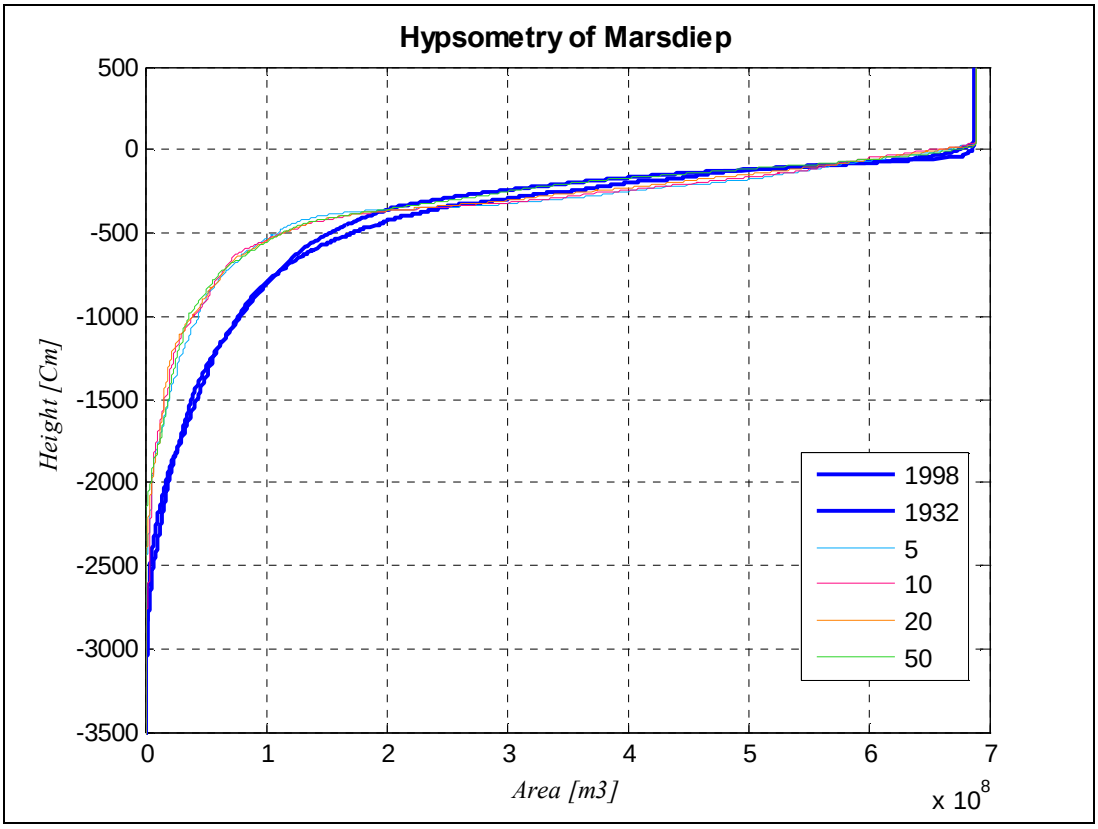

Figure 4-17: Hypsometry of Marsdiep basin in the runs with different α_{bn}

The cross section of the Texel inlet after 300 years of morphological modeling is shown in the figure 4-18. As it is shown in the figure 4-18 by increasing the α_{bn} the inlet tends to have only one main channel.

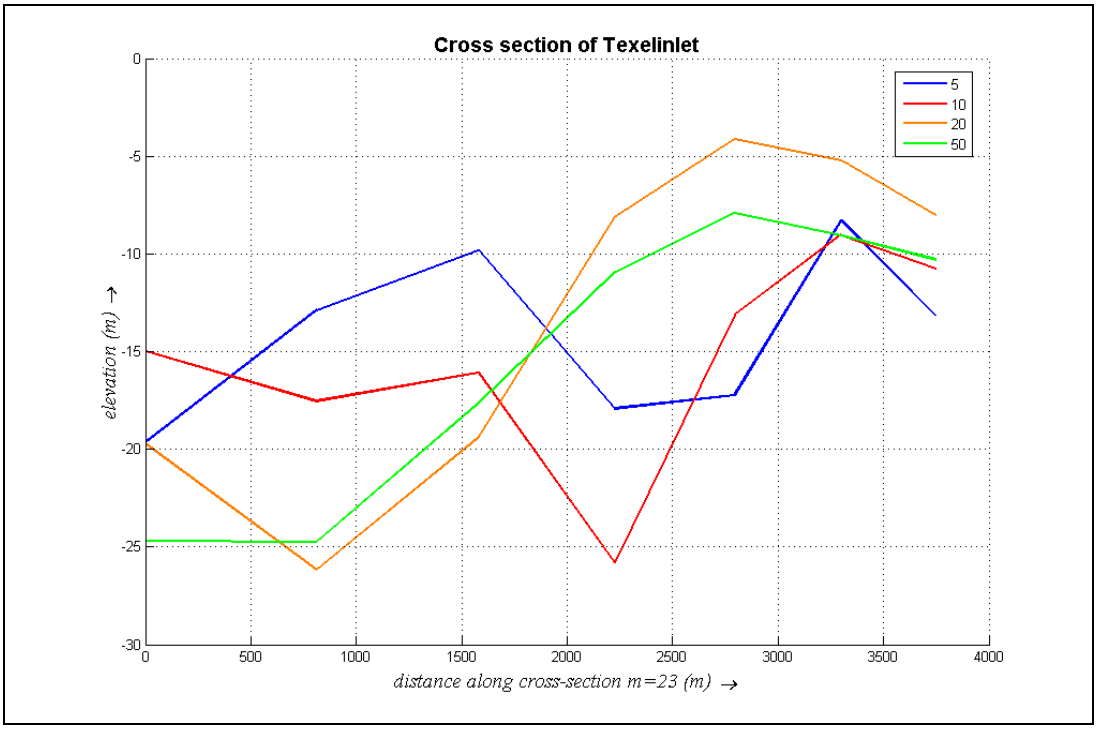

Figure 4-18: Cross section of Texel inlet in the runs with different α_{bn}

Clearly, by increasing α_{bn} the amount of sediment transport is increasing as well. This is shown in figure 4-19, by plotting volume changes inside the Marsdiep basin.

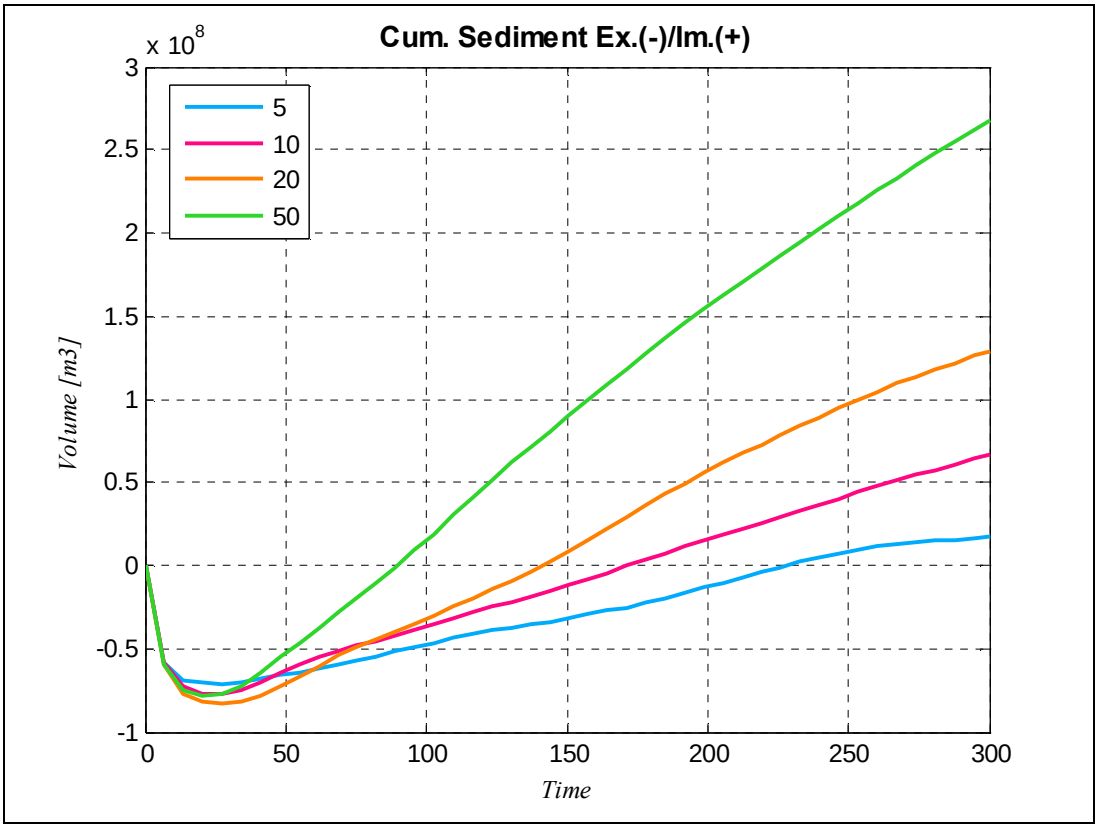

Figure 4-19: Cumulative Sediment import/export from the Marsdiep basin in time (300 years of modeling) in the runs with different α_{bn}

By plotting the result of these runs for Marsdiep on the Friedrichs and Aubrey graph, it is shown that all the basins move toward the same direction on the graph. While the runs with α_{bn} of 5 and 10 are almost the same, by increasing α_{bn} the model of Marsdiep basin gets shallower with more inter-tidal storage volume. (Figure 4-20)

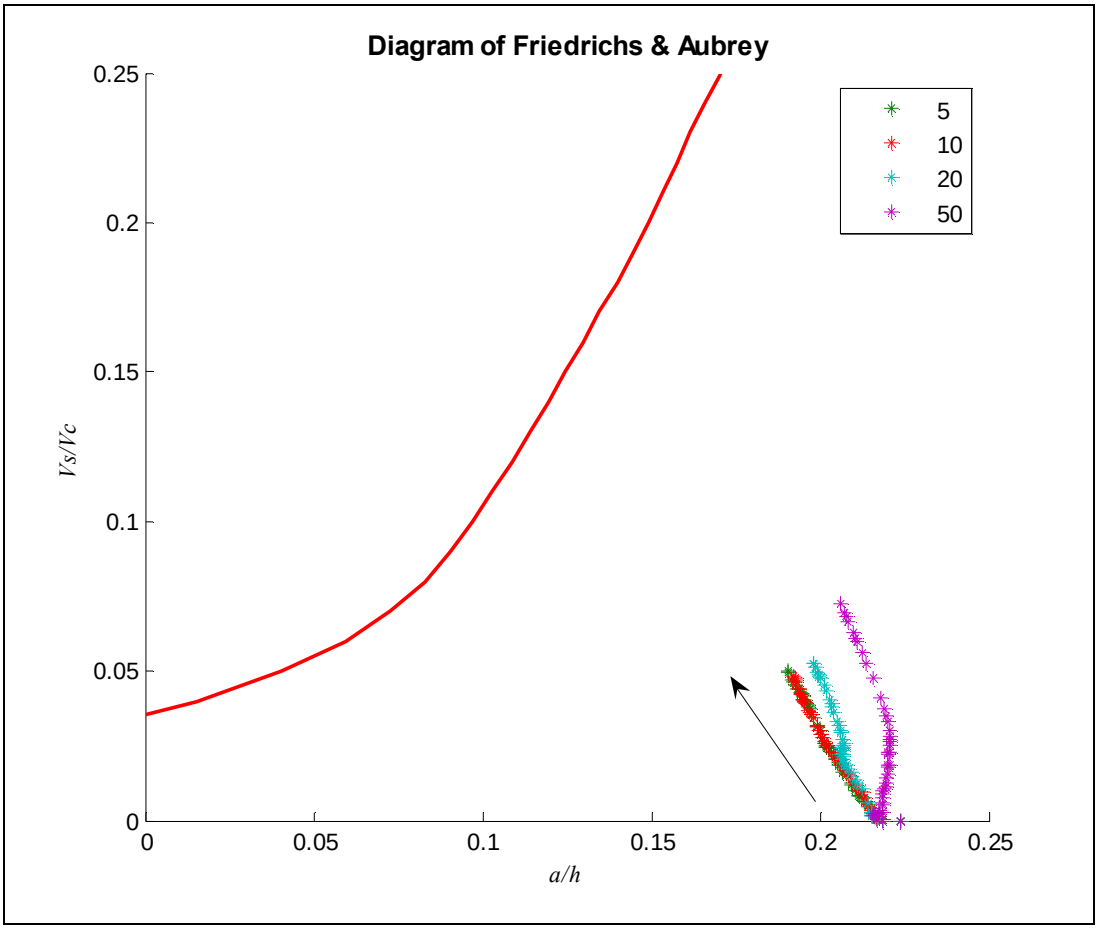

Figure 4-20:Friedrichs and Aubrey graph for the data of Marsdiep in the simulations with different α_{bn} during 300 years of modeling

Comparing the result of theses runs the value of 10 is chosen for the runs with the flat bathymetries, for the α_{bn} less than 10 after a while the sediment transport mechanism stops which is not realistic, on the other hand for larger values some unrealistic high velocities take place and increase the sediment transport. For the runs with real bathymetry the effect of α_{bn} is discussed separately.

The final bathymetry of the Western Wadden Sea in the simulations with different α_{bn} is illustrated in following figures. It is clearly showed that the main effect of α_{bn} is on the channel and shoal patterns, especially on channel depth.

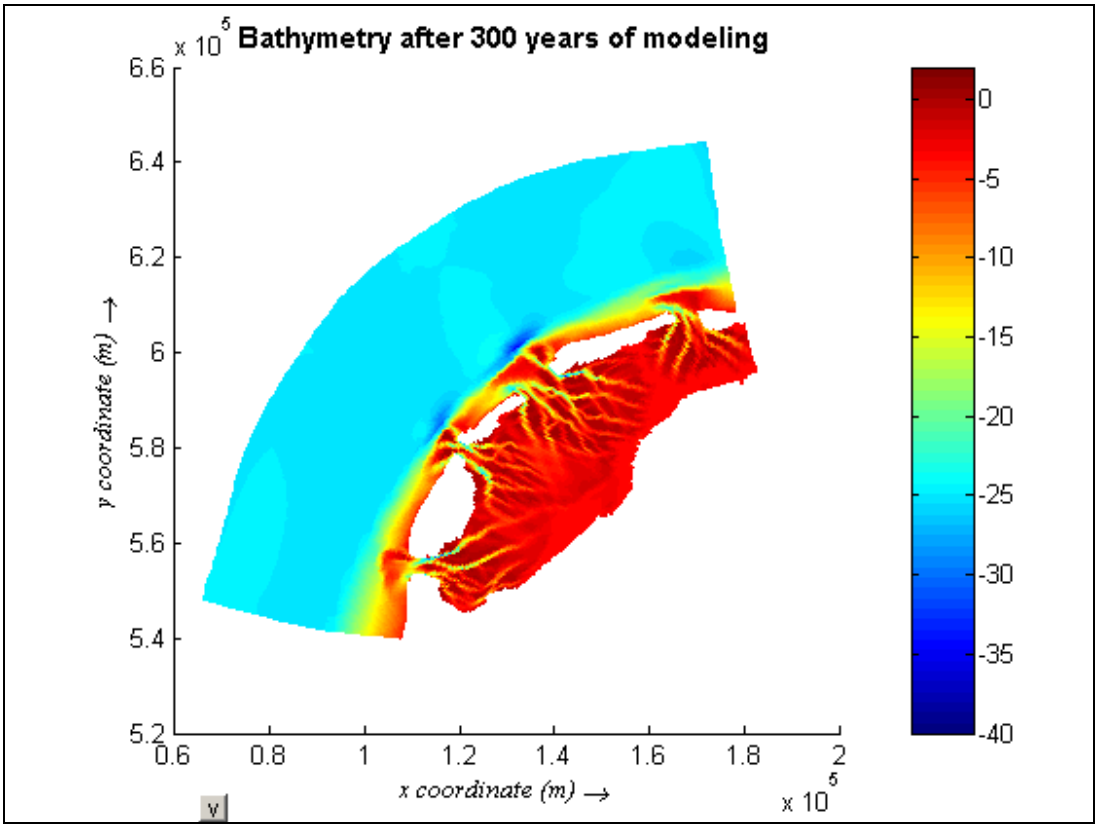

Figure 4-21: Final bathymetry of Western Wadden Sea in the simulations with α_{bn}=5

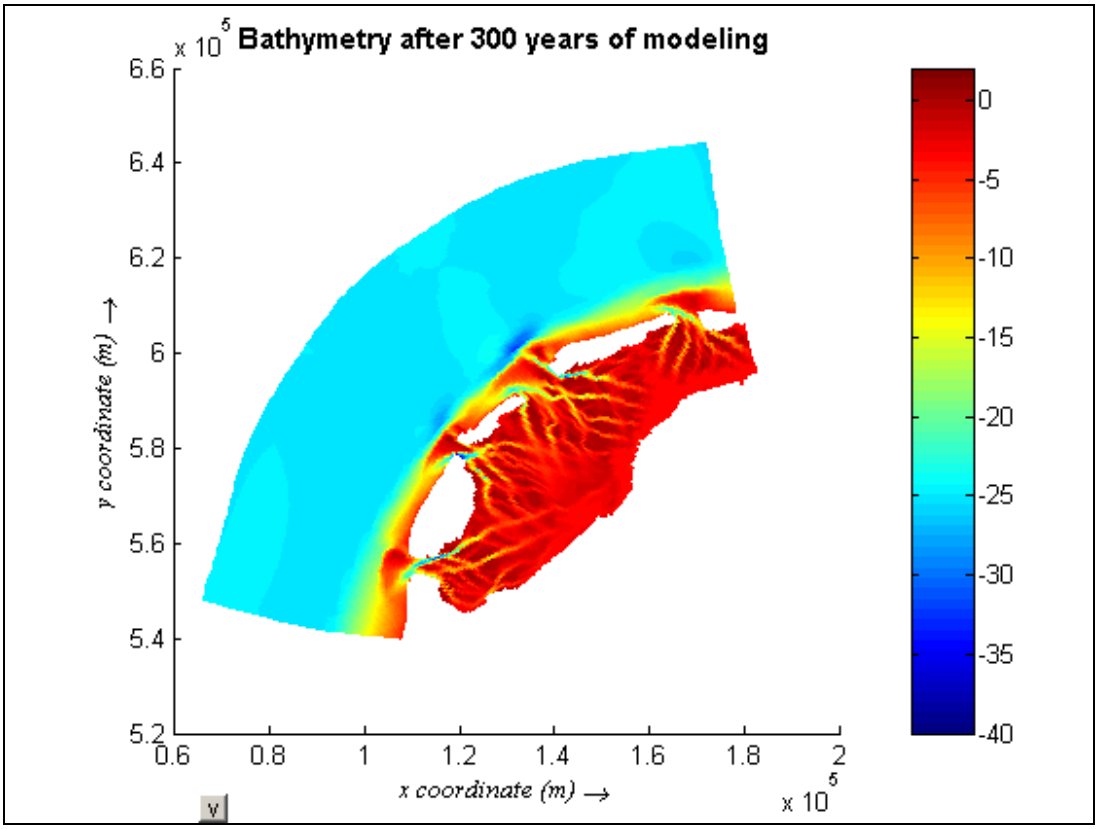

Figure 4-22: Final bathymetry of Western Wadden Sea in the simulations with α_{bn}=10

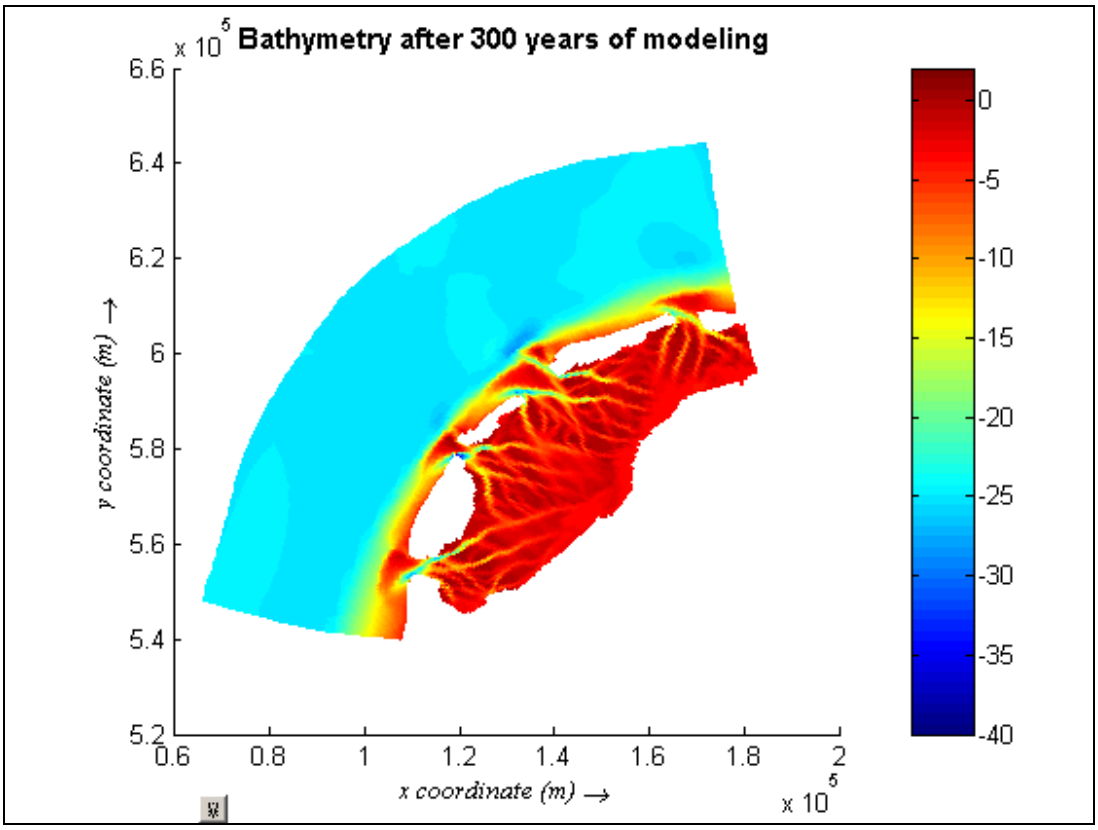

Figure 4-23: Final bathymetry of Western Wadden Sea in the simulations with α_{bn}=20

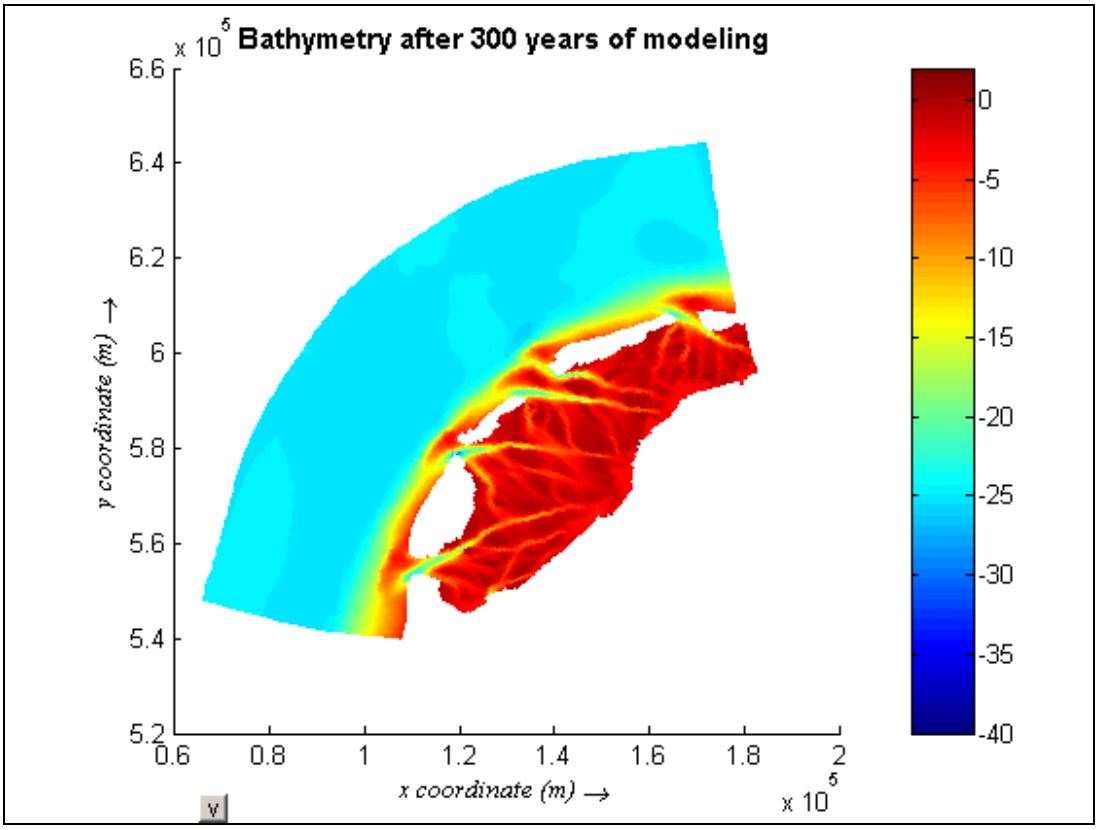

Figure 4-24: Final bathymetry of Western Wadden Sea in the simulations with α_{bn}=50

4.7 Setup of different runs

Seeking the hypothetical equilibrium condition in Marsdiep and other tidal basins in the Western Wadden Sea some different simulations were carried out. These simulations can be categorized in two main different scenarios, schematized bathymetry simulations and real bathymetry simulations. In all the runs due to computational time and the size of output files the hydrodynamic time is 7 years. The value of 300 is chosen for 'Morphological Factor', so the morphological modeling time is 2100 years. The Chézy coefficient is 65 and the eddy viscosity is 1.0 in all the runs.

4.7.1 Schematized bathymetry simulations

To show the effect of initial bathymetry on the equilibrium condition in the model, different runs with different flat bathymetries and the sloping bathymetry (See section 4.5) were carried out. In all these runs except one (L06) the $ZM_2M_4M_6$-$M_2M_4M_6$ forcing boundary condition is used. To illustrate the changes in the results with only M2 forces (lack of tidal asymmetry) one simulation (L06) is done using ZM_2-M_2 forcing boundary condition (See section 4.3). The runs in this scenario which are analyzed in this report are summarized in table 4-4.

Table 4-4: Different runs with schematized bathymetry

Run ID	Forcing	Bathymetry	α_{bn}
L01	$ZM_2M_4M_6$-$M_2M_4M_6$	Flat (d=3.62)	10
L06	ZM_2-M_2	Flat (d=3.62)	10
L02	$ZM_2M_4M_6$-$M_2M_4M_6$	Flat (d=4.54)	10
L11	$ZM_2M_4M_6$-$M_2M_4M_6$	Flat (d=5.02)	10
L03	$ZM_2M_4M_6$-$M_2M_4M_6$	Flat (d=8.00)	10
L04	$ZM_2M_4M_6$-$M_2M_4M_6$	sloping	10

4.7.2 Real bathymetry simulations

Another goal of this study is to simulate the mega scale changes of the basins from now on. In this regard 4 main simulations with $ZM_2M_4M_6$-$M_2M_4M_6$ forcing boundary condition (See section 4.3) were carried out. The only changing parameter in these runs is α_{bn} which was shown to have an effect on the channel and shoal patterns. These runs are introduced in table 4-5.

Table 4-5: Different runs with real bathymetry

Run ID	Forcing	Bathymetry	α_{bn}
L07	$ZM_2M_4M_6$-$M_2M_4M_6$	1998	5
L05	$ZM_2M_4M_6$-$M_2M_4M_6$	1998	10
L12	$ZM_2M_4M_6$-$M_2M_4M_6$	1998	20
L13	$ZM_2M_4M_6$-$M_2M_4M_6$	1998	50

4.7.3 Corresponding hydrodynamic runs

Since the morphological time of the simulation is long (2100 years) the changes in the bathymetry of the basins affect the tidal properties. On the other hand in these morphological models each tidal cycle represents around half a year of morphological changes. Therefore if at a specific time any kind of hydrodynamic characteristic is needed, a short-term hydrodynamic run should be carried out with the modeled bathymetry at that time but without any morphological changes. In this study the duration of these hydrodynamic runs is 5 tidal cycles. In the scenario with schematized bathymetries the hydrodynamic run is carried out once for each morphological simulation with the resulting bathymetry after 2100 years of morphological modeling. For real bathymetry scenarios for one morphological model, 5 hydrodynamic simulations are done in morphological years of 0, 200, 700, 1200, and 2100. All the hydrodynamic runs are summarized in the table 4-6.

Table 4-6:Different Hydrodynamic runs

Scenario	Run ID	Corresponding Morphological Model	Morphological Year
Schematized bathymetry	H01	L01	2100
	H02	L02	2100
	HB2	L02	0
	H04	L04	2100
Real Bathymetry	HB5	L05	0
	HC5	L05	200
	HD5	L05	700
	HE5	L05	1200
	H05	L05	2100

5 Analyzing the Results and Discussion

5.1 Analyzing assumptions and method

The result of the morphological modeling with Delft3D software should be analyzed and interpreted to tidal basin characteristics. In order to do that, the time history of the bed levels in the Western Wadden Sea basins during the simulation period are extracted from Delft3D results and exported as .mat file (MATLAB® data structure) by QUICKPLOT as well as the time history of tidal levels in front of the tidal inlets. Some analyzer routines were written in MATLAB® environment to analyze these data. the input of this analyzer is the bed level time history, morphological factor and Mean high water, Mean Low water and Mean water level in front of each basin and also the boundaries, according to which the basins are defined. The analyzer first calculates the area of each grid cell, then separates the data for each basin based on the introduced boundaries. The next step in the analyzer is to create a hypsometry for each basin with the accuracy of 1.0 cm. When the hypsometry of a basin is ready by using the tidal elevations all the basin parameters such as: changes in sediment volume in each basin, tidal prism, inter-tidal flat area, inter-tidal flat volume, channel area, channel volume, volume of inter-tidal storage, height of flats, etc. are calculated in all time steps.(See Appendix B for more details) All these parameters can be plotted in time or against each other to check different equilibrium indicators. Figure 5-1 shows the flow chart of the Analyzer.

In this study the Analyzer time steps for long-term simulations is 40 (39.95) morphological years. Although the temporal and spatial changes in tide have an effect on the analysis of the basin parameters, to simplify the analyses, in this study the tidal elevations in front of each inlet in the last morphological year are chosen as the representative tidal elevations throughout the basin area as well as during the simulation period. The (small) effect of this assumption on the accuracy of the results is discussed in Appendix A. The boundaries of the basins in most of the simulations is the boundary defined by RIKZ in 'Vaklodingen' data base, except in one analyze which shows the changes in the boundaries.

5.2 Limitation of the simulations

Before discussing the results the main limitations of the simulations in this study are summarized in this section:

- The forcing of the model is only tide with water boundary in the sea side and Neumann boundaries in lateral boundaries.
- Only M_2,M_4 and M_6 components are chosen for tide.
- One sediment fraction is used in the model which is available till depth of-45 in all the grid points.
- Obviously the minimum width of the channels at each depth can not be smaller than the grid lines spacing (500 m on average)
- Relatively large value of 300 is used as the morphological factor.
- No sea level rise is taken into account in this study.

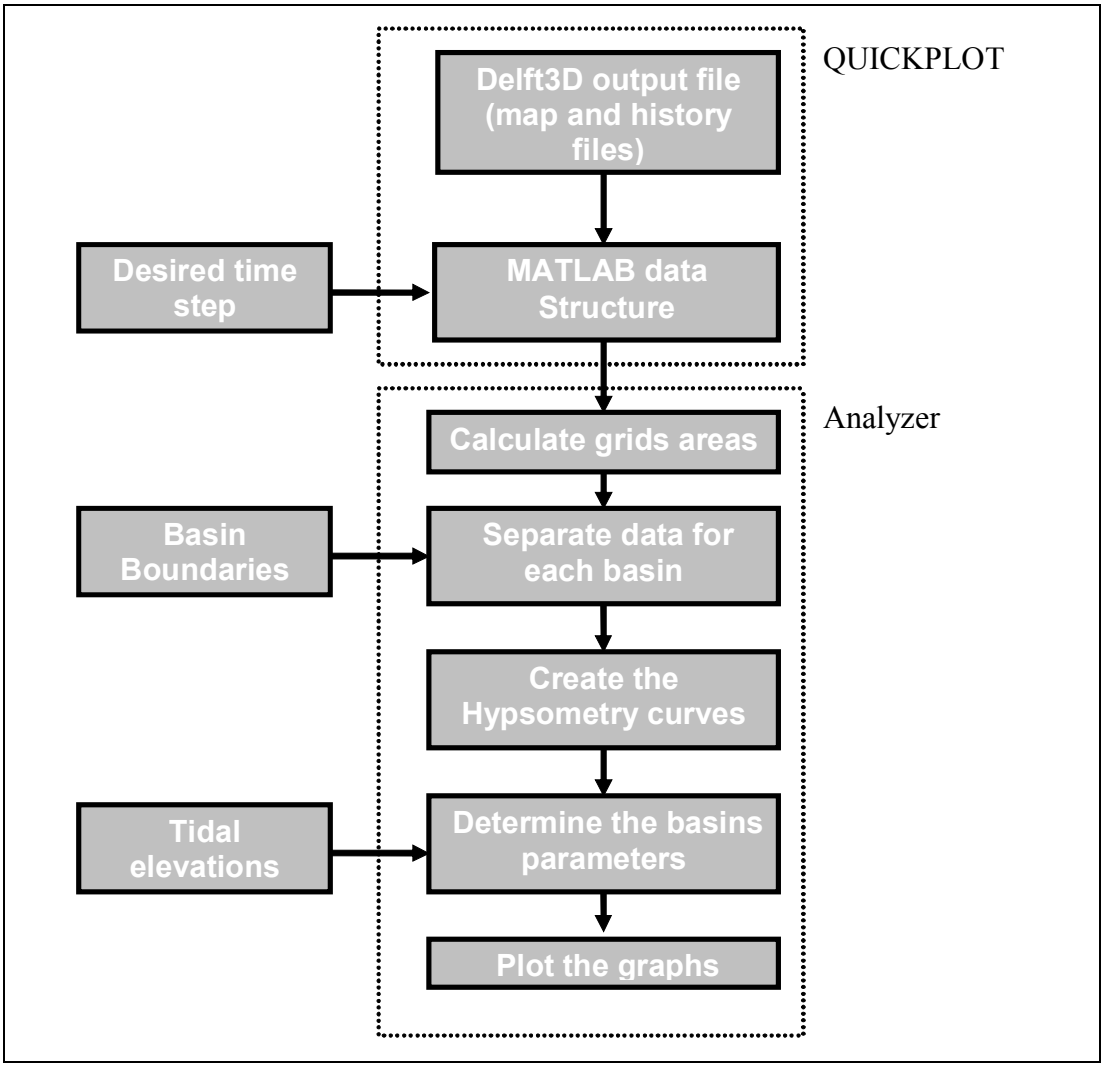

Figure 5-1:Flow chart of the Analyzer

5.3 Schematized bathymetry scenario

5.3.1 Morphological development

Starting with the schematized bathymetry inside the basin, the model shows the evolution of the ebb-tidal delta and channel and shoal patterns inside the basins. For example in run L02 during the first 100 years of modeling the ebb-tidal delta in front of the Marsdiep inlet is formed, also main entrance channel is developed during this period (Figure 5-2). This is followed by evolution of the main channel and shoal patterns inside Marsdiep basin. After almost 400 years of modeling the main channel and shoal pattern inside Marsdiep basin is almost defined, however the dynamic behavior of this pattern is obvious (Figure 5-2). The ebb-tidal delta migrates towards the inlet as well as down-drift coastline. In reality there is a channel on the north side of the Marsdiep ebb-tidal delta (Texel Island) but in the model this channel is not clearly formed. The main channel inside the basin clearly stretches eastward and does not change its orientation during the time while other channels shows a fractal

dynamic behavior till the basin reaches its relatively stable channels with three originating from the entrance channel.

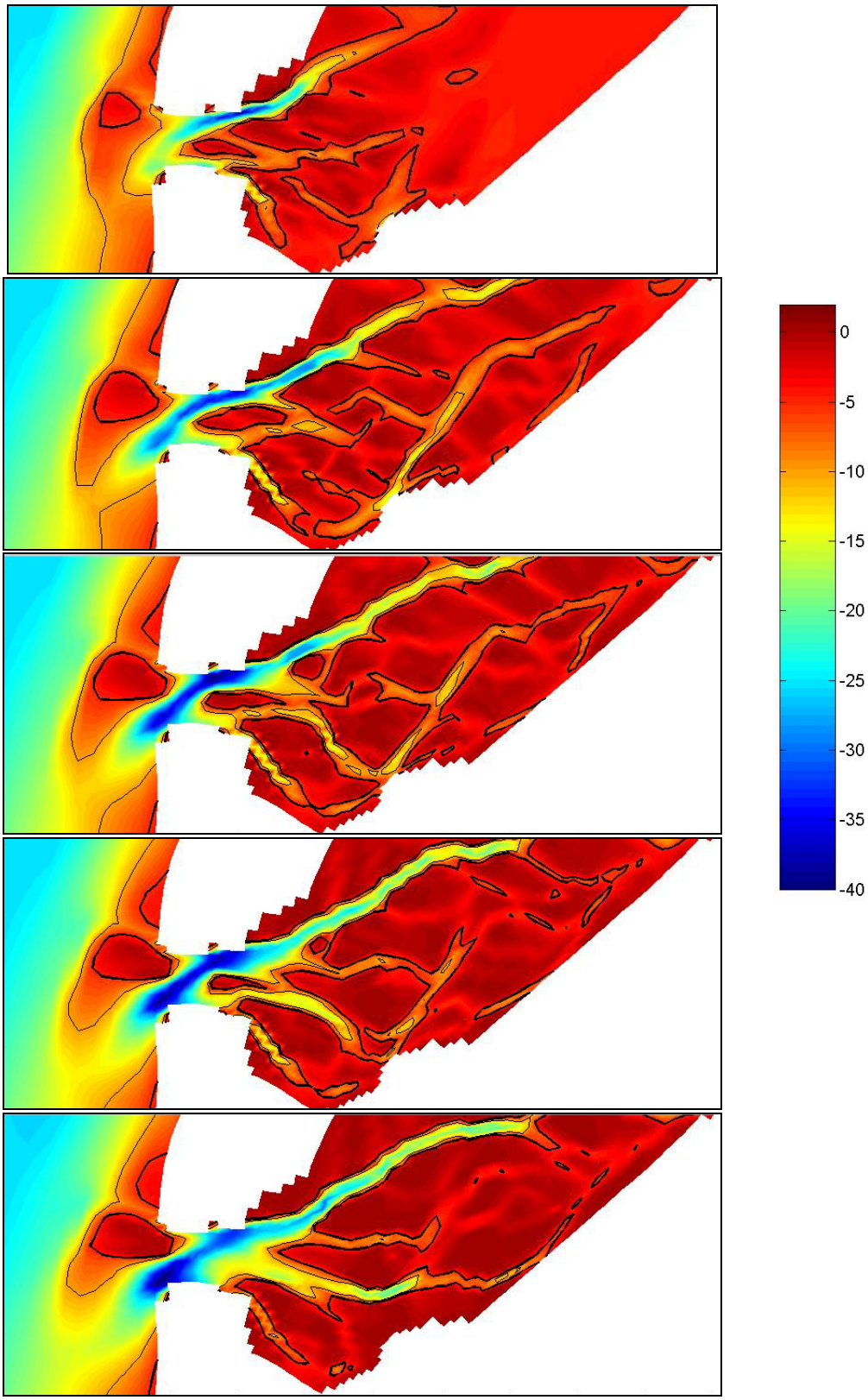

Figure 5-2: Evolution of Marsdiep Basin and its ebb-tidal delta, in morphological years of 120,400,800,1200, and 2100 for simulation L02

Looking at the whole modeled area (Figure 5-3), it is clear that unlike the reality all three basins, Marsdiep, Eierlandse Gat, and Vlie are in the same order in size and affect each other's evolution a lot. So differences amongst them in reality especially in the case of Eierlandse Gat should be due to some geological or historical differences.

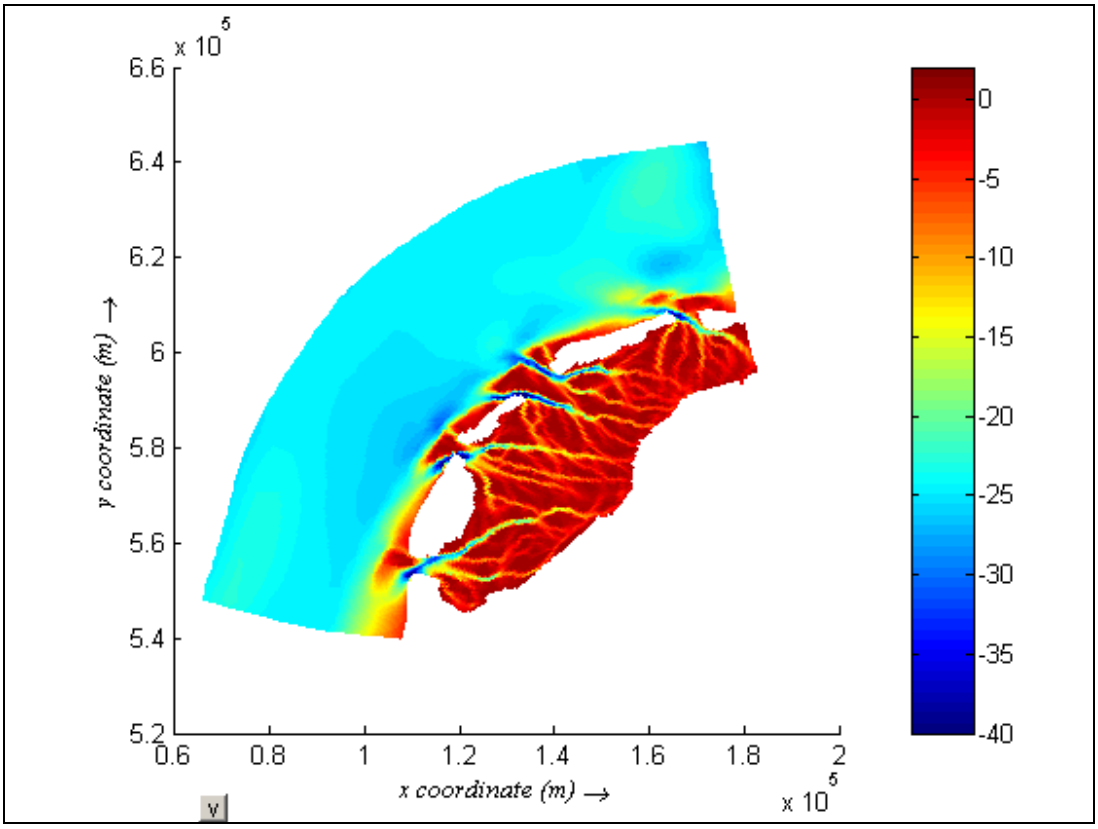

Figure 5-3:The resulting bathymetry of L02 simulation after 2100 years

About Vlie inlet it is interesting that in all the runs with schematized bathymetries two main channels are developed in that inlet, which means that this inlet is too wide for a single entrance channel.

The same phenomena are observed in all the simulations with schematized bathymetries, except in run with the deepest Wadden Sea (L03). In this run due to lack of sediment in the model, the basins import sediment from the adjacent coastlines from the beginning and there is not enough sediment to form an ebb-tidal delta. The Bathymetry of the Marsdiep after 2100 years of morphological modeling for different initial conditions (different simulations) are shown in figure 5-4.

Using one fraction of sand in the model leads to some unrealistic morphological shapes in the results, for example in the seaward side of the Vlie ebb-tidal delta very steep slopes are developed under the MSL .

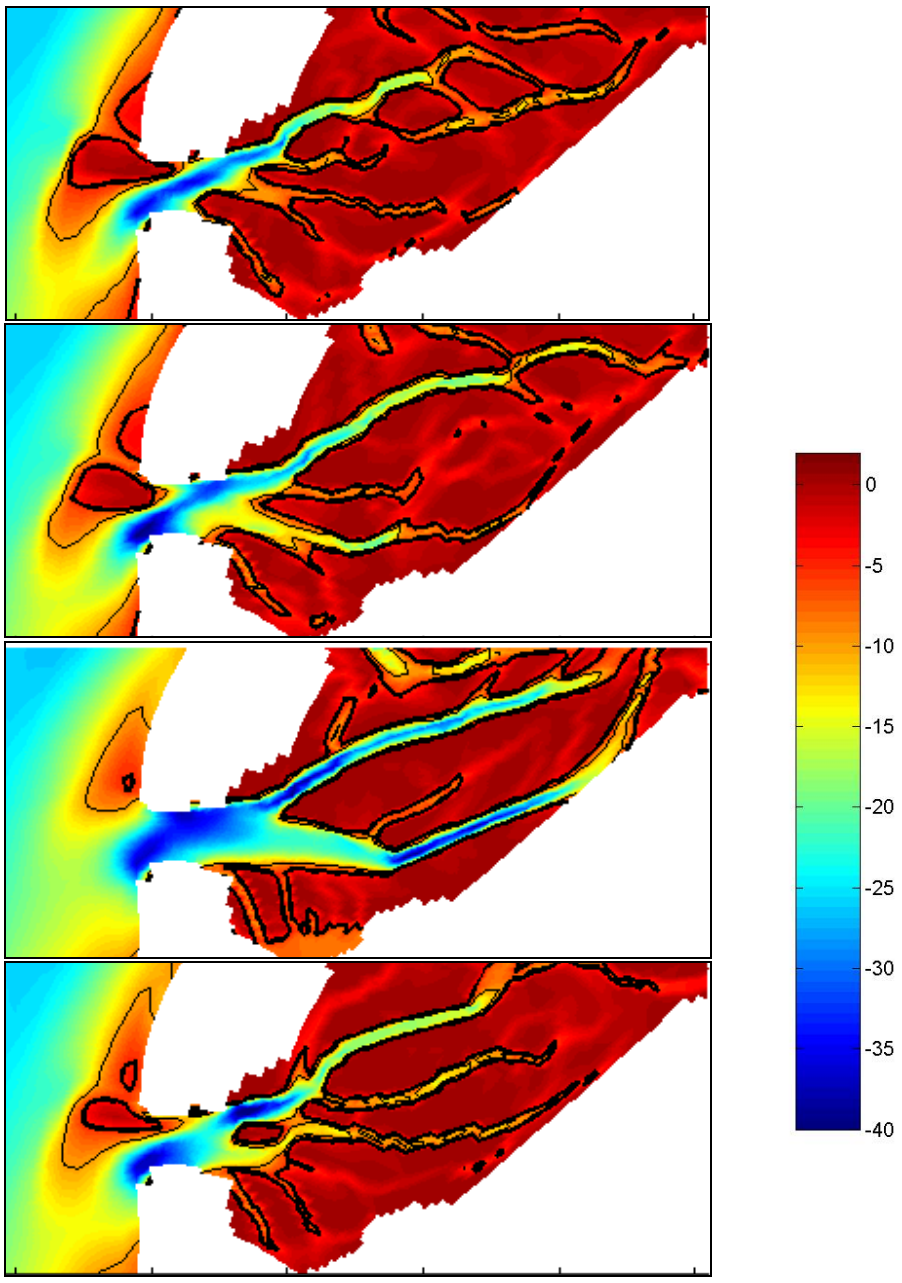

Figure 5-4:Bathymetry of Marsdiep after 2100 years of morphological modeling in different simulations (from up to down L01,L02,L03 and L04)

In the following sections the main equilibrium indicators and relations in each basin for each simulation are discussed.

5.3.2 Sediment balance

The changes in the available sediment in each basin during the simulation time are calculated by using the basin boundaries defined in 'Vaklodingen' database and with respect to an arbitrary level to show the difference between the initial values, and shown in following figures. (simulation L03 which is the deepest one is excluded from the results and simulation L11 included)

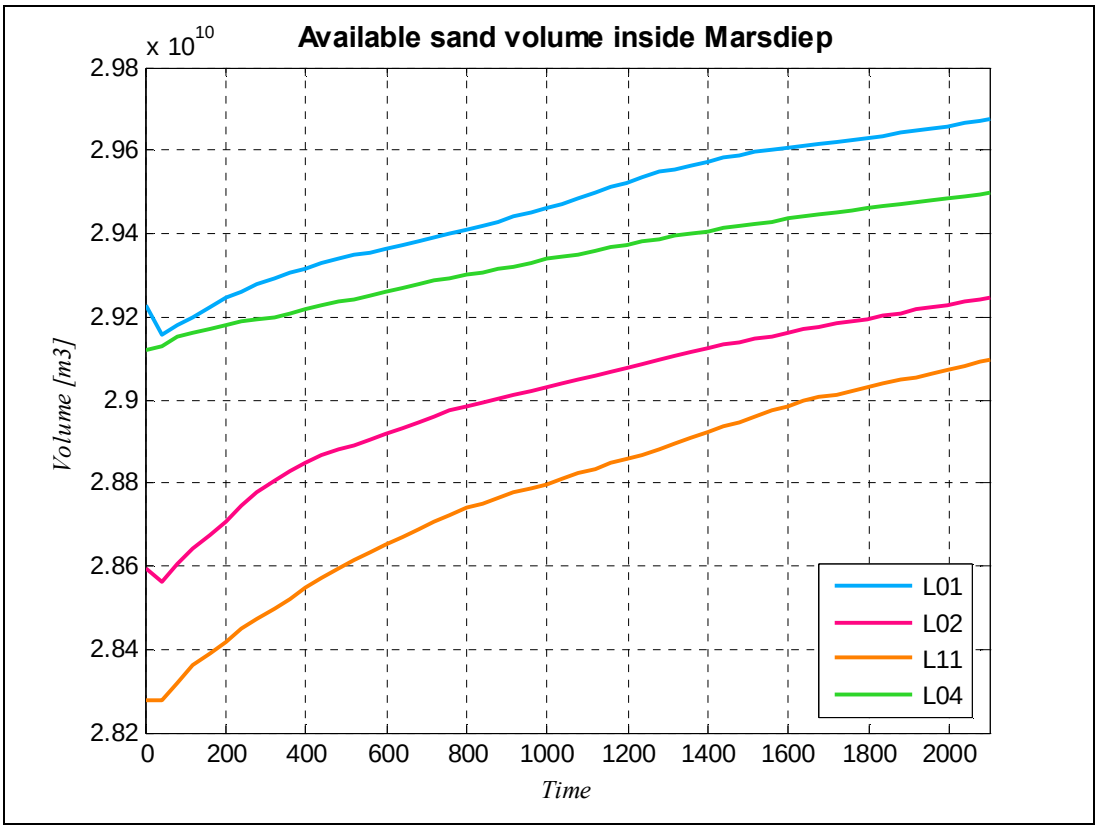

Figure 5-5:Changing in available sediment inside the Marsdiep basin during the simulation time (2100 yrs)

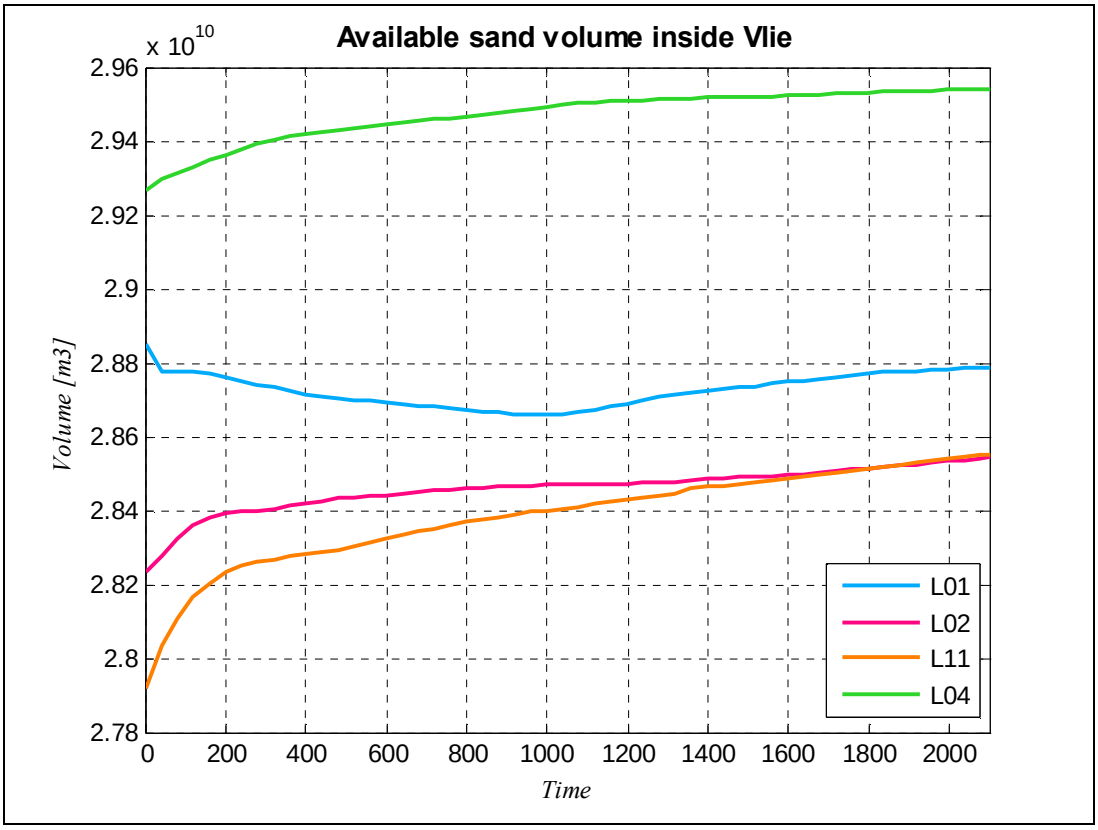

Figure 5-6:Changing in available sediment inside the Vlie basin during the simulation time (2100 yrs)

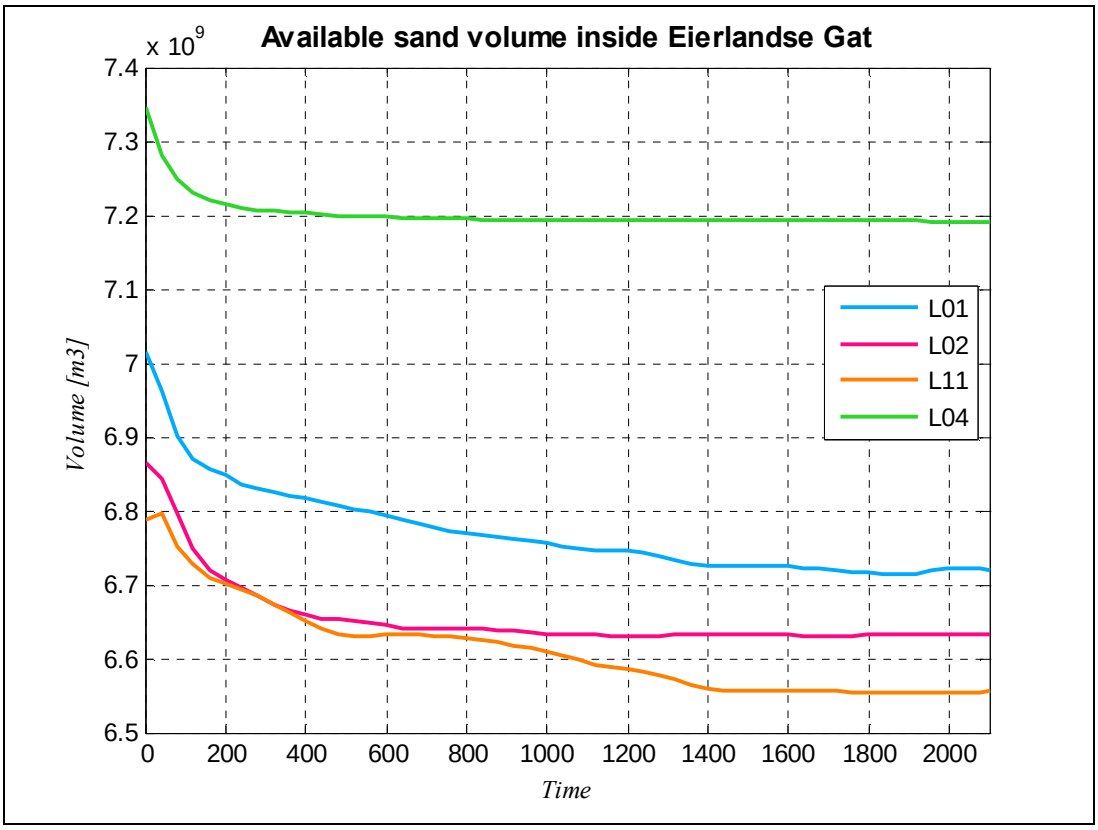

Figure 5-7:Changing in available sediment inside the Eierlandse Gat basin during the simulation time (2100 yrs)

From the figures it is obvious that in the first years of simulations (order of 300 years) the rate of sediment exchange is much more than the last years, from this point of view it can be claimed that the basins are going toward the stable available sediment, especially in Eierlandse Gat in simulation L04, but clearly this equilibrium is dependent of the initial condition. But in a closer look to Marsdiep results it is shown that in this basin even after 2100 years of modeling still the exchange exists although its rate is decreased (in the order of 250,000 m^3 per year). On the other hand Vlie shows different behavior, the available sediment in two simulations with uniform depth of 5.02 and 4.54m goes to the ***same*** value and shows import to the basin, the L01 simulation with the shallower depth of 3.62m, shows export for the first 1000 years, going toward the values of L02 and L11 simulations, and then moves parallel to those two runs. These behaviors may be due to this fact that the defined boundaries for basins are not accurate for the runs with schematized bathymetry.

5.3.3 Flat characteristics

Eysink (1990) claims that one of the first parameters which goes to an equilibrium value, in relatively short time, is the height of flats which is related to the tidal amplitude. To check this hypothesis in the results of process based modeling, the development of flats in Marsdiep basin from flat or sloping bathymetries, is shown in the figure 5-8.

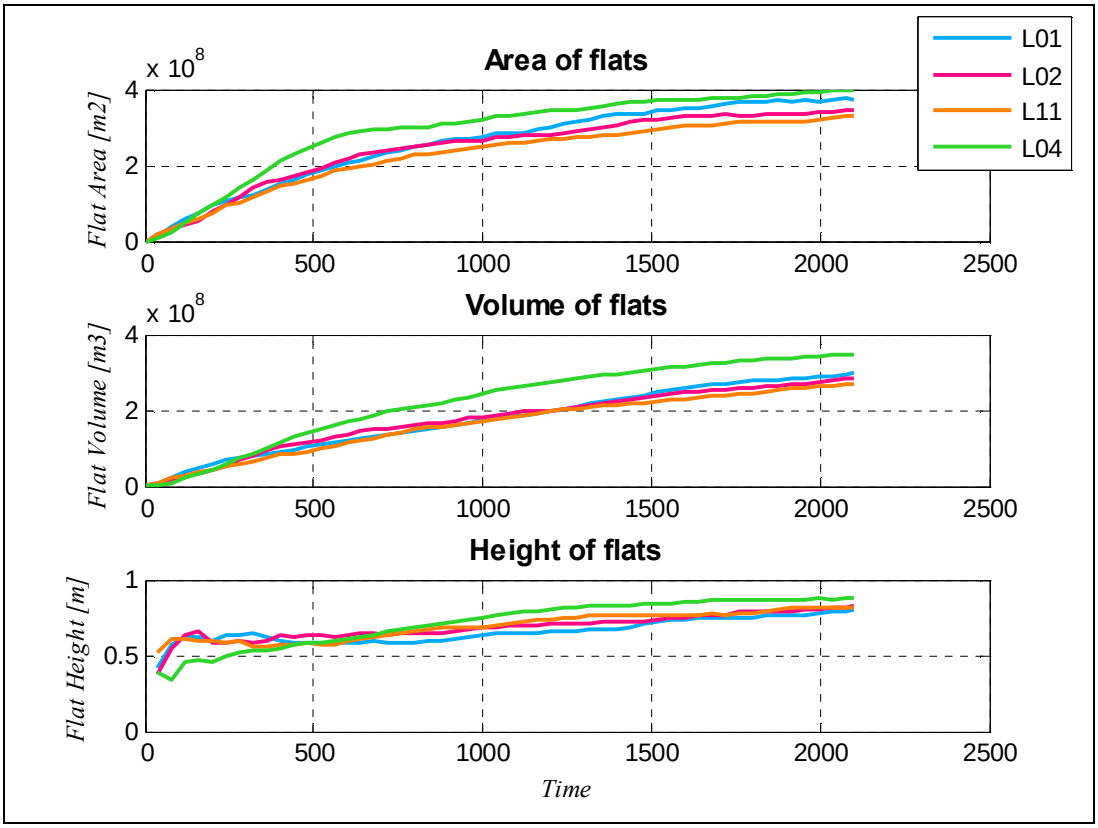

Figure 5-8: Development of flat characteristics in Marsdiep from different initial conditions

Figure 5-8 shows that flat characteristics tend toward some equilibrium values but the flat height is not adjusted as fast as Eysink (1990) claims. Also it is shown that these equilibrium values are also dependent on the initial condition. This dependency is less pronounced in flat height but in volume of flats obviously the initial sloping bathymetry (L04) developed more flat volume and also it developed more flat area, so the longitudinal distribution of the sediment in initial bathymetry also affects the result for flat characteristics . The final height of flat in all the simulations with flat initial bathymetries are almost the same but far from the equilibrium value suggested by Eysink (1990), which is around 0.4 m in this case.

Another flat characteristic that is among the equilibrium indicators is relative flat area or the ratio between area of flats and total area of basin. The evolution of this indicator for Marsdiep basin from different initial conditions is shown in figures 5-9 and 5-10.

Since the borders of the basins are fixed in this analysis, if the relation of Renger and Partenscky (1974) is examined, the equilibrium value for A_f/A_b remains constant during the simulation time. This value and the changes in A_f/A_b are shown in figure 5-9. It shows that A_f/A_b also tends to some stable values but again different for different initial conditions and not in agreement with theory.

This value is also plotted on the suggested graph for Wadden Sea basins by Eysink (1991) in figure 5-10 , in this figure also the results are not in the range suggested by him.

Only in the case of Eierlandse Gat and the sloping initial bathymetry the theoretical value matches the resulted value from the model (Figures 5-11 and 5-12).

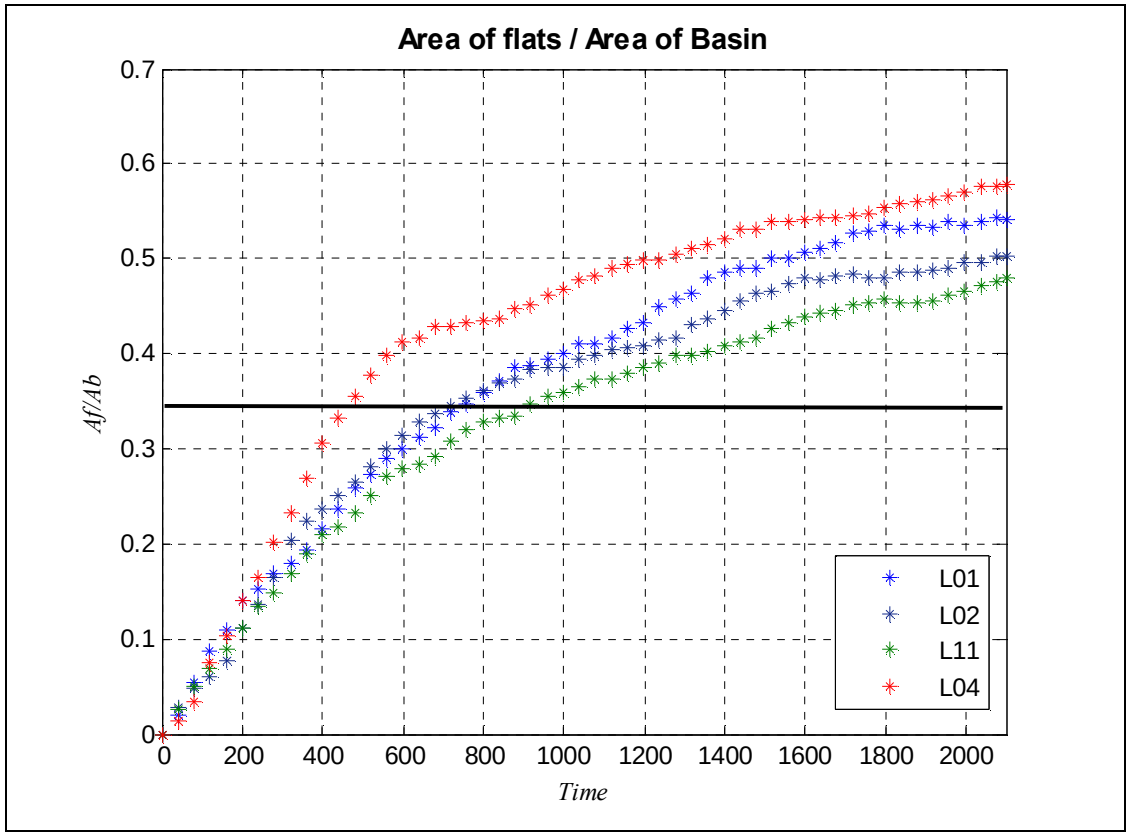

Figure 5-9: Relative flat area in Marsdiep during the simulation period

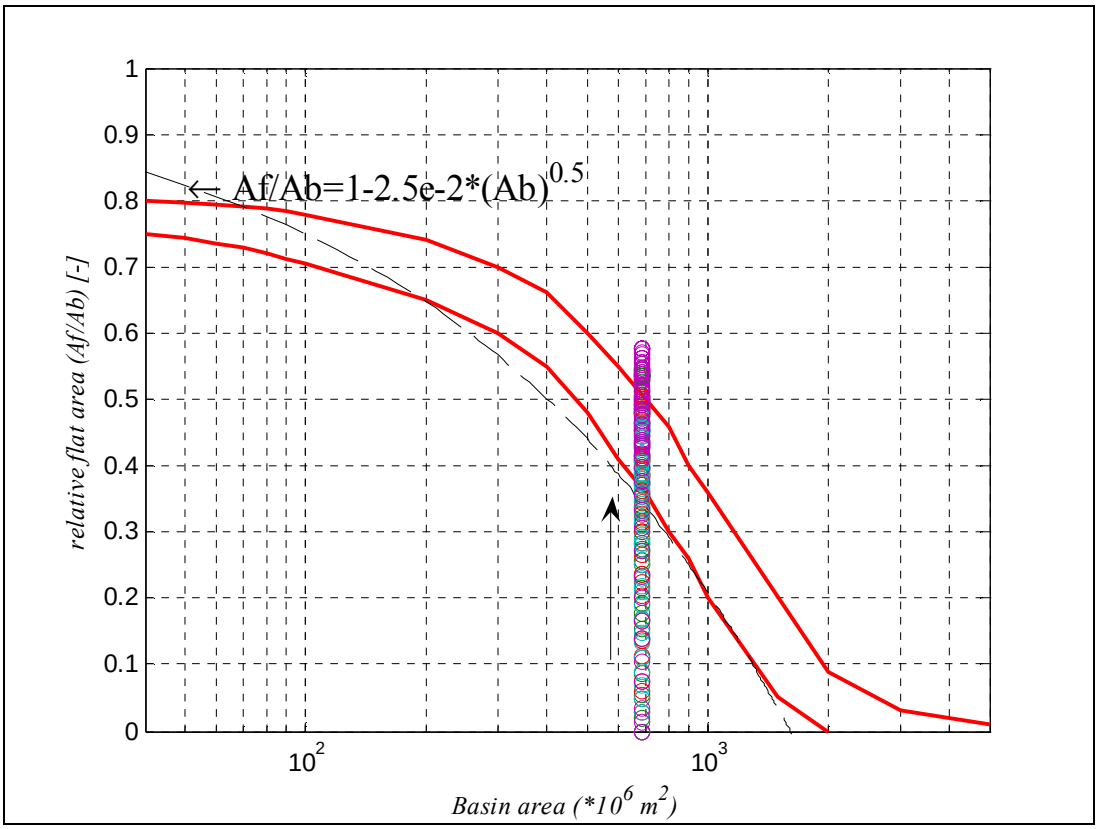

Figure 5-10: Relative flat area in Marsdiep on Eysink (1991) graph

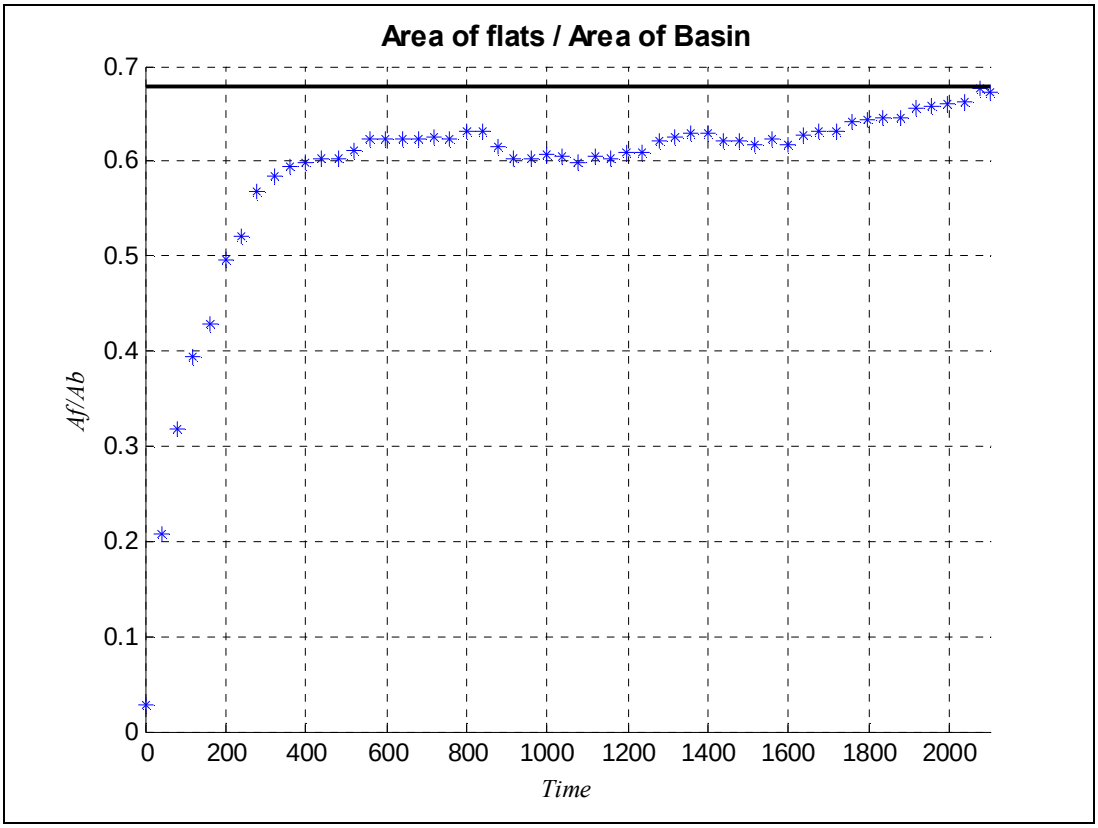

Figure 5-11: Relative flat area in Eierlandse Gat during the simulation period with theoretical value

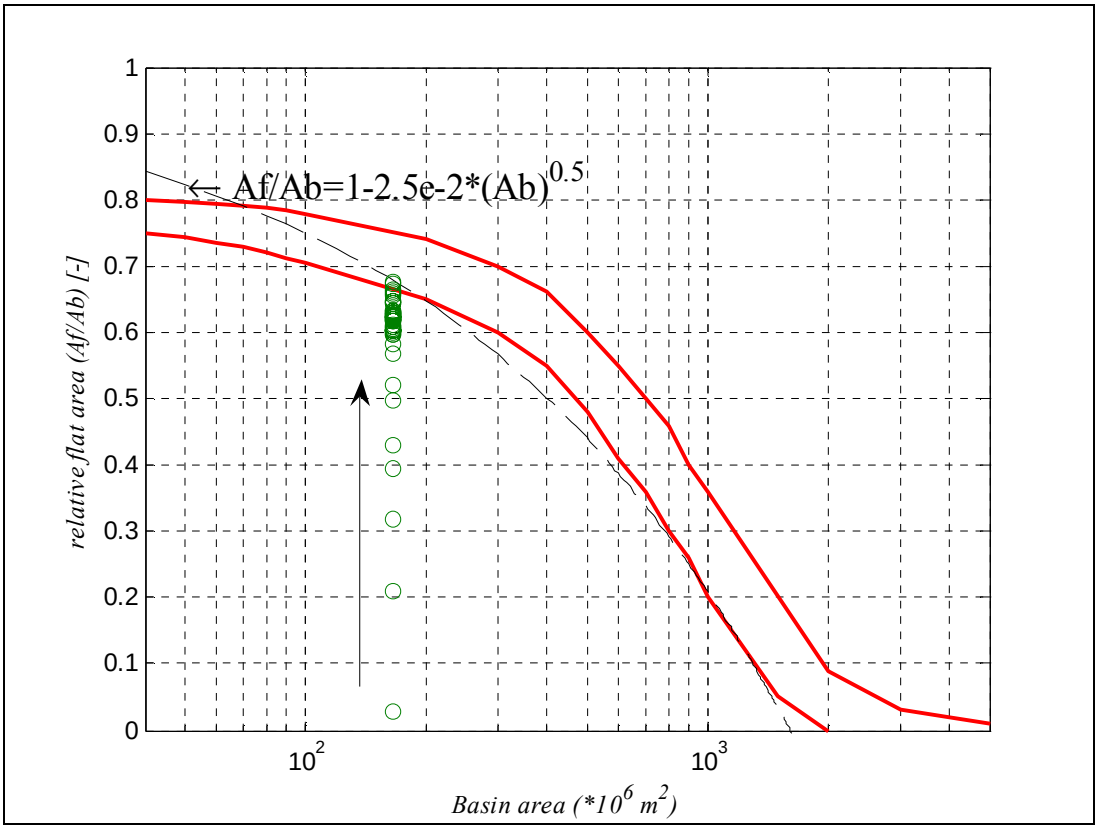

Figure 5-12: Relative flat area in Eierlandse Gat on Eysink (1991) graph

5.3.4 Friedrichs and Aubrey graph

The parameters for Friedrichs and Aubrey graph are calculated from the result of the model for different basins. These results are shown in following figures. In all the simulations and all the basins the development of the basin according to this graph is toward the ebb and flood dominant separation line; this development is faster in early years of modeling than at the end. When the basin condition is near that line it begins to scatter and develop almost parallel with the line; this is shown in the case of Vlie for the simulation with sloping initial bathymetry and Eierlandse Gat in all the simulations. This line in Friedrichs and Aubrey graph is suggested to be some indicator of equilibrium, so it can be concluded that all the basins from all initial conditions are going toward this equilibrium. The difference between the value of a/h in different simulations is due to different initial depths (h) rather than the different in tidal amplitude (a).

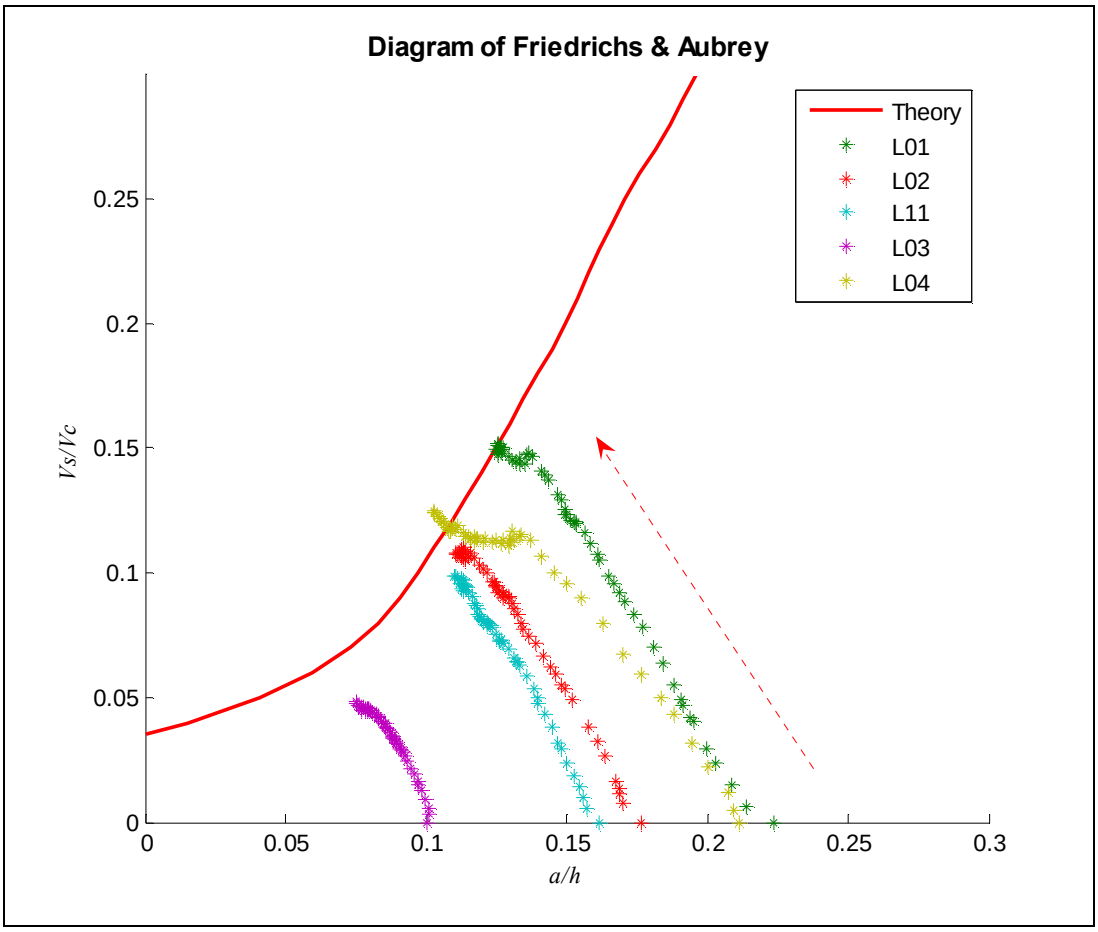

Figure 5-13: Friedrichs and Aubrey diagram for modeled Marsdiep with different initial condition, the arrow shows the direction of changes during the time

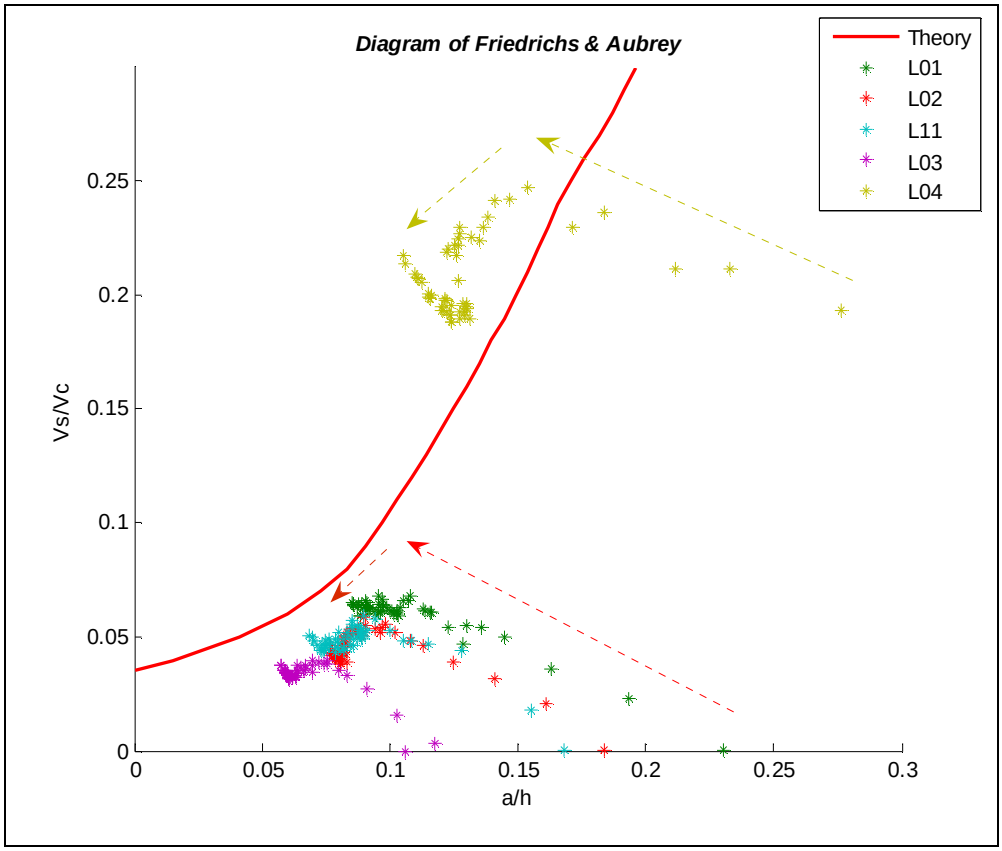

Figure 5-14: Friedrichs and Aubrey diagram for modeled Eierlandse Gat with different initial condition.

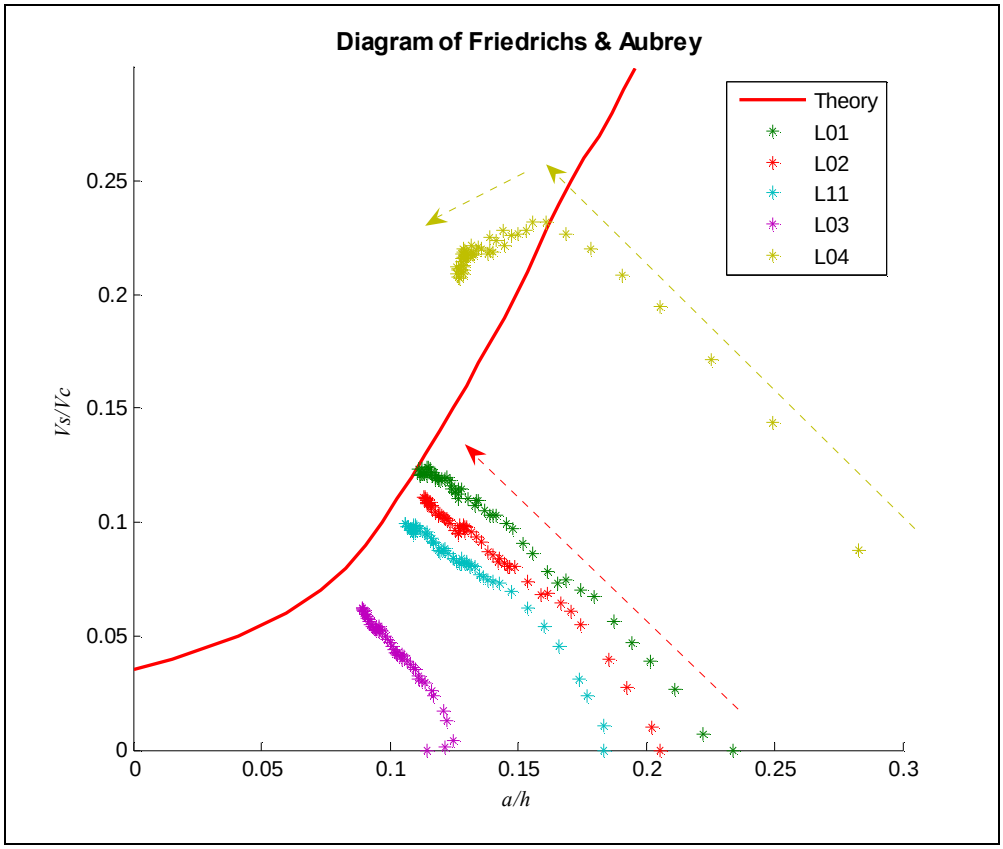

Figure 5-15: Friedrichs and Aubrey diagram for modeled Vlie with different initial condition

5.3.5 Channel volume relation

Eysink (1992) suggested another equilibrium relation in tidal basins relating channel volumes with the tidal prism. This relation for the current simulations is shown in figure 5-16 for Marsdiep.

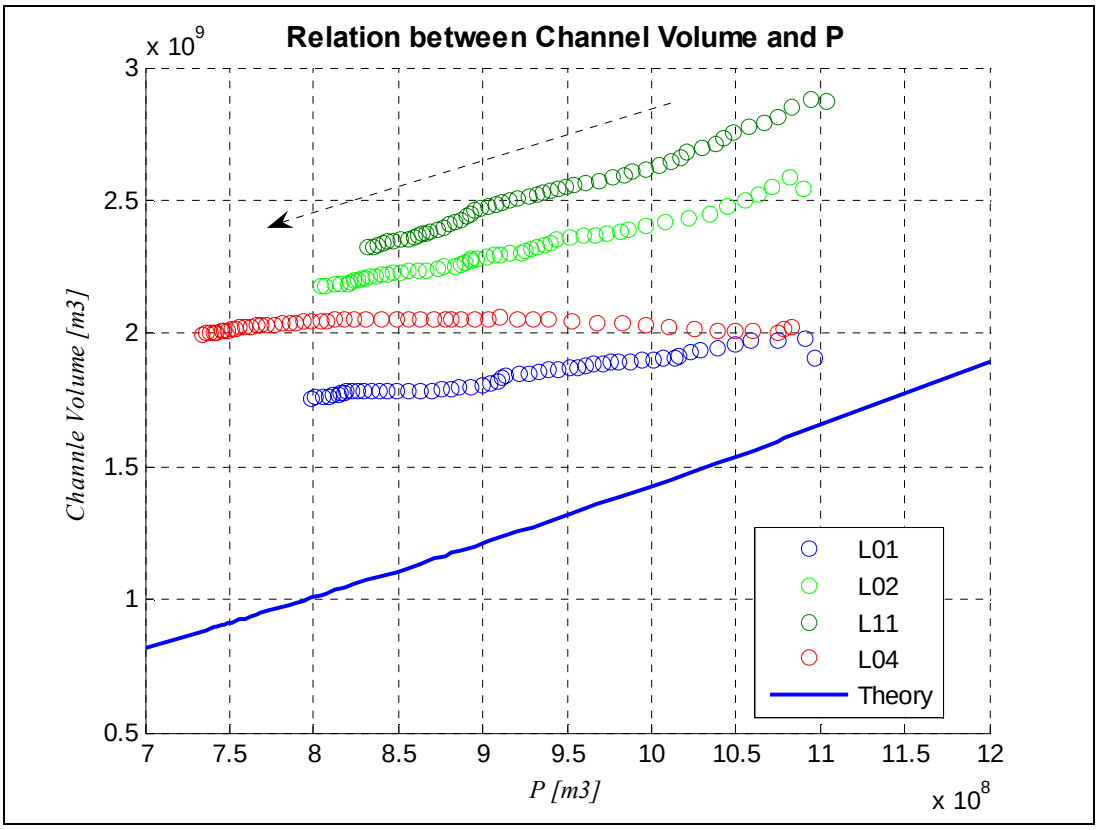

Figure 5-16: Relation between channel volume and tidal prism in Marsdiep

This figure shows that although in some simulations like L02 and L11 the trend of development is parallel to the theoretical line, it is far from the suggested value. Changes of coefficient in Eysink (1992) relation between channel volume and tidal prism (α_c) during 2100 of morphological modeling in Marsdiep is shown in figure 5-17

In this figure it is clear that the current model could not simulate any kind of stability or equilibrium regarding to this kind of relations. The simulations with flat bathymetry inside the Wadden Sea (L01,L02,L11) show the same slope in increasing α_c while the simulation with sloping bathymetry shows a steeper slope. Also in all the runs the value of α_c get far from the value which is suggested in equilibrium relation (= 16e-6).

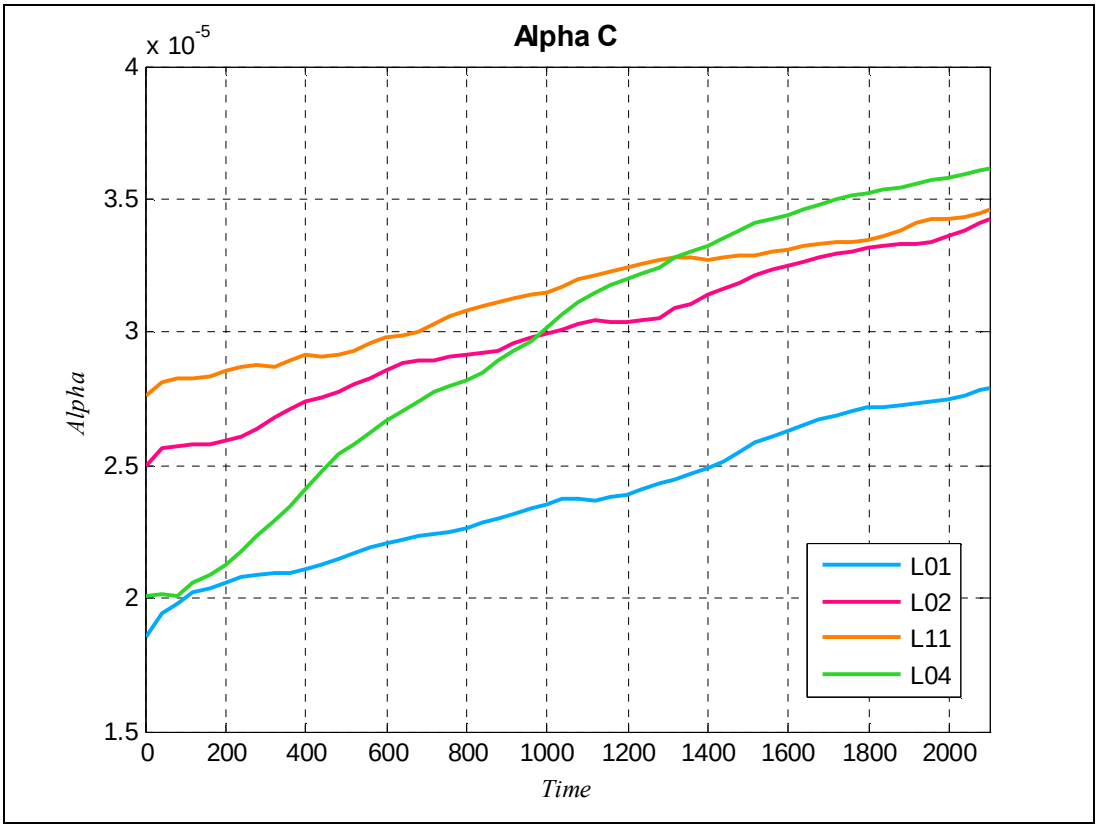

Figure 5-17:Changes of coefficient in the relation between channel volume and tidal prism (α_c) during 2100 of morphological modeling in Marsdiep

5.3.6 Effect of different tidal forcing on the results

In order to check the effect of different tidal forces on the result, one simulation is carried out with the forcing boundary condition based on only M_2 component. Comparing the changes of available sediment inside the Marsdiep basin in this simulation (L06) and the one with the same initial condition but M_2,M_4 and M_6 components (figure 5-18) reveals that forcing boundary condition based on only M_2 can not model the desired mechanism of building the ebb-tidal delta and importing sediment into the basin. It means that the tidal asymmetry due to M_4 and M_6 has an important role in morphological evolution of the tidal basins in this process based model.

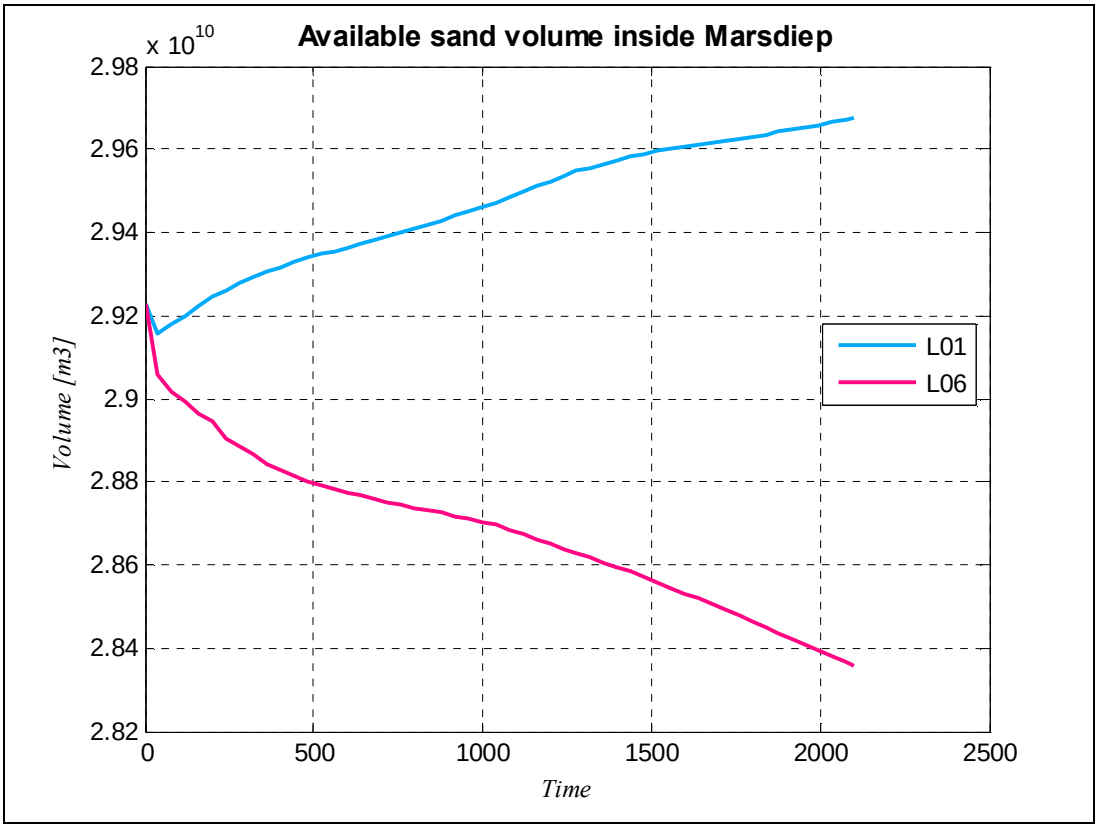

Figure 5-18:Changing in available sediment inside the Marsdiep basin during the simulation time (2100 yrs) under the effect different kind of tidal forcing

5.4 Real bathymetry scenario

The other set of simulations in this study is that with real bathymetry of 1998 as the initial bathymetry. The only parameter which is different in this set, is the transverse bed slope effect in Delf3D input file (See table 4.5). The results of these simulations are also analyzed with the analyzer to determine the characteristics of basins and described in this section.

5.4.1 Hypsometry

The final hypsometry of Marsdiep basin in this set of simulations is shown in figure 5-19. It clearly shows that the resulting Marsdiep after 2100 years of morphological modeling is much deeper than the current Marsdiep, with more flat areas; in other words the model erodes the channels and dumps the sand on the flat areas. This result can be due to the fact that the size of the grid cells in this model is relatively large, so any erosion on one grid cell is acting on the area of 0.25 km^2 in average.

On the other hand this graph shows that similar to simulations with schematized bathymetries, in these simulations also the hypsometry of Marsdiep does not change with different coefficient for the transverse bed slope effect (α_{bn}).

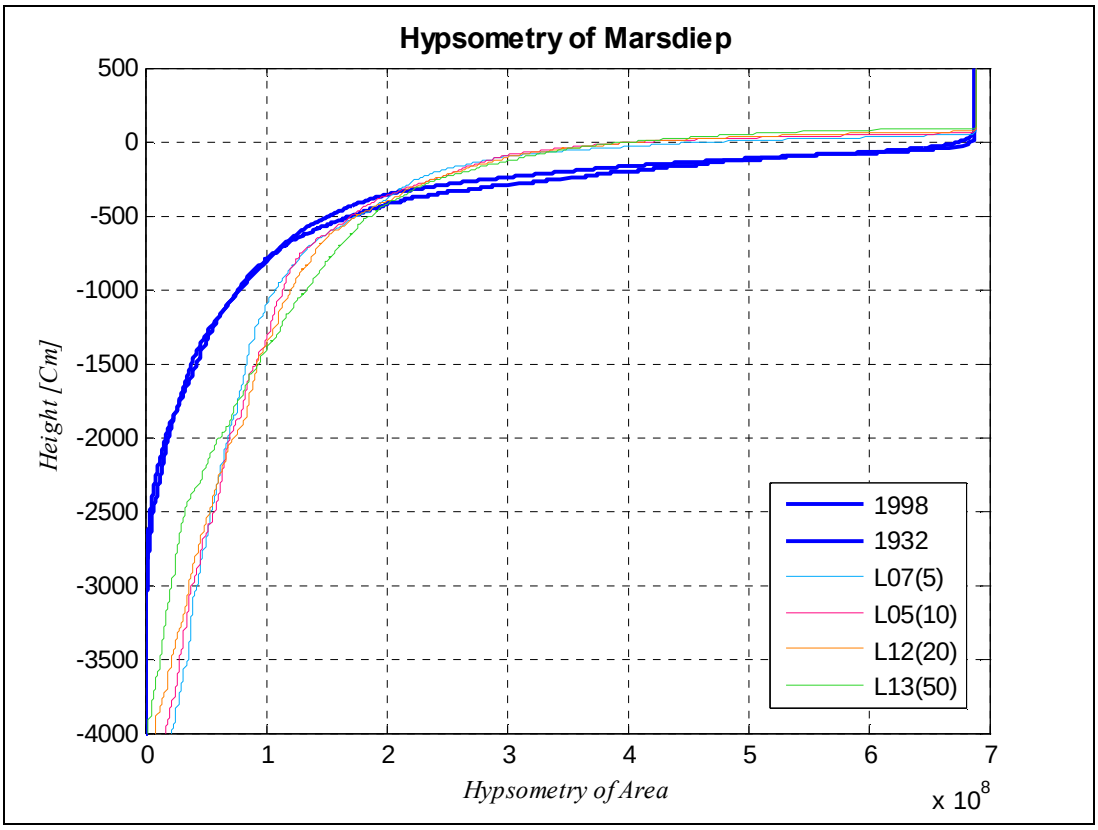

Figure 5-19:Final hypsometry of Marsdiep basin after 2100 years of simulation with real bathymetry (Legend : RunID(α_{bn}))

5.4.2 Friedrichs and Aubrey graph

Development of Marsdiep basin in this set of simulations on the Friedrichs and Aubrey graph is shown in figure 5-20. This graph shows that development of Marsdiep basin in the runs with real bathymetries similar to the simulation with schematized bathymetries is toward the ebb and flood dominant separation – equilibrium – line, and at some point near this line it begins to follow a trend parallel to that, which was shown in the result of simulations with schematized bathymetry for Vlie and Eierlandse Gat basins before. Amazingly in the simulation with α_{bn} equal to 10 this pivot point is exactly on the equilibrium line and the rest of development is exactly on the line.

The same graphs for Eierlandse Gat (Figure 5-21) and Vlie (Figure 5-22) are more scattered than the one for Marsdiep but still shows the same trend toward the equilibrium line and then parallel to that except in the Eierlandse Gat model with α_{bn} equal to 50, in which the movement toward the equilibrium line happens as a S shape curve.

Since the simulations with the value of 50 for α_{bn} shows some different behavior, for the rest of analyses this run is excluded.

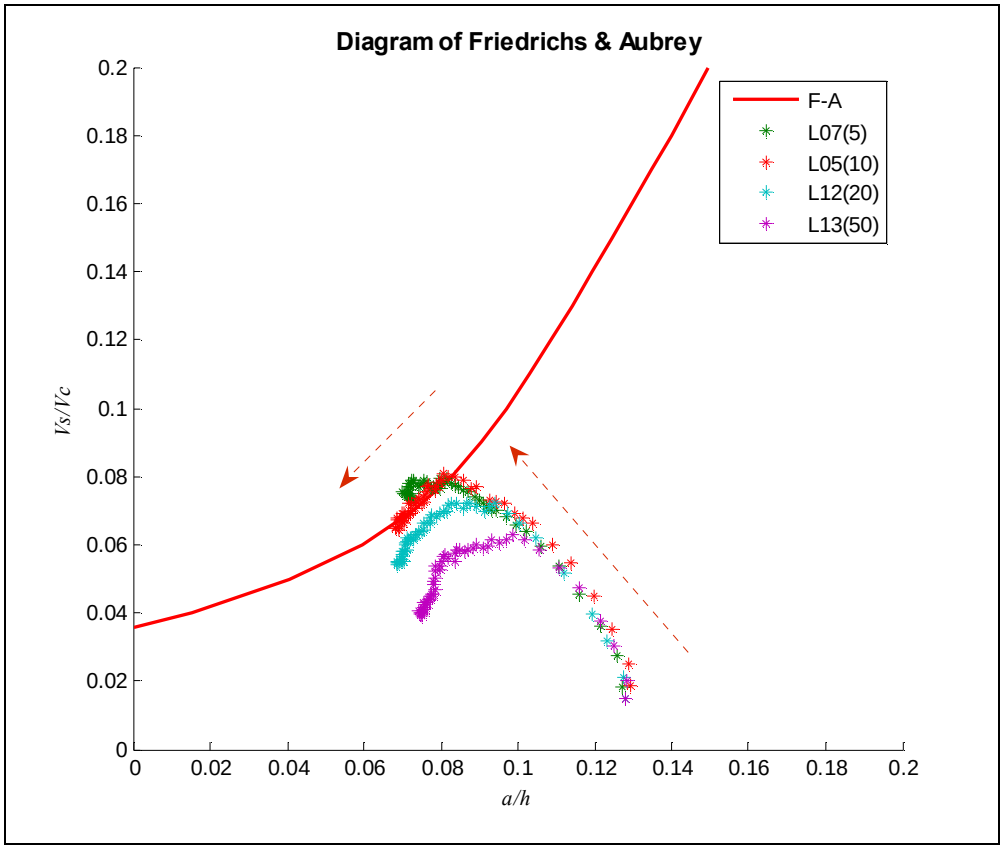

Figure 5-20:Friedrichs and Aubrey diagram for modeled Marsdiep with real bathymetry, (Legend : RunID(α_{bn}))

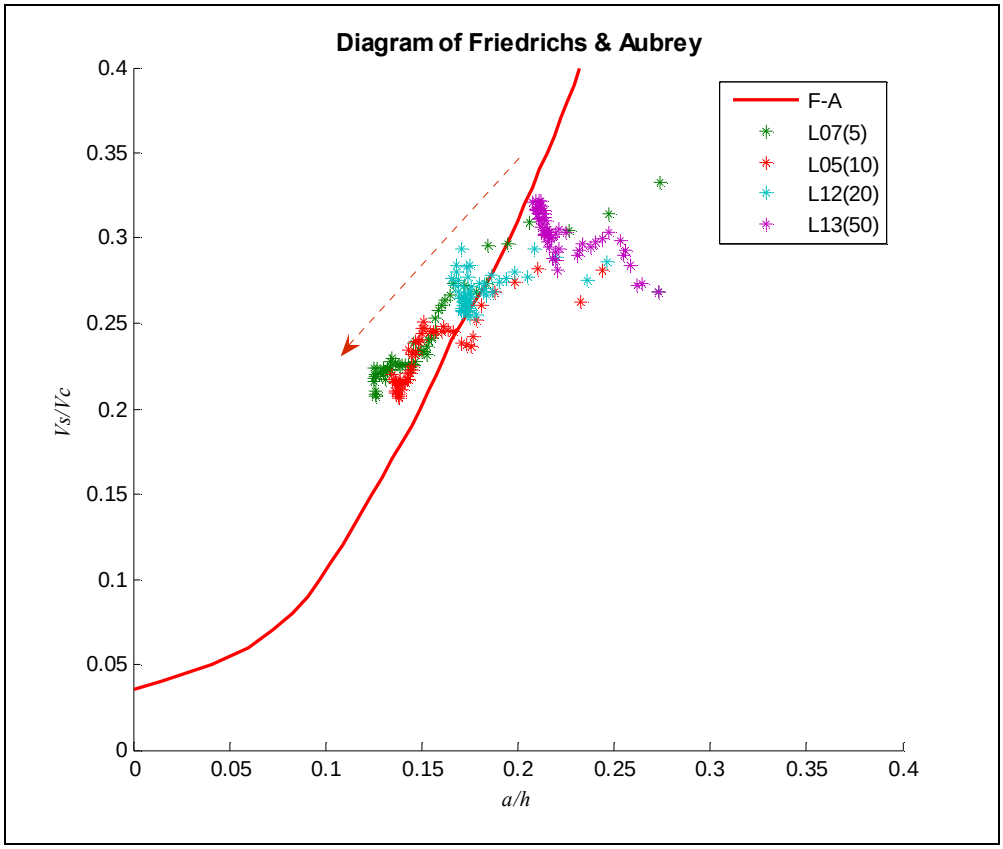

Figure 5-21:Friedrichs and Aubrey diagram for modeled Eierlandse Gat with real bathymetry

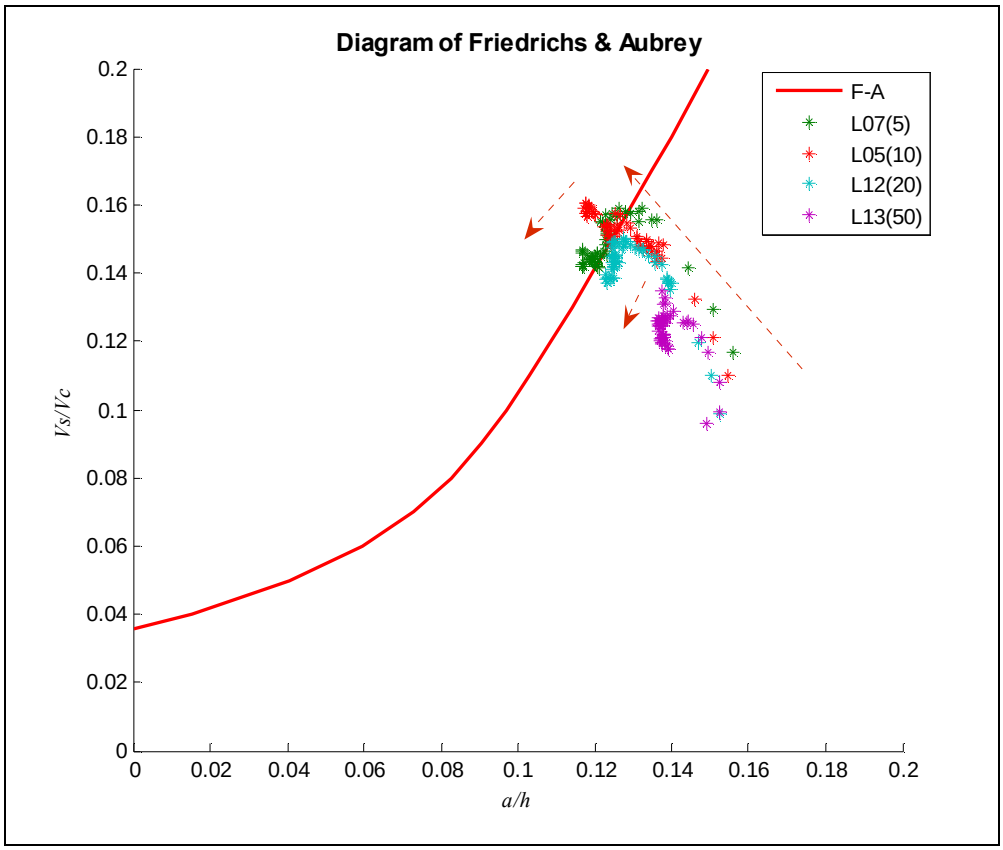

Figure 5-22:Friedrichs and Aubrey diagram for modeled Vlie with real bathymetry

5.4.3 Flat characteristics

The flat characteristics in Marsdiep basin in this set of simulations also shows the tendency of the model to reach an equilibrium value (Figure 5-23), but like the simulations with schematized bathymetry not towards the suggested equilibrium values (0.4 m for flat height).

For flat area the value of α_{bn} does not change the final equilibrium value, which can be expected from the hypsometry curves as well. But flat volume and therefore flat height for α_{bn} equal to 5 is less than α_{bn} of 10 and 20, which are almost the same. Obviously this is due to less sediment transport due to transverse bed slope effect with α_{bn} of 5.

Also the relative flat area A_f/A_b for these simulations goes to more or less the same value (Figure 5-24), which is again different from the value suggested by Renger and Partenscky (1974). (This value is shown in the same figure with straight line). This value is plotted on the Eysink (1991) graph too, (Figure 5-25). In this case also the basin develops toward the equilibrium suggested by him but does not stop in the range and continues to pass the suggested range of relative flat area for the Western Wadden Sea.

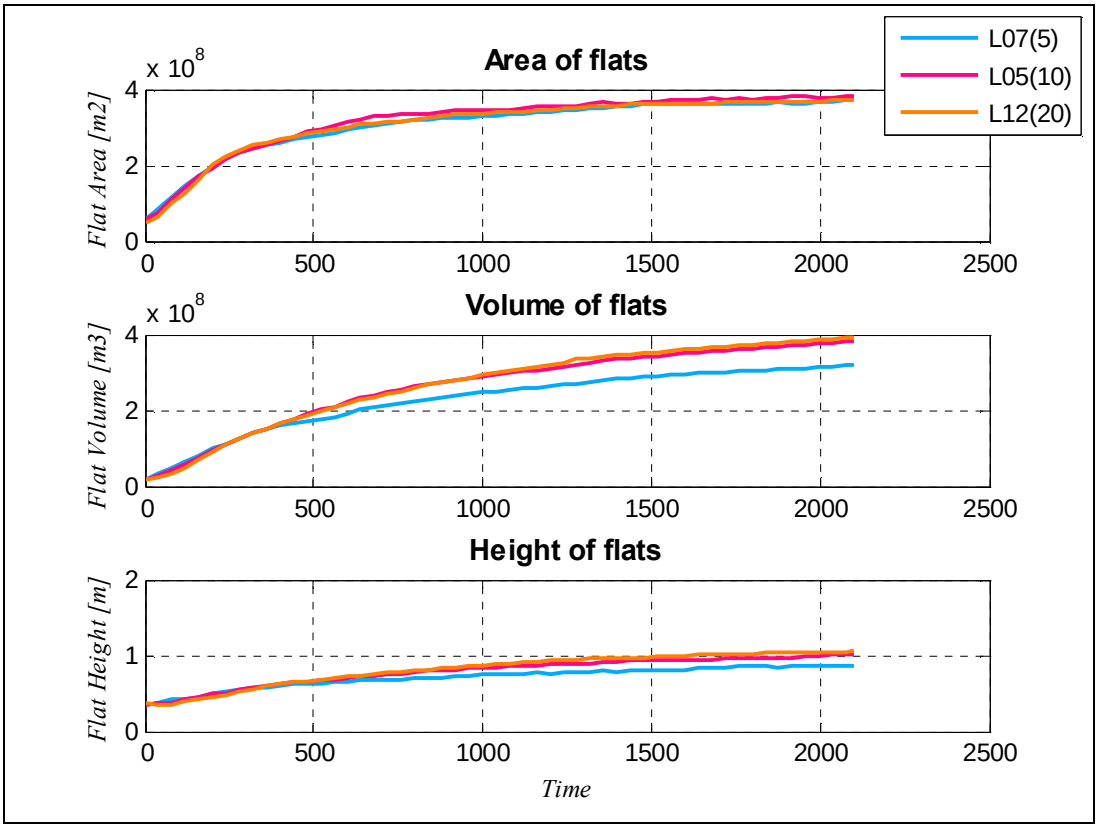

Figure 5-23: Development of flat characteristics in Marsdiep from real bathymetry, (Legend : RunID(α_{bn}))

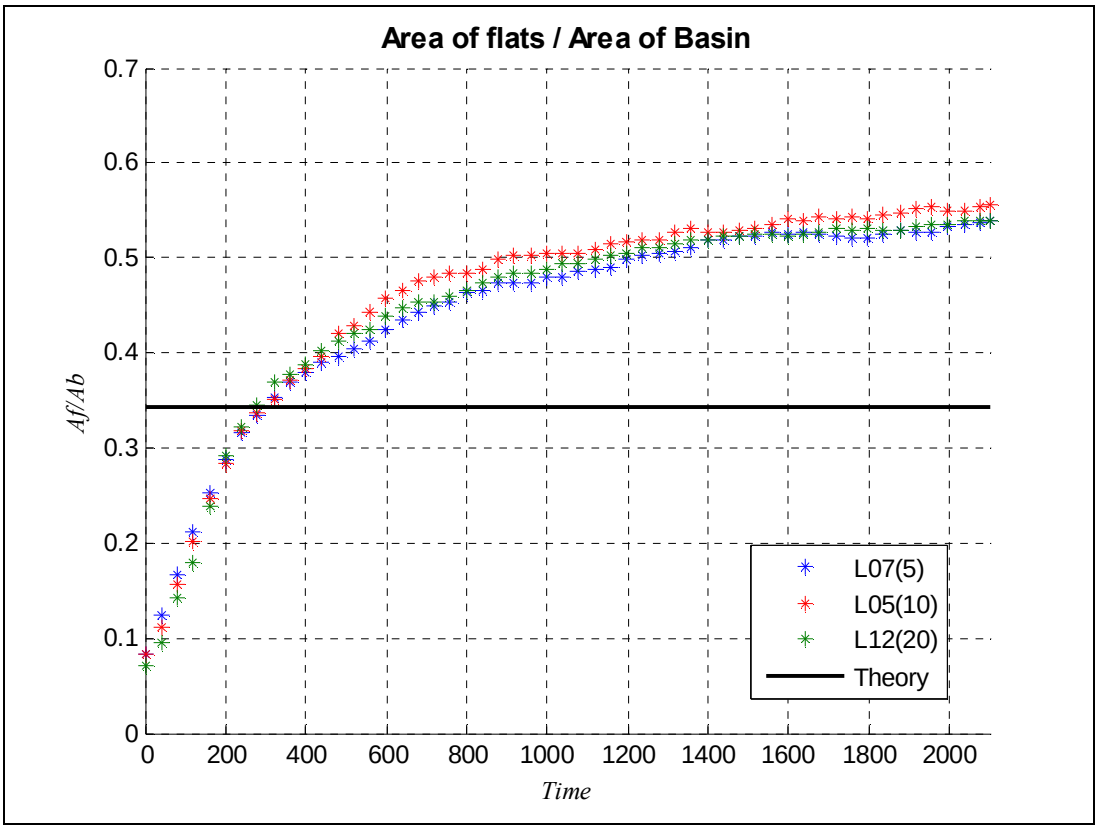

Figure 5-24: Relative flat area in Marsdiep during the simulation period with real bathymetry, (Legend : RunID(α_{bn}))

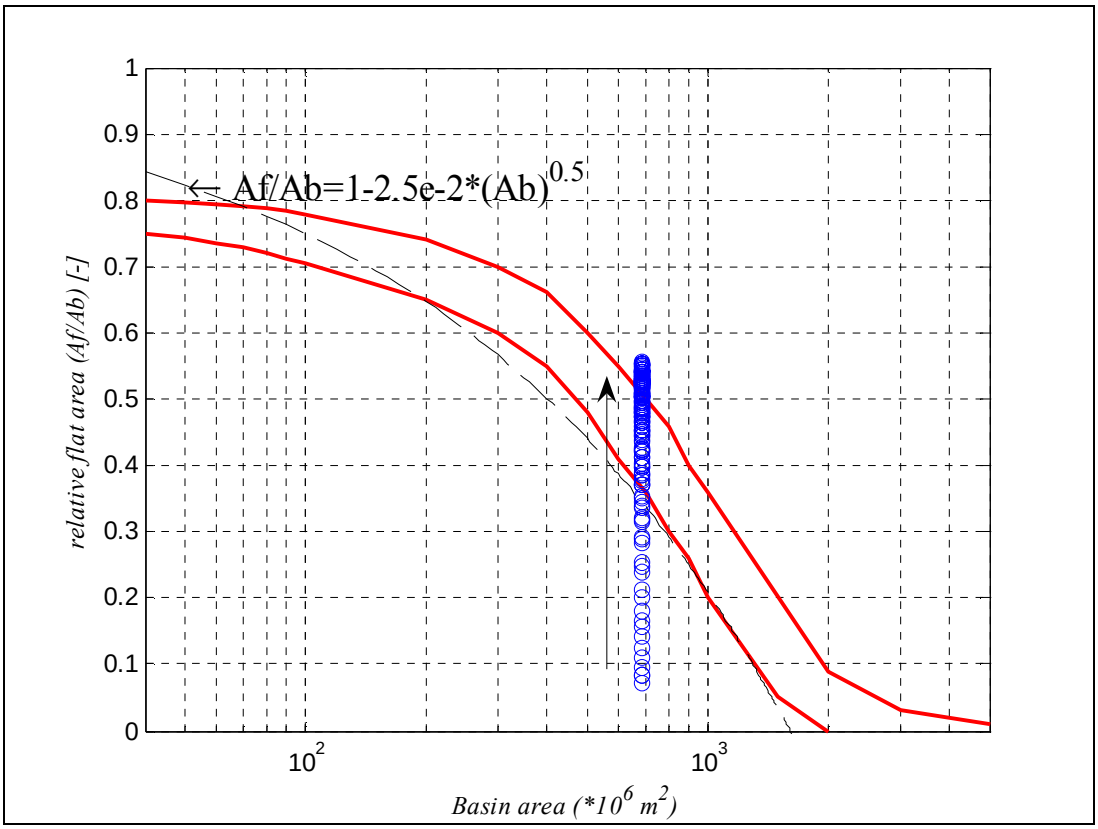

Figure 5-25: Relative flat area in modeled Marsdiep from real bathymetry on Eysink (1991) graph

5.4.4 Channel volume relation

In this scenario like the other simulations the model could not reach any stable condition for the relation between channel volumes and tidal prism. Changes of α_c in Eysink (1992) relation between channel volume and tidal prism is shown in figure 5-26 . The suggested equilibrium value for α_c is 16e-6.

5.4.5 Sediment balance

Changes in available sediment inside the Marsdiep, defined in 'Vaklodingen', data base is shown in figure 5-27. This figure shows that Marsdiep in this model imports about 400 Mm^3 during 2100 years of simulation, which is in order of 0.2 Mm^3 per year. But this rate is not constant during 2100 years. The main portion of the sediment import takes place in the first 300 year. During first 300 years about 300 Mm^3 of sand enters the Marsdiep with a maximum rate of about 3 Mm^3 per year in the first 40 year. While in last years of modeling this rate reduces to only 30,000 m^3 per year which is negligible so it can be claimed that from sediment exchange point of view the model reaches an equilibrium condition. On the other hand in reality if the effect of tidal current in sediment exchange of basin reduces to such extent, other forces such as wave and wind will have the main role in sediment transport, which are neglected in this study. Also it should not be neglected that sea level rise is not included in this study.

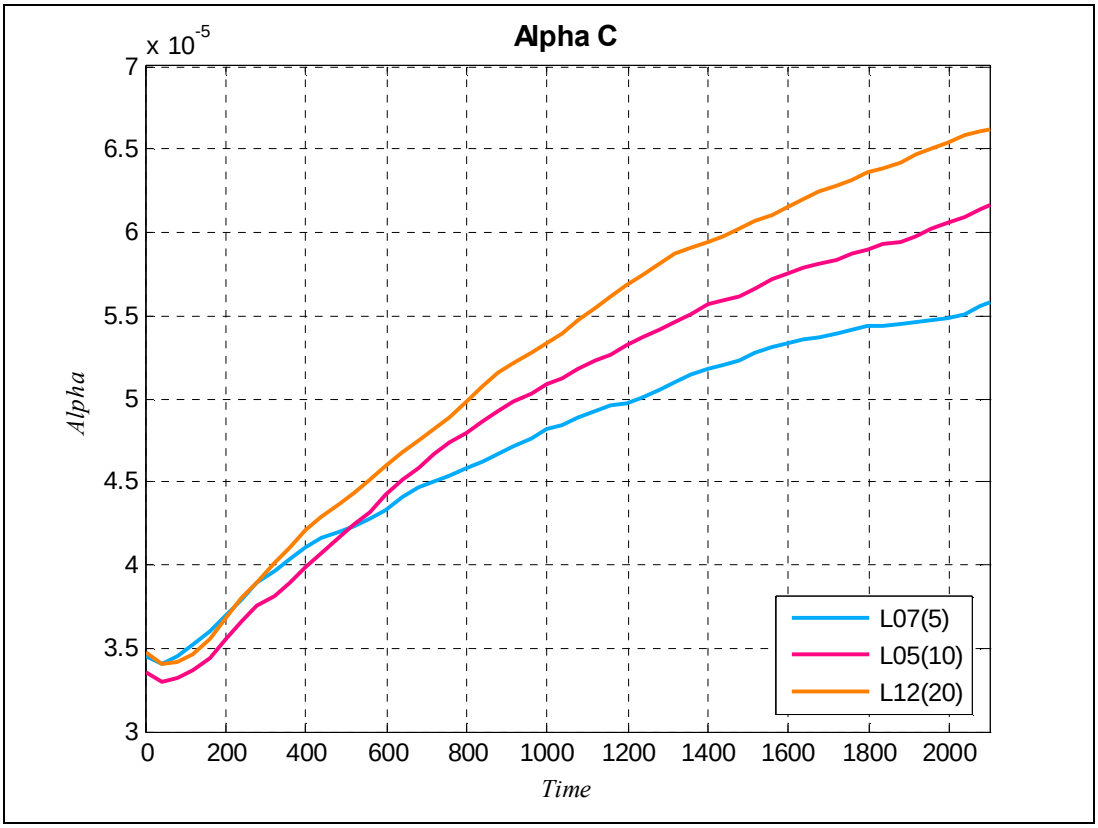

Figure 5-26: Changes of coefficient in the relation between channel volume and tidal prism (α_c) during 2100 of morphological modeling in Marsdiep from real bathymetry, (Legend : RunID(α_{bn}))

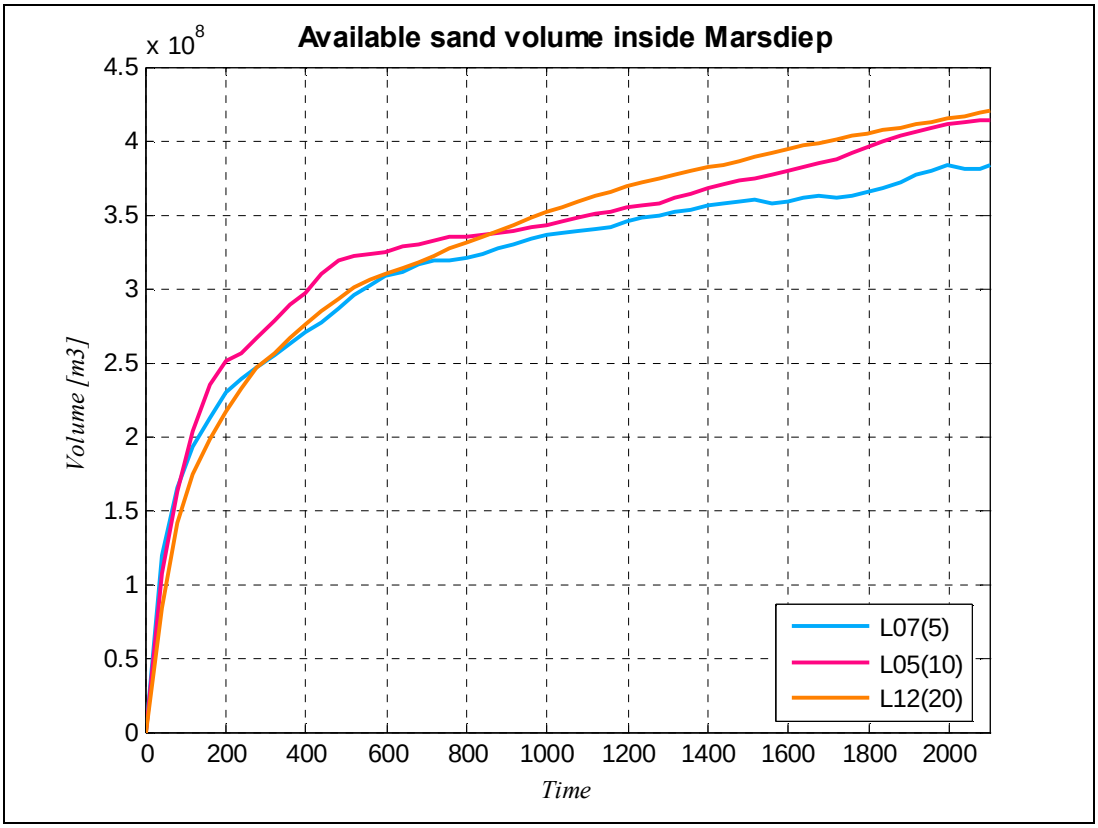

Figure 5-27: Changes in available sediment inside the defined border of Marsdiep in the simulations with real bathymetry, (Legend : RunID(α_{bn}))

5.4.6 Morphological development

Although the goal of this study is not to model the detail morphological changes, in this section some morphological developments in Western Dutch Wadden Sea simulation are discussed. This chapter is mainly based on the L05 simulation which is the run with real initial bathymetry and α_{bn} of 10. However, the effect α_{bn} on meso-scale phenomena is stronger.

5.4.6.1 Channel and shoal pattern

The cumulative erosion and sedimentation in western Dutch Wadden Sea is shown in figure 5-28. Due to simulation with only one fraction of sediment, the main channels of all three basins got much deeper and flats got shallower and wider. But the main interesting phenomenon which is observed in the model is the rotation of channels in Marsdiep and Vlie. As it can be seen in the figure, in Marsdiep the part of the main channel located behind the barrier island migrated towards the south west, while the channels inside the basin near the Afsluitdijk stretched in north east direction. In Vlie also the main channel moved toward the south west edge of the inlet while again the fractal structure of inside channels migrated toward the east. Mainly it can be claimed that both basins stretched their borders to the east.

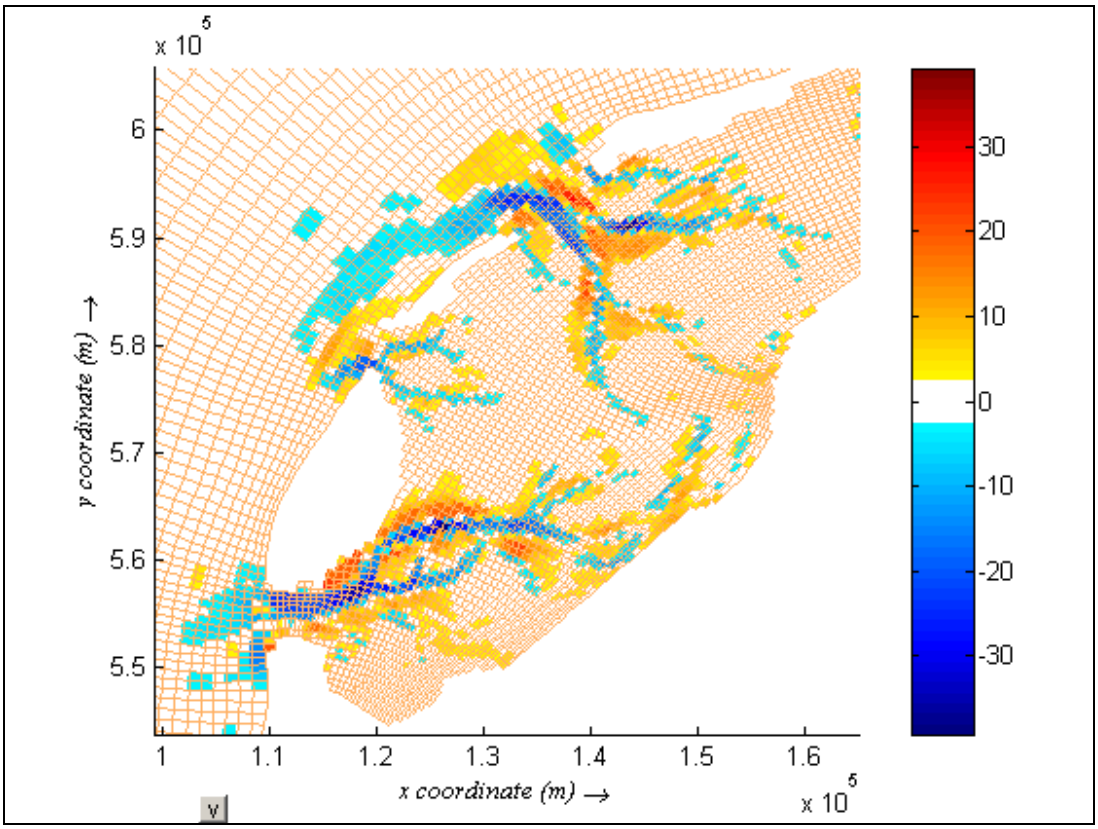

Figure 5-28a: Cumulative erosion and sedimentation in western Dutch Wadden Sea after 500 of morphological modeling from real bathymetry, with the orientation of channel migration.

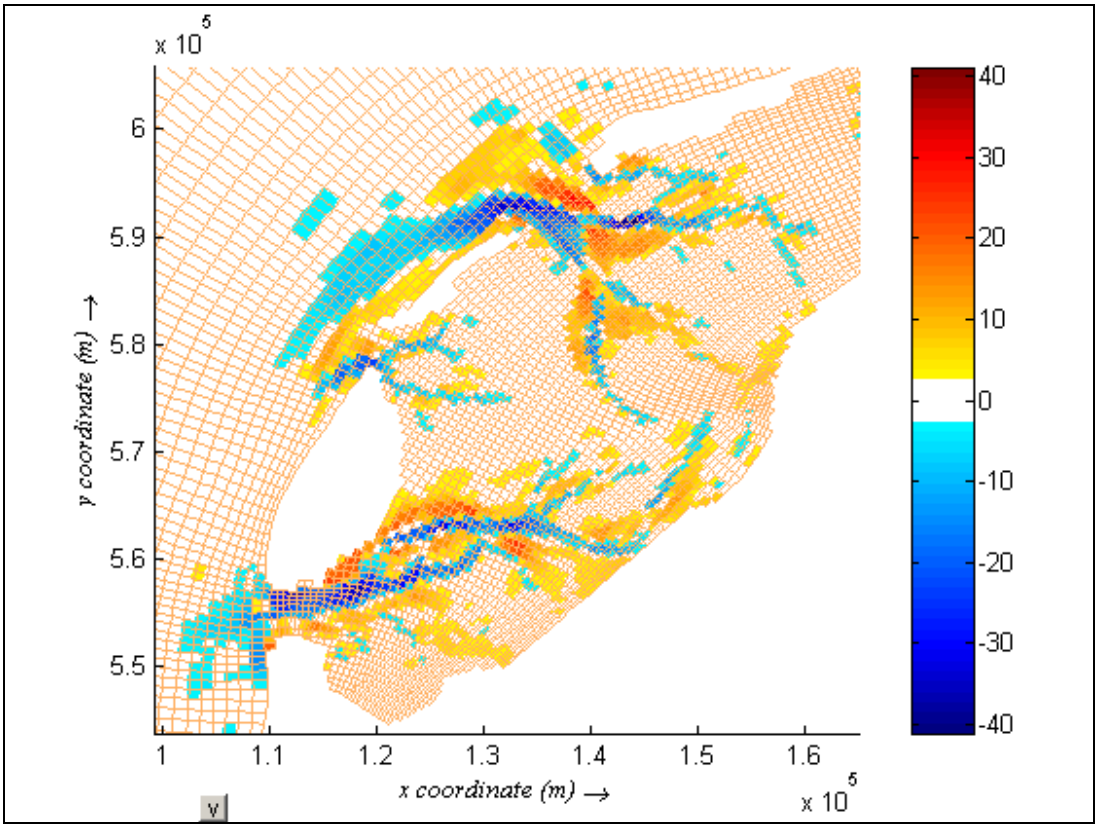

Figure 5-29b: Cumulative erosion and sedimentation in western Dutch Wadden Sea after 1000 of morphological modeling from real bathymetry, with the orientation of channel migration.

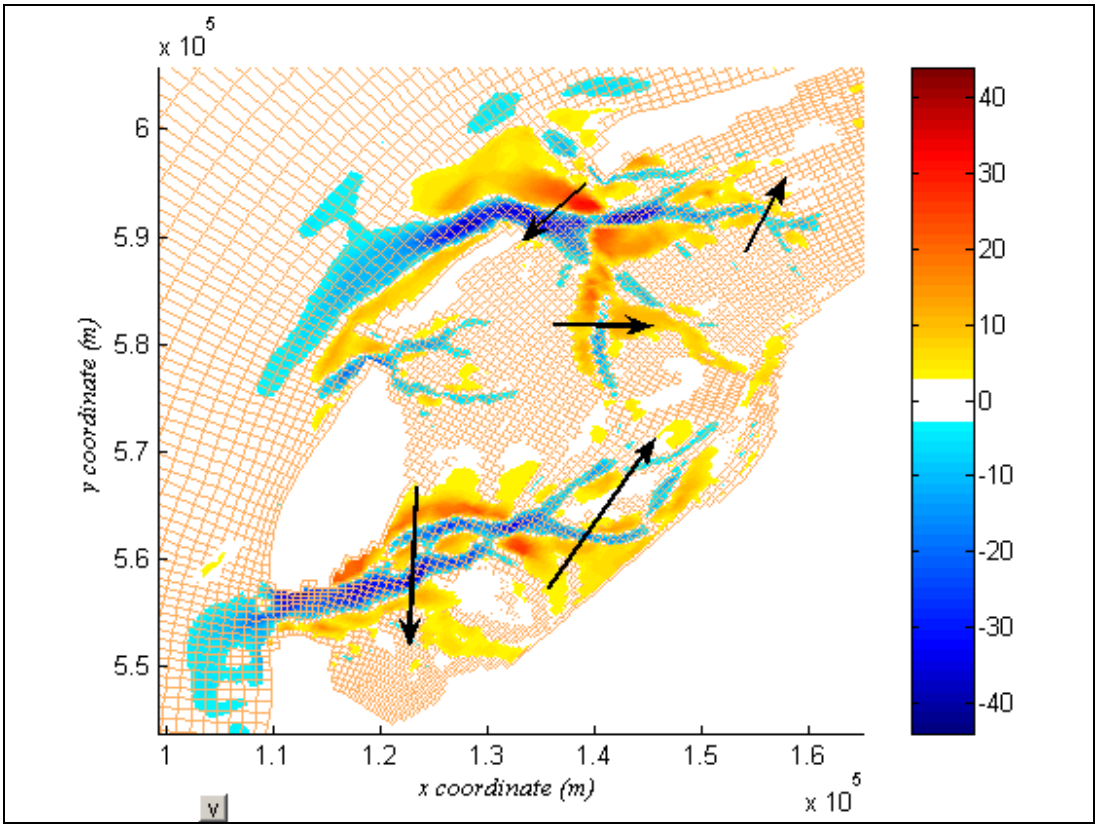

Figure 5-30c: Cumulative erosion and sedimentation in western Dutch Wadden Sea after 2100 of morphological modeling from real bathymetry, with the orientation of channel migration.

5.4.6.2 Marsdiep ebb-tidal delta

It is shown before that in this simulation Marsdiep basin imports sediment with relatively large rates in the first decades. The main source of this sediment is its ebb-tidal delta. Figure 5-29 and 5-30 show the erosion of this delta during the simulation in the L05 run, the contour line of -5m has almost disappeared after 250 years of simulation and later this erosion continues while some sediment is also eroded from the adjacent coastline.

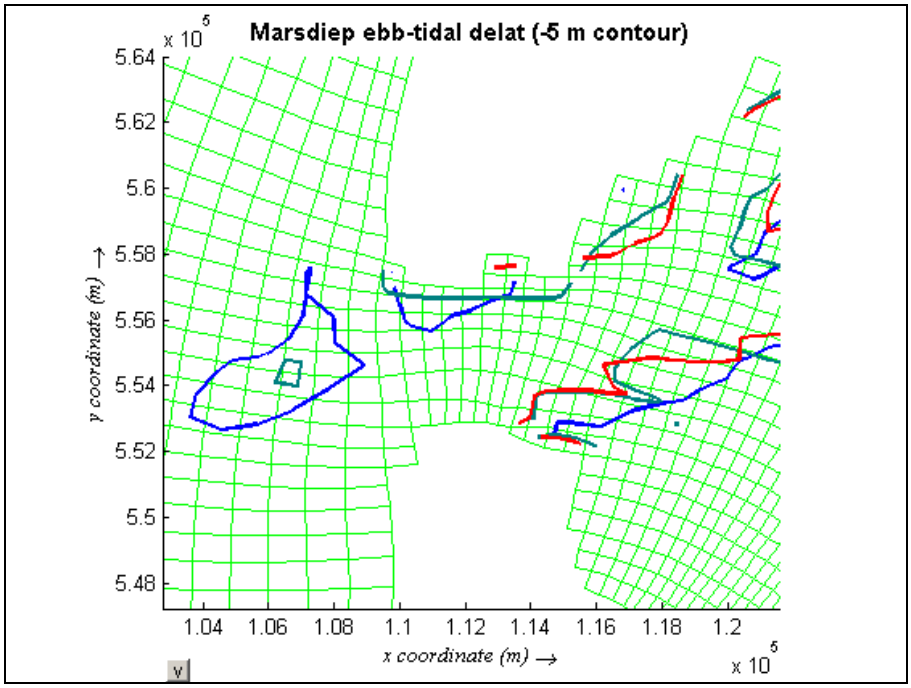

Figure 5-31:Contour line of -5 m for Marsdiep ebb-tidal delta in initial bathymetry (blue), After 240 years (green) and after 2100 years (red) in simulation L05

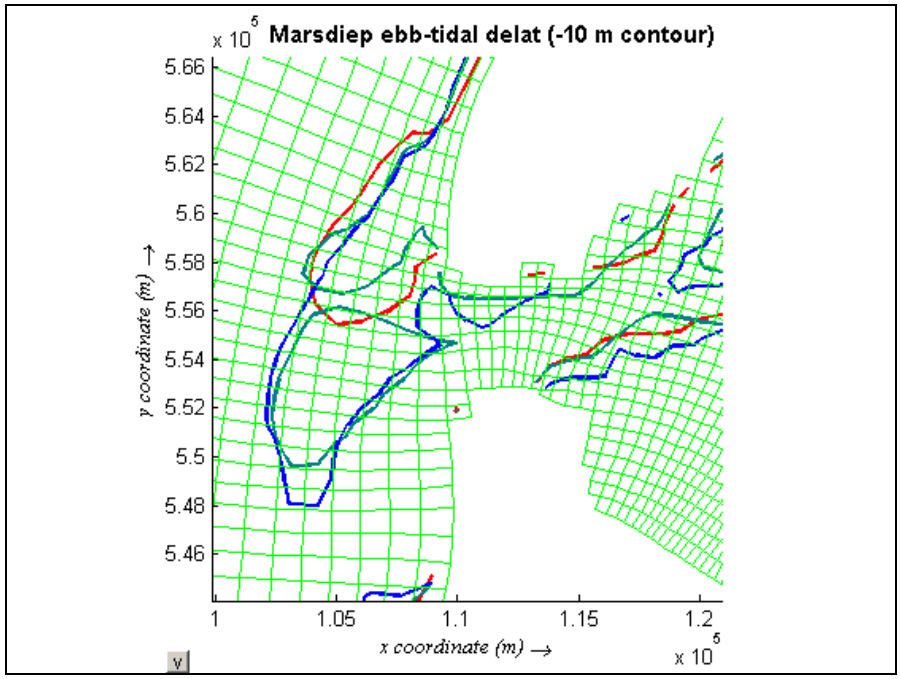

Figure 5-32:Contour line of -10 m fro Marsdiep ebb-tidal delta in initial bathymetry (blue), After 240 years (green) and after 2100 years (red) in simulation L05

If the same figure is produced for other simulation with lower α_{bn} (L07), which means lower sediment transport capacity the outcome will be different. It is shown in figure 5-31 that in this simulation the ebb-tidal delta is eroded but not completely and another channel is developed north of the delta, while the sediment is imported from adjacent coastlines more in this simulation. So, as it was expected the effect of transverse bed slope coefficient on the patterns of channels and shoals is not negligible.

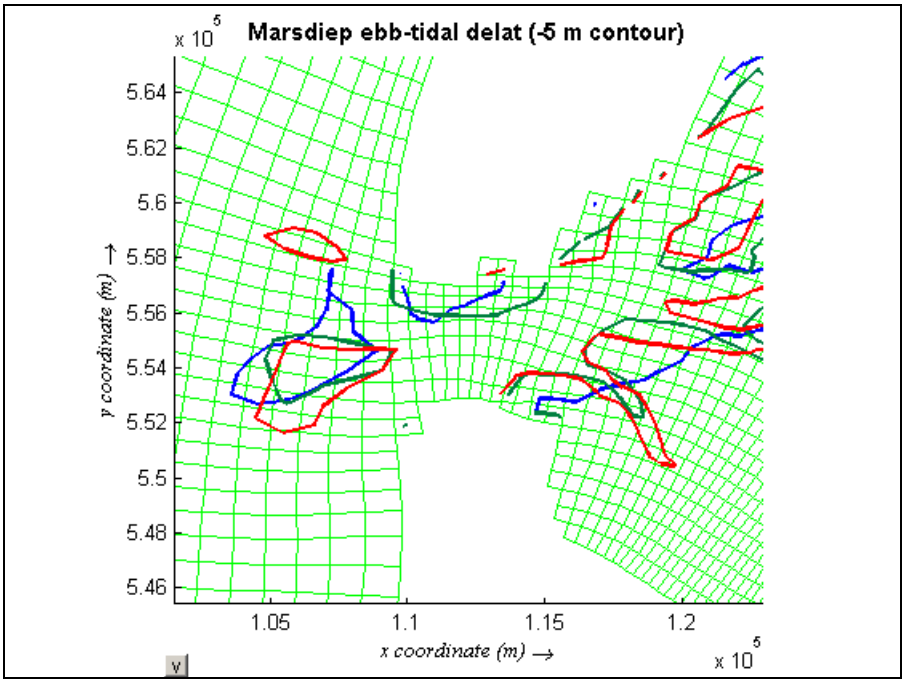

Figure 5-33:Contour line of -5 m fro Marsdiep ebb-tidal delta in initial bathymetry (blue), After 240 years (green) and after 2100 years (red) in simulation L07

5.4.6.3 Vlie inlet

The other morphological changes are in Vlie inlet. It was claimed in schematized bathymetry scenarios that the Vlie inlet in this model is too wide for one main entrance. In the simulation with real bathymetry it is observed that the main channel migrated toward south west and the second channel developed at the north side of the inlet, which resembles the two main channel condition resulted from schematized bathymetry simulations. Migration of main channel of Vlie has been observed in reality as well.(See sec. 3.4.3.2)

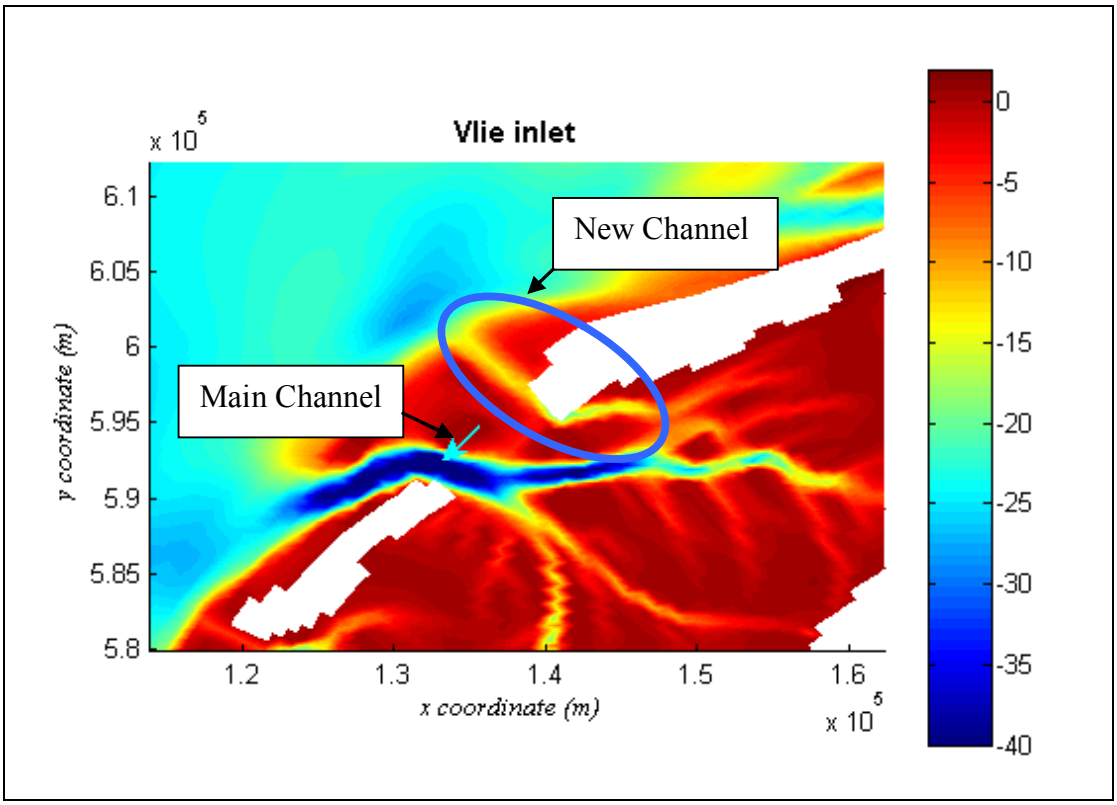

Figure 5-34:Vlie inlet bathymetry after 2100 years of morphological simulation

5.5 Analyzing basin boundary changes

After abovementioned observations especially the morphological development in simulations with real initial bathymetry, it seems that the boundaries which are defined in 'Vaklodingen' data-base for different basins in the Western Wadden Sea may not be a good choice in long periods. Also the important role of this boundaries in analyses are mentioned in other studies in the same region, but to the knowledge of the author, no extensive study has been done on this issue yet and most of the investigations are based on this predefined boundaries. In this section of this report, the changes in boundaries of tidal basins in the study area are discussed briefly. To study the change of the boundary, results of one simulation with real initial bathymetry are used (L05) and resulting bathymetry of morphological modeling is extracted from the results in years 0,200,700,1200, and 2100. Then to provide the corresponding flow field in all these years, 5 hydrodynamic simulations for 5 tidal cycles are carried out using the extracted bathymetries. Having the bathymetry and flow field in each case it is possible to define the boundaries between tidal basins in the model of the Western Dutch Wadden Sea.

5.5.1 Definition of the boundary

The physical boundary between tidal basins is the tidal divide, but to find it in the result of simulations this definition should be translated to flow field or bathymetry characteristics. In this study it is suggested that the line of minimum standard deviation of (depth averaged) velocities is the tidal divide. Standard deviation of velocities can be calculated for all the velocity points in grid cells by Delft3D toolbox.

5.5.2 Validation of definition

To check the abovementioned definition the result of hydrodynamic simulation for the initial bathymetry of the morphological simulation is used (Run ID : HB5). The flow field is analyzed to find the standard deviation of the velocity and the 'Vaklodingen' boundaries is drawn on the map of velocity standard deviation (Figure 5-33). It is clear that these boundaries match the minimum values on the map, so this definition can be used to define the boundaries in different years of morphological simulation.

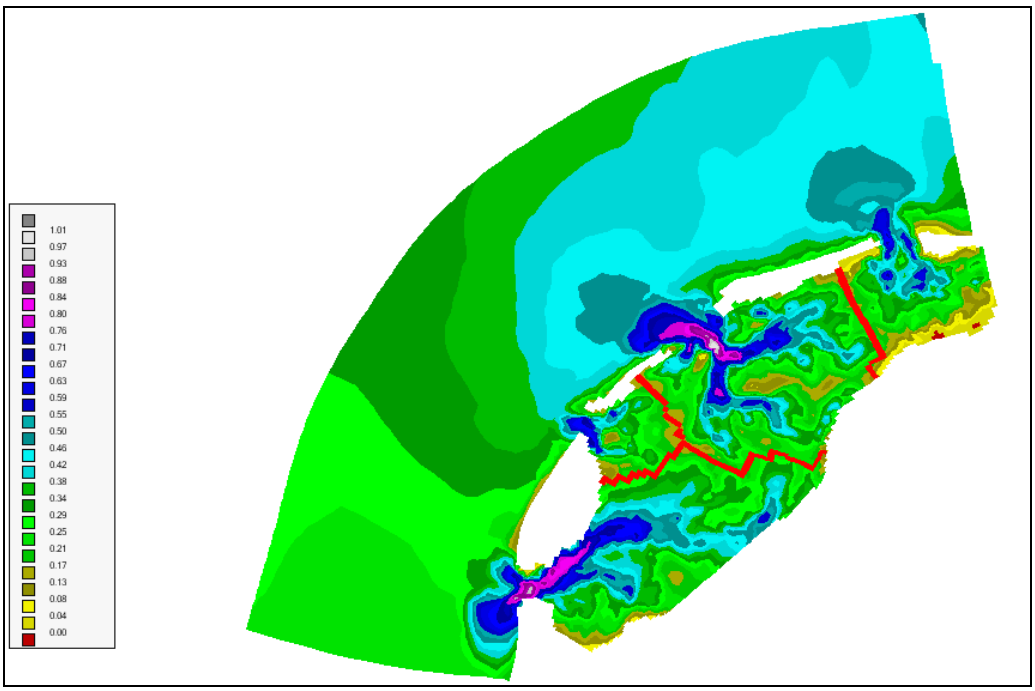

Figure 5-35: Vaklodingen boundaries (red lines) on the map of standard deviation of mean velocity for the initial bathymetry

5.5.3 Application of definition

To use the same method to determine the boundaries in morphological years of 200,700,1200, and 2100, the corresponding hydrodynamic simulations are analyzed to determine the standard deviation of the velocities. Then the line of minimum values is determined visually and used as the boundary of basins in different analyses. The result of this procedure for year 2100 is shown in figure 5-34.

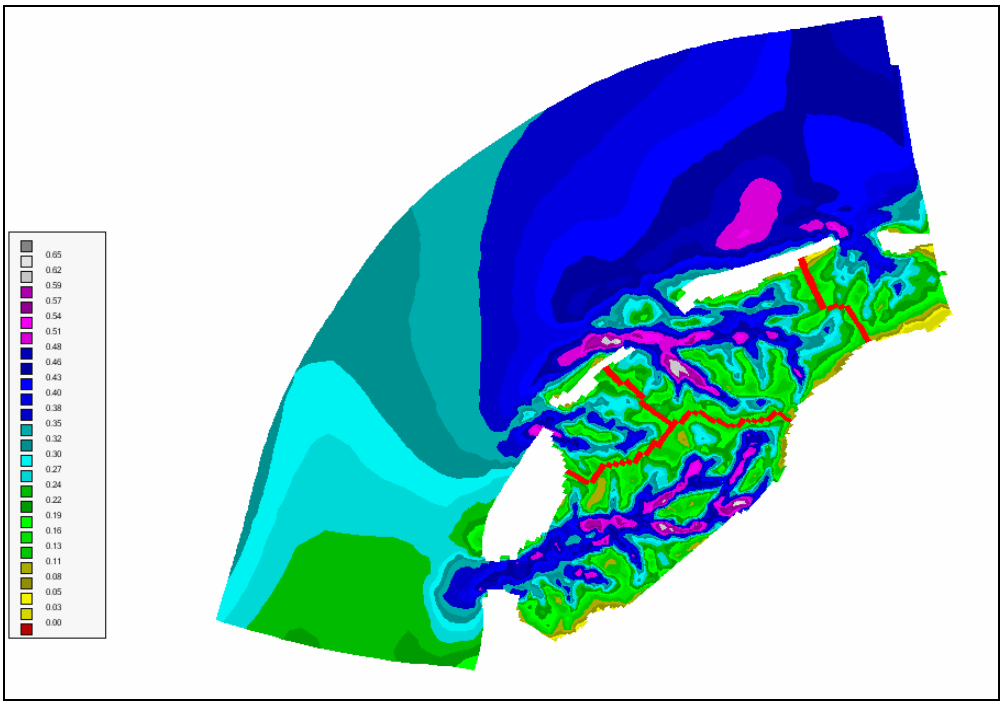

Figure 5-36:Map of standard deviation of velocity and visually defined boundaries after 2100 years of morphological modeling.

5.5.4 Changes in the boundaries

Applying the definition of boundary on result of different years, boundary of the basins are defined and plotted on the bathymetry in different morphological years.(Figures 5-35 to 39)

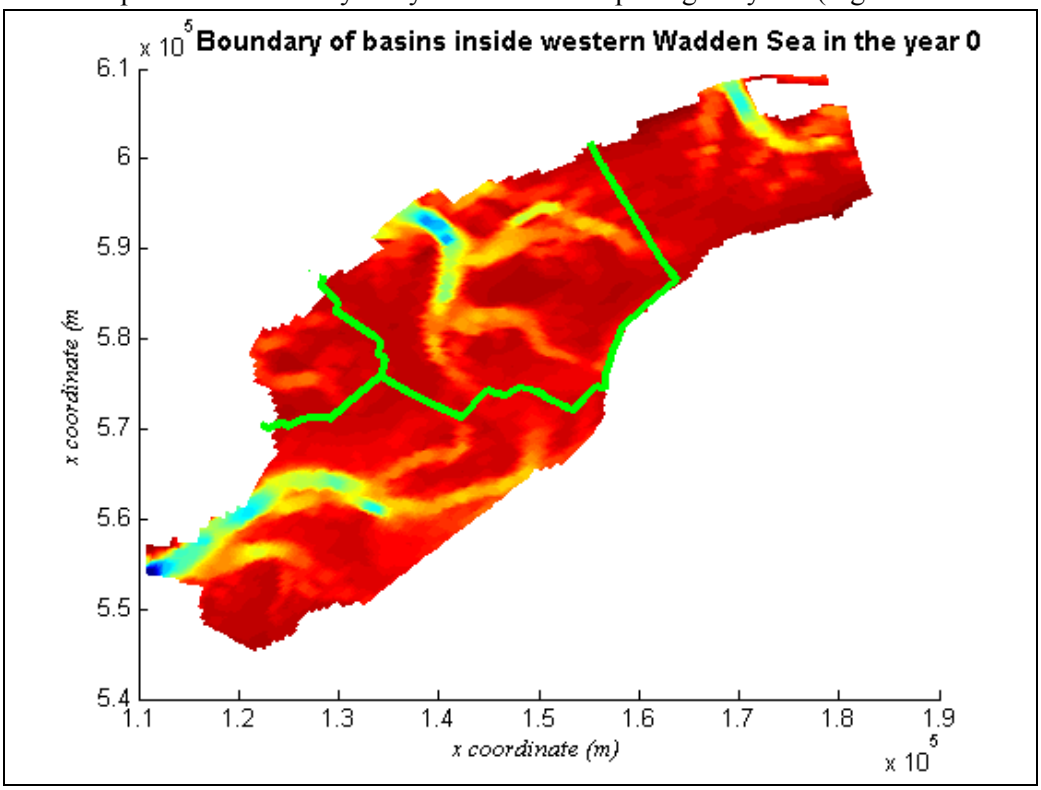

Figure 5-37: Boundary of basins inside the Western Wadden Sea, at the beginning of simulation

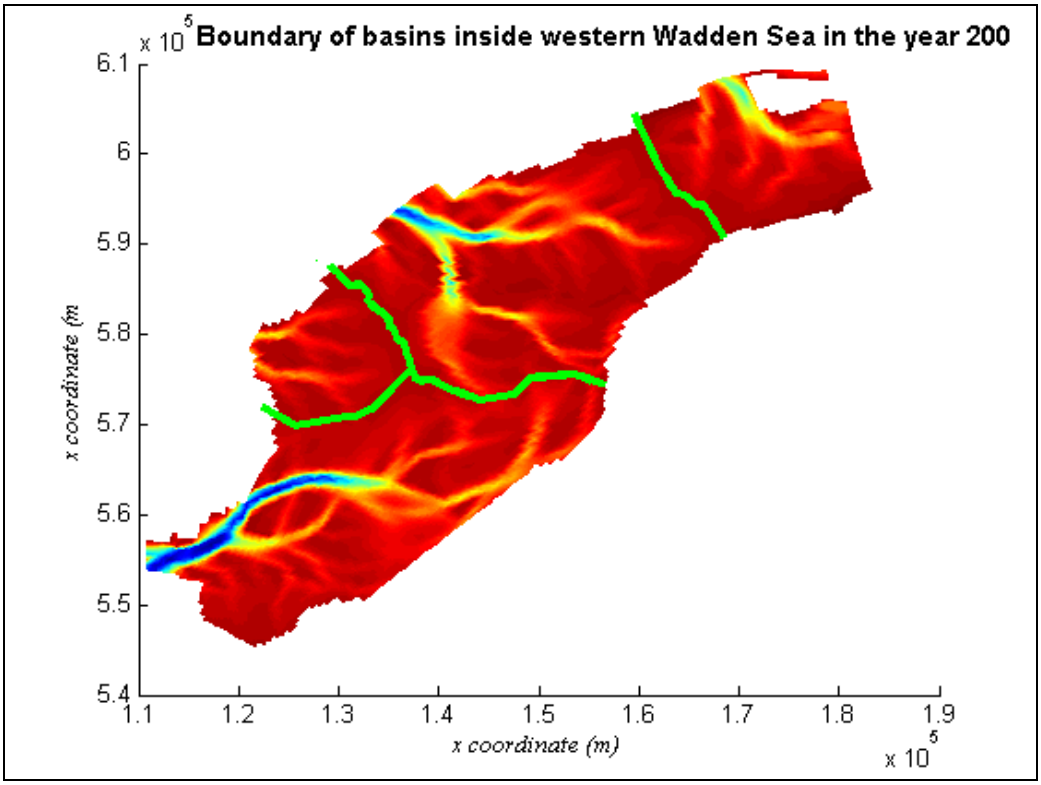

Figure 5-38: Boundary of basins inside the Western Wadden Sea, after 200 years of morphological simulation

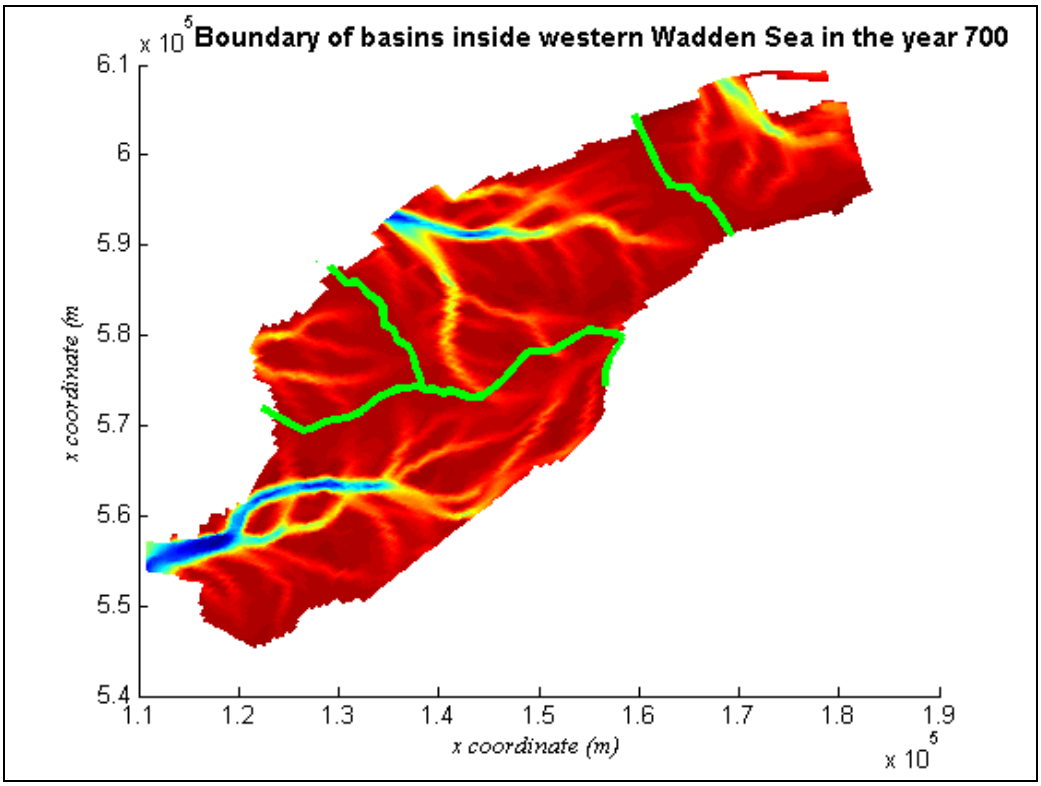

Figure 5-39: Boundary of basins inside the Western Wadden Sea, after 700 years of morphological simulation

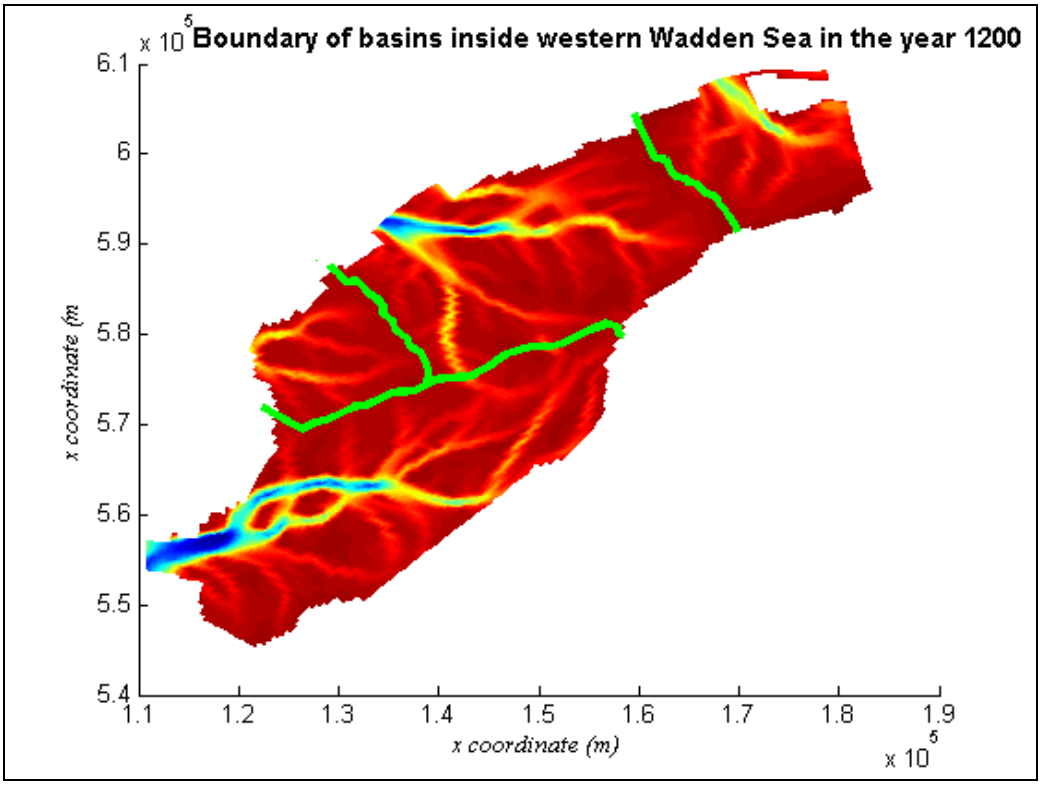

Figure 5-40: Boundary of basins inside the Western Wadden Sea, after 1200 years of morphological simulation

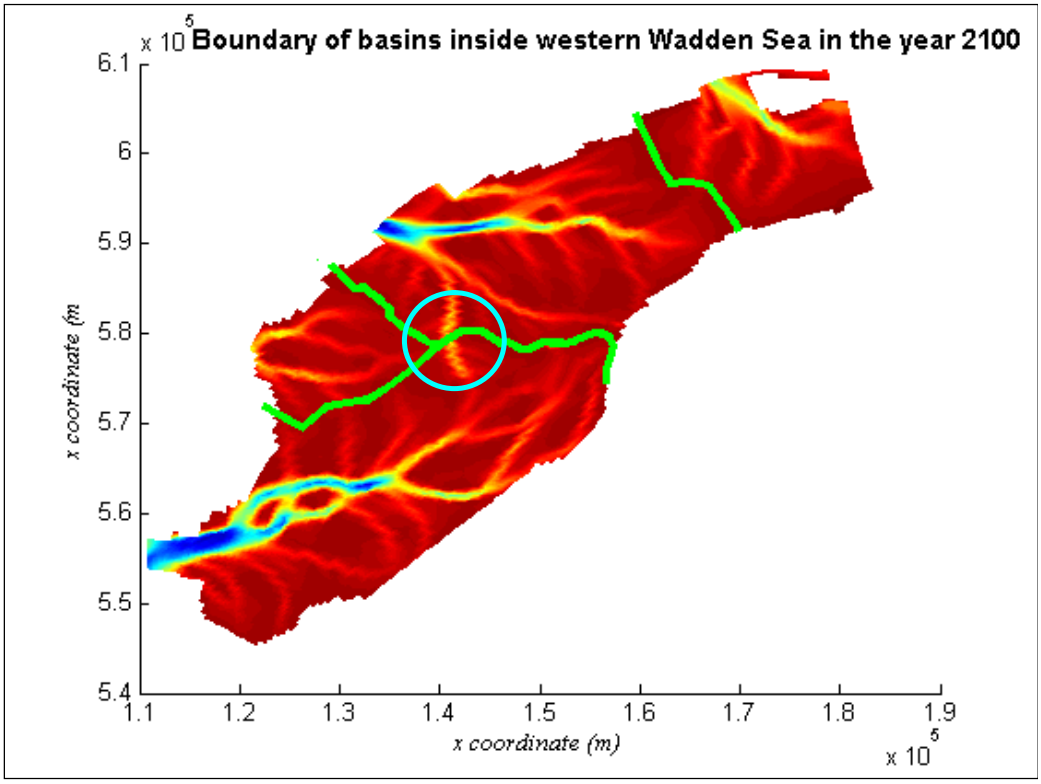

Figure 5-41: Boundary of basins inside the Western Wadden Sea, after 2100 years of morphological simulation

The results clearly show that the boundaries of the basins are stretching eastward; Marsdiep is gaining area from Vlie, while Vlie in its turn is extending its boundary into the Ameland. But in the case of Eierlandse Gat the boundary of this basin does not expand, this boundary only rotates toward east. Plotting the boundaries over the bathymetry also shows a good agreement between the defined boundaries and expected boundaries of the basins from bathymetry. Only in one case in morphological year of 2100, there is channel that the suggested boundary divides it between Marsdiep and Vlie, This contradiction can be explained by the fact that this channel is an old channel which is abandoned and the new channel inside the Vlie basin is developing in the east side of this channel.

This simulation is in agreement with the available hypothesis about stretching Marsdiep basin to the east. Also in parallel study on the measured data during 1926-2006 the same behavior is observed (figure 5-40 from Van Geer, 2007).

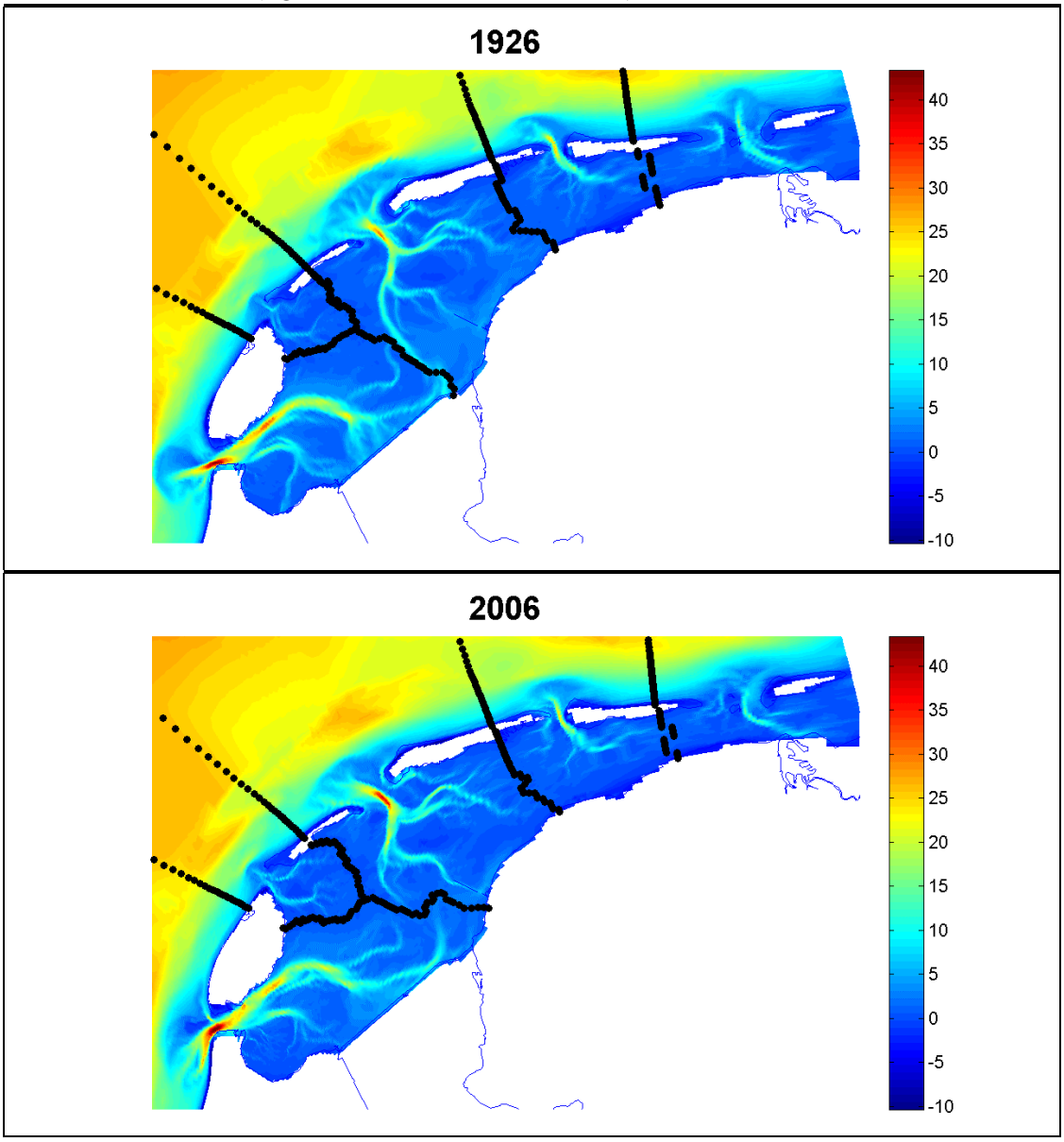

Figure 5-42:Boundaries of the basins in Dutch Wadden Sea defined on bathymetry in years 1926 and 2006 (Van Geer, 2007)

The result of the model in this study can be distorted by two different issues, first human interventions which are not modeled in this simulation, mainly the Pollendam near Harlingen, and second the boundary of the simulation area in the north east, that restrict the boundary of Ameland basin and does not let this boundary to move to east.

In next section the characteristics of the basins are determined using different boundaries for different morphological years.

5.5.5 Characteristics of basins with moving boundaries

Unlike previous analyses in this section the analysis of basin characteristics is based on the changing boundaries. The characteristics of Marsdiep, Vlie and Eierlandse Gat basins are determined for morphological years of 0,200,700,1200, and 2100 according to new boundaries in each year.

One of the most important differences in this case is that the area of the basin is not constant during the time any more. The changes in the area of the basin are shown in figure 5-41. It is clear that area of Marsdiep is increasing while Vlie basin is decreasing in size, on the other hand the area of Eierlandse Gat does not change extensively during the simulation.

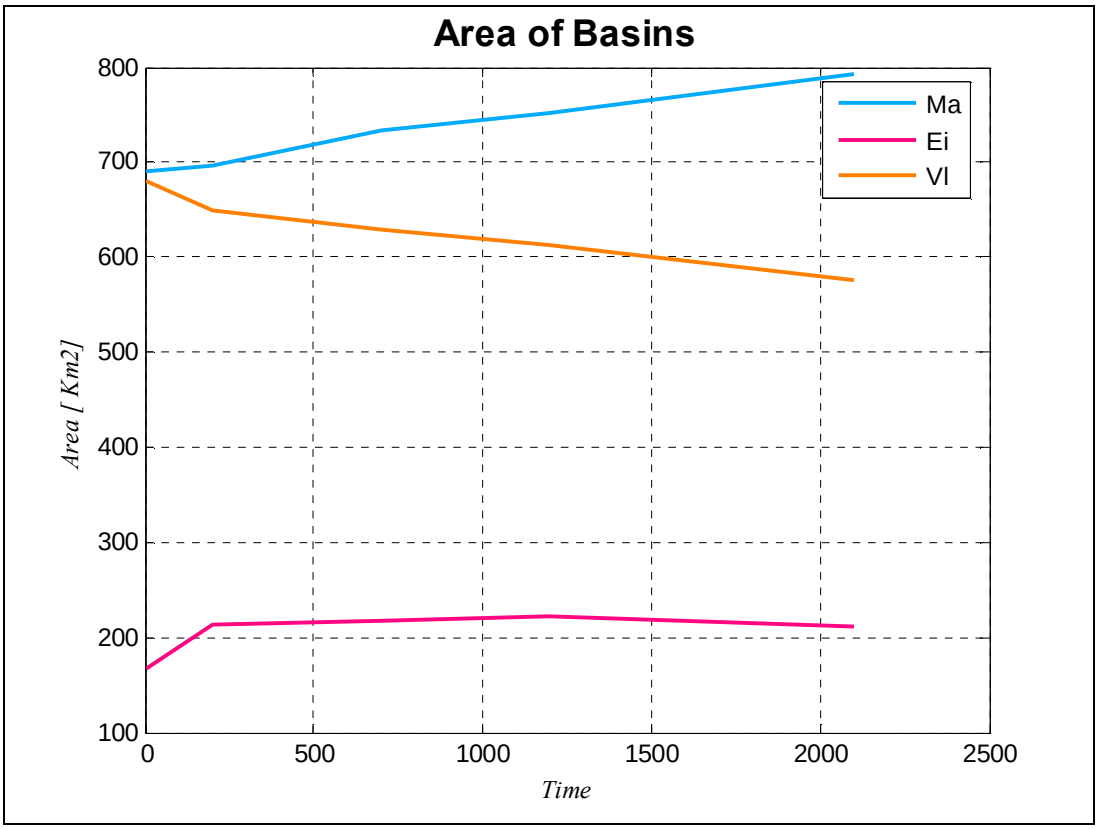

Figure 5-43:Development of basin areas during the simulation time

The development of flats for the basins are shown in figure 5-42; the behavior of this basins from this point of view is almost the same as the result from the fixed boundaries. In this case the development of flat height toward the stable (equilibrium) value is faster but still it is far from the value suggested by Eysink (1992).

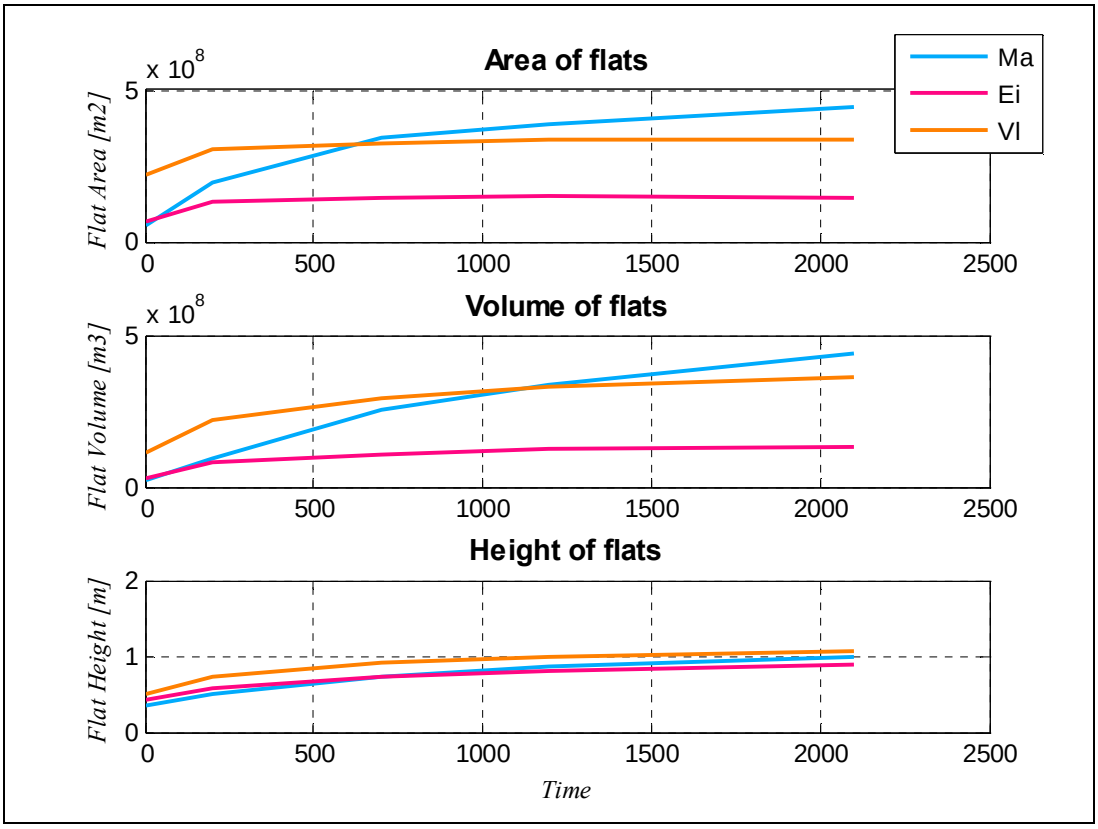

Figure 5-44:Development of flat parameters for different basins during the simulation, considering changing boundaries

An other parameter which is affected by changing the area of basins is the relative flat area (A_f/A_b). Development of this parameter for basins is illustrated in figure 5-43 and also in figure 5-44 on Eysink (1991) graph for Wadden Sea basins.

Clearly the relative flat area in different basins tends to be stable and reach an equilibrium value but as it is shown in figure5-44, for Marsdiep basin the final value is not in the range that Eysink (1991) suggested for the basins in Wadden Sea, Also the final value in both Marsdiep and Vlie basins are far from the suggested relation for German bights by Renger and Partenscky (1974). It seems that both suggestions are more accurate for small basins than large or very large basins. It should be notified that both suggestions are based on measured data of recent condition of tidal basins, but clearly some of the basins which are used in development of these relations such as Marsdiep, are not in equilibrium yet. Therefore this relation may be subjected to some distortion.

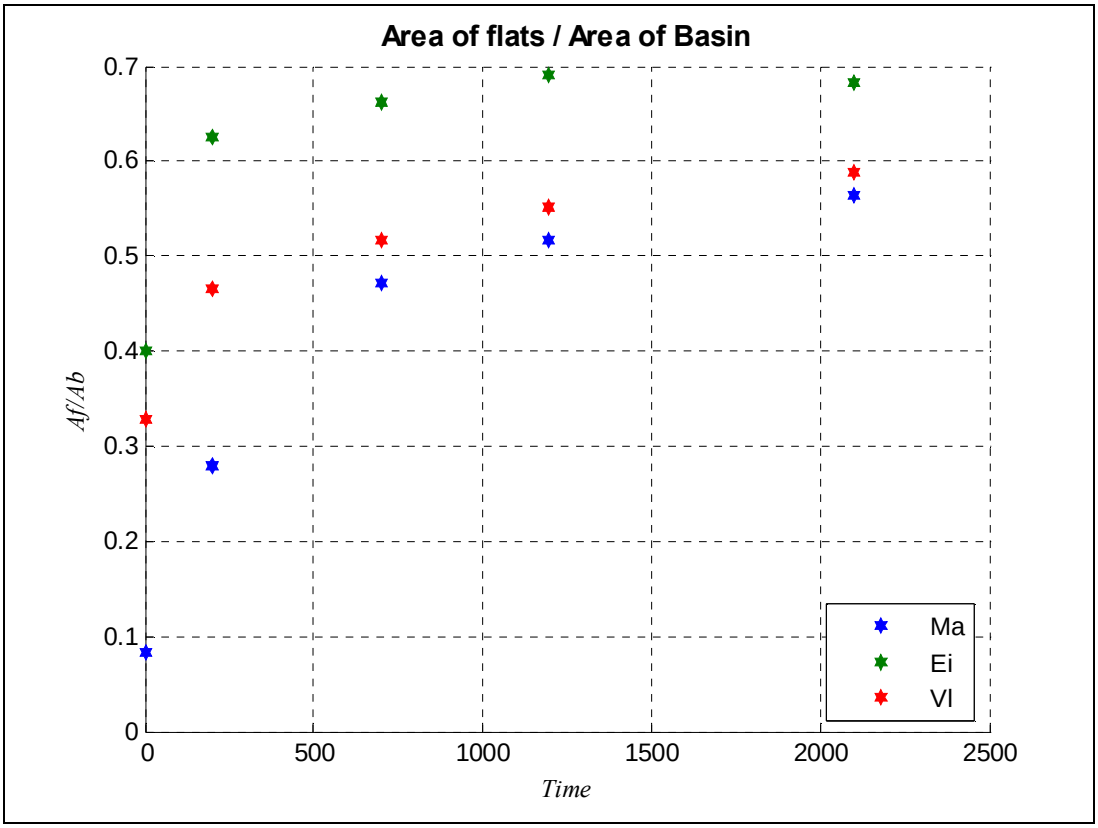

Figure 5-45: Development of relative flat area of basins during the simulation, considering varying boundaries

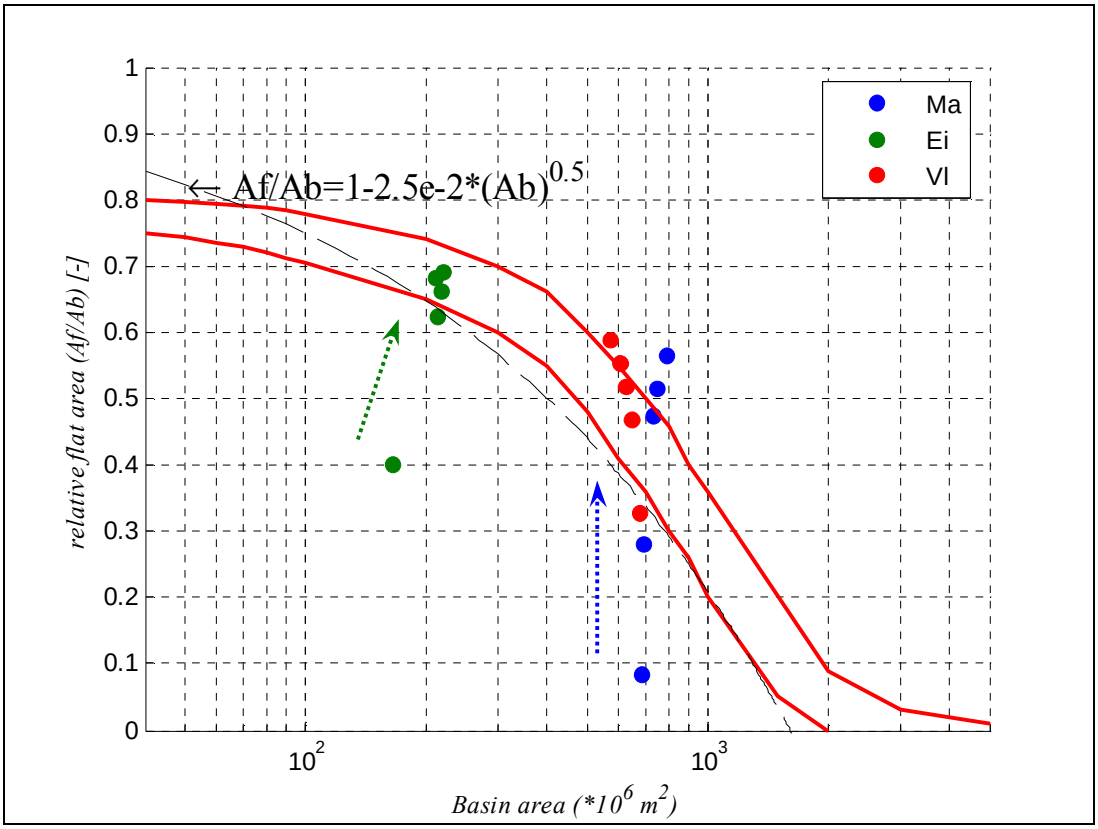

Figure 5-46: Development of relative flat area of basins during the simulation plotted on Eysink (1991) graph for Wadden Sea, considering changing boundaries

The result of this new analysis is also plotted on Friedrichs and Aubrey graph in figure 5-45. The outcome shows that as it is expected from previous results the basins develop through the equilibrium line and then continue to develop parallel or on that line. Marsdiep reaches the line after 700 years while Eierlandse Gat passes the line before year 200, and Vlie begins to develop more or less parallel to the line after 200 years.

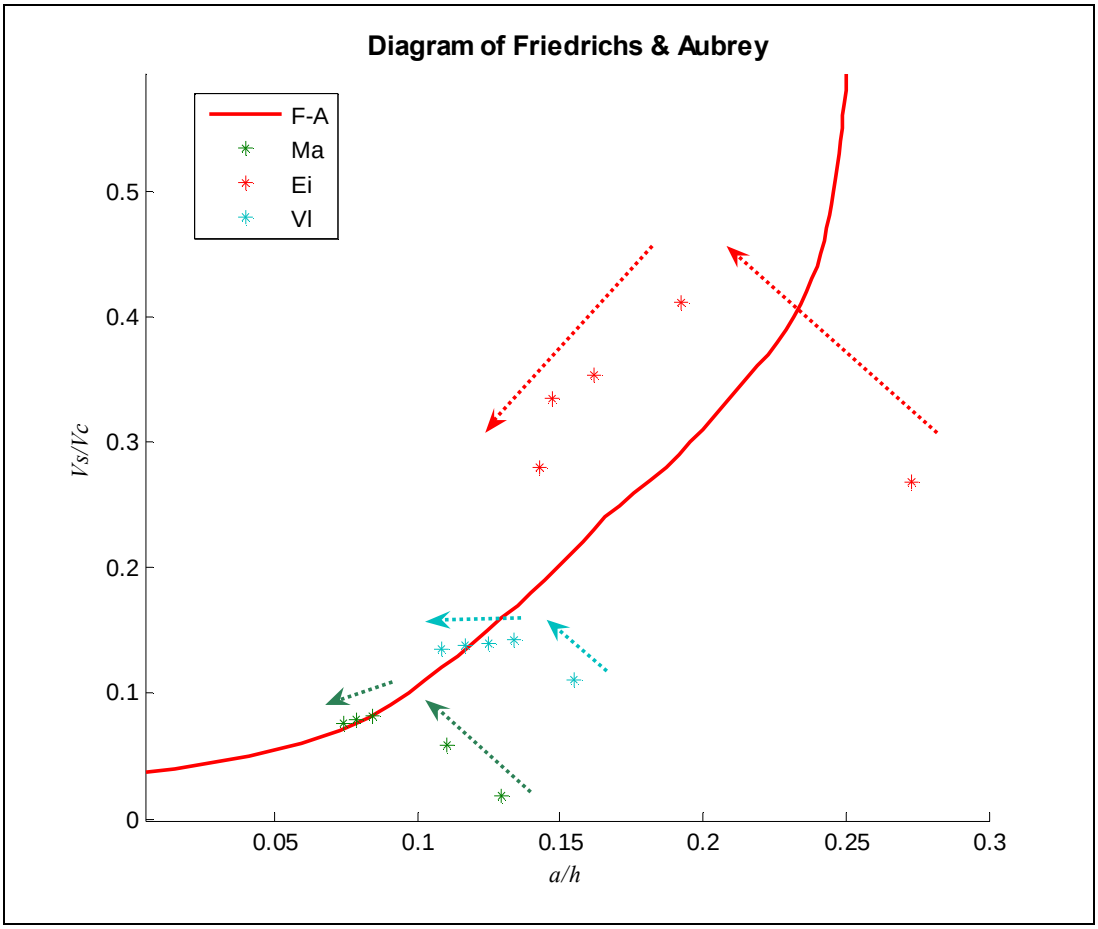

Figure 5-47:Development of basins on the Friedrichs and Aubrey graph considering varying boundaries

The relation between the channel volume and tidal prism can be checked also for these results, similar to all the previous results, the outcome of current model can not reproduce the relation between channel volume and tidal prism, as it is shown in figure 5-46, only in case of Eierlandse Gat the result of model is in good agreement with the theoretical relation. In two other basins the development is not toward the theoretical line.

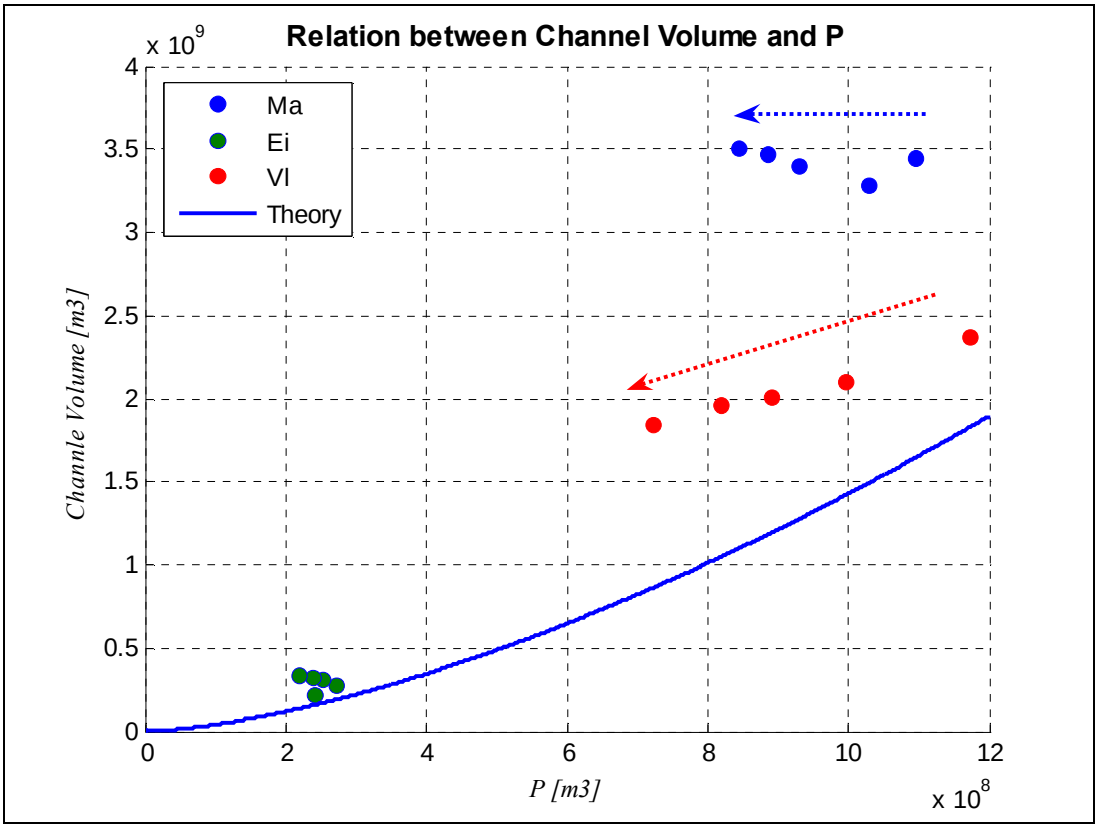

Figure 5-48:Relation between channel volume and tidal prism, considering varying boundaries

5.6 Summary of the results

During the previous sections the result of different morphological simulation of Western Dutch Wadden Sea using a process based model was discussed and compared with empirical equilibrium relations. It is shown that in this case, the process based model (Delft3D, morphological model) simulates the evolution of the basins toward the equilibrium suggested according to the ***Friedrichs and Aubrey graph***, the best. For flat characteristics especially ***flat height*** also the development through an equilibrium value is simulated but this value is not in agreement with the value suggested in the literature; the same is true in the case of ***relative flat area*** (A_f/A_b). Assuming that the result of the model from the initial real bathymetry analyzed with varying boundary of basins is a good representative of equilibrium condition of the basins, the coefficients of empirical relations is re-calculated for flat height and relative flat area.

In the case of flat height the suggested form of equilibrium equation suggested by Eysink (1990) is :

$$h_f = \alpha_{fe} \cdot 2a$$

$$\alpha_{fe} = \alpha_f - \beta \cdot A_b$$

In which

h_f [m] : Height of flat
A_b [m^2] : Total Area of basin
a [m] : Tidal amplitude

and coefficients are
α_f [-] : 0.41
β [-] :0.24e-9

recalculated coefficients from the result of model, which are in the same order of magnitude are :
α_f [-] : 0.33
β [-] :0.40e-9

In the case of relative flat are the suggested relation based on Renger and Partenscky (1974) work is (Areas in Km^2) :

$$\frac{A_f}{A_b} = 1 - 0.025 \cdot A_b^{0.5}$$

and the relation with new coefficients based on the results of simulation is :

$$\frac{A_f}{A_b} = 1 - 0.087 \cdot A_b^{0.24}$$

This new relation is plotted with original relation, the suggested graph by Eysink (1991), and the result of the simulation in figure 5-47 .

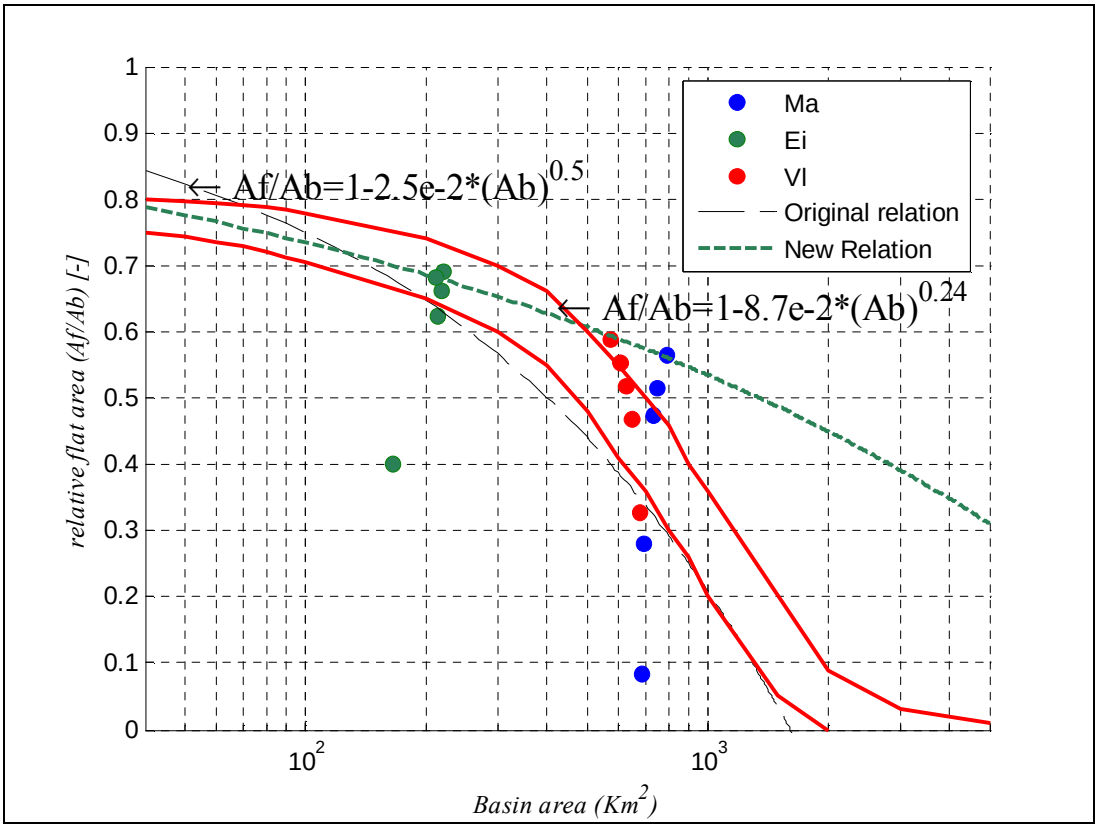

Figure 5-49:New relation for relative flat area, original suggestion and model results with real initial bathymetry and varying boundaries

The evolution of relative flat area of Marsdiep in some of simulations with schematized bathymetries (L04 and L01) also goes toward this new line (Figure 5-48).

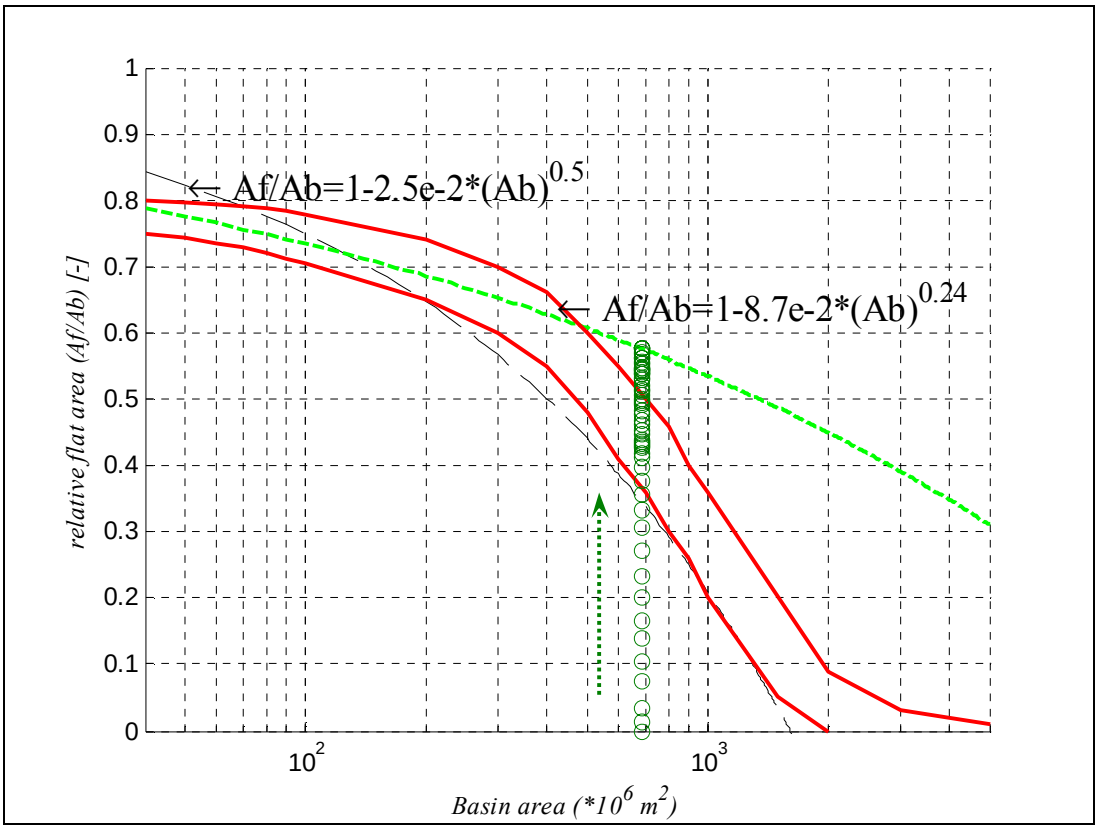

Figure 5-50:New relation for relative flat area, original suggestion and model results for Marsdiep with schematized sloping bathymetry (L04)

Although the coefficients are re-calculated, this does not mean that the relations with new coefficients can predict the equilibrium values better than the original ones, but it shows that the result of a process based model can lead to the same form of equations.

On the other hand the results of the model could not show a relation between the ***tidal prism and channel volume***, which can be compared with empirical relation. This may be due to this fact that to calculate the basin parameters including tidal prism, the tidal elevation of the last year of simulation is used, the main effect of this schematization is on tidal prism more than other parameters.

6 Conclusions and Recommendations

In this section the outcome of the study is concluded based on the research questions:

Can a mega-scale stable situation of the Marsdiep Basin be predicted using a schematized long-term morphological modeling and given constant boundary conditions?

The process-based model which is used in this study could not simulate one single *mega-scale* stable (equilibrium) condition in the Western Wadden Sea including Marsdiep for all initial conditions for the *duration of the simulations*, but with each initial condition in many aspects such as sediment exchange and some basic characteristics of tidal basins, a *mega-scale* stable (equilibrium) condition is simulated, which is dependent not only on the given boundary condition but also on the initial condition.

In the Western Dutch Wadden Sea M_4 and M_6 components of the tide are very important in simulating the morphological behavior of tidal basins and it can not be modeled with the tidal force based on M_2 only.

How much sand is needed to import to Marsdiep to reach this hypothetical stable morphological situation and is this amount of sediment available?

If the simulation with the initial real bathymetry is accepted as a good representative of the *mega-scale* stable (equilibrium) of Marsdiep, this basin imports about 400 Mm^3 during 2100 years of simulation. The main portion of the sediment import – 300 Mm^3 -takes place in the first 300 years with a maximum rate of about 3 Mm^3 per year in the first 40 year.

What is the effect of nearby basins in Wadden Sea, especially Vlie Basin, on the morphology of Marsdiep Basin?

It is shown in the analyses that the effect of close-by basins on each other can be interpreted as varying in the boundaries of basins. From this point of view Marsdiep basin is stretching eastward and gaining some area from Vlie, while Vlie also is expanding toward east.

Generally the changes in the boundaries of different tidal basins in a multi-inlet tidal system such as Dutch Wadden Sea play a significant role in determining the basin characteristics.

Is the result of schematized long-term morphological modeling of Marsdiep Basin in agreement with empirical models?

In this study it is shown that the result of current process based model follow the empirical equilibrium equations for flat characteristics and relative flat area qualitatively, while the results are in very good agreement with the equilibrium suggested based on Friedrichs and Aubrey graph.

Although there are numerous studies being carried out about tidal basin equilibrium especially in the Dutch Wadden Sea, there is still a lot to do. Some recommendations for new studies on this topic are as follows:

- There are two other famous empirical relations suggested for tidal basin characteristics which are not checked in this study: relation between ebb-tidal delta volume with the tidal prism and cross section of inlet with the tidal prism; to check these relations a finer model of tidal basin is needed so it is recommended to model a smaller tidal basin with finer grids to examine the behavior of the process-based model according to these relations.

- The model which is used in this study is forced by harmonic boundaries (Water level at the sea side and Neumann at the lateral boundaries), it is recommended to use astronomical boundaries and calibrate the model more accurately for tidal elevations in front of inlets.

- Another way to schematize the initial bathymetry in tidal basins, which is recommended, is to calculate the volume of sediment according to existing equilibrium relations and distribute it in the basin to have the same shape of hypsometry as now.

- In the current model all the human interventions except the Afsluitdijk are neglected; some of these interventions may have a significant effect on the result, especially on the analyses of the boundaries between basins. So it is recommended to run some models with those interventions, such as the Pollendam as well.

- One of the main distortions in the result of the current study is the unrealistic deepening of the main channels of basins. To avoid this, it is recommended to use a finer model with different sediment fraction and/or armoring of the channel beds.

- Sand nourishment on the coastline and ebb-tidal deltas plays its role in providing the sediment for basins; in this model no nourishment was modeled. Since the rate of sediment exchange is changing a lot during the long simulation time, the normal dredging and dumping modules of Delft3D can not be efficiently used. It is recommended to develop a module to dump sand on the ebb-tidal delta as much as it is eroded, or in other words to keep the ebb-tidal delta in the same size and shape as it is in the initial bathymetry.

- Sea level rise is excluded from the current study, while it has an effect on morphological changes in tidal basins in the Dutch Wadden Sea. In future studies it should be included as well

- The other recommendation is to investigate the tidal basin parameters in *one* basin with several inlets without separating the basins.

- It can also be suggested to exclude the effect of nearby basins on each other and study the behavior of each single basin. This can be done by adding thin dams on the ‘Vaklodingen’ boundaries.

7 References

Ahnert, F. 1960. “Estuarine meanders in Chesapeake Bay are” Geographical Review 50, 390-401.

Bruun, P. and Gerritsen F. 1959. “Natural bypassing of sand at coastal inlets” Journal of the Waterways and Harbors, 85, 75-107.

Cayocca, F. 2001. “Long-term morphological modeling of a tidal inlet: the Arcachon Basin, France” Coastal Engineering, 42, 115-142.

Cleveringa, J. and Oost, A. P. 1999. “The fractal geometry of tidal-channel systems in the Dutch Wadden Sea” Geologie en Mijnbouw, 78, 21-30.

Davis, R. A. and Hayes, M. O. 1984. “What is a wave-dominated coast?” Marine Geology, 60, 313-329.

De Vriend, H. J. 1991. “Mathematical modeling and large-scale coastal behavior, Part 1: physical processes.” Journal of Hydraulic Research, 29, 727-740.

De Vriend, H. J. 1996. “Mathematical modeling of meso-tidal barrier islands coasts. Part 1: Empirical and semi-empirical models” Advances in coastal and ocean engineering, P. L. F. LIU, ed., World Scientific Publishing Company, Singapore, 150-197.

De Vriend, H. J. and Ribberink, J. S. 1996. “Mathematical modeling of meso-tidal barrier island coasts. Part II: Process-based simulation models.”, Advances in Coastal and Ocean engineering, P. L.-F. LIU, ed., World Scientific Publishing Company., Singapore, 150-179.

De Vriend, H.J., Capobianco, M., Chesher, T., De Swart, H.E., Latteux, B. and Stive, M.J.F., 1993b. “Approaches to long term modeling of coastal morphology: a review.” Coastal Engineering 21 (1-3), 225-269.

De Vriend, H. J., Louters, T., Berben, F. M. L. and And Steijn, R. C. 1989. "Hybrid prediction of intertidal flat evolution in an estuary" International Conference Hydraulic and Environmental Modeling of Coastal, Estuarine and Rivers waters, Bradford, U.K.

Dean, R.G. and Walton, T.L. 1975. “Sediment transport processes in the vicinity of inlets with special reference to sand trapping” Estuarine research, L.E. Cronin, Academic Press, 2, 129-150.

Delft 3D user manual, 2006, Delft Hydraulic, Delft, The Netherlands.

Elias, E. 2006. “Morphodynamics of Texel Inlet” IOS Pres, The Netherlands.

Elias, E. P. L., Stive, M. J. F., Bonekamp, J. G. and Cleveringa, J. 2003b. “Tidal inlet dynamics in response to human intervention” Coastal Engineering Journal, 45(4), 629-658.

Escoffier, F. F. 1940. “The stability of tidal inlets.” Shore and Beach, 114-115.

Eysink, W.D. 1990. “ Morphological response of tidal basins to change” Proc. 22nd Coastal Engineering Conference, ASCE, Delft, Juky 2-6, Vol. 2, the Dutch coast, paper no. 8, 1990, pp. 1948-1961.

Eysink, W.D. 1991. “ISOS*2 Project : Impact of sea level rise on the morphology of the Wadden Sea in the scope of its ecological function, phase 1” Delft Hydraulic report H1300, Delft, The Netherlands.

Eysink, W.D. and Biegel, E.J. 1992. “ISOS*2 Project : Impact of sea level rise on the morphology of the Wadden Sea in the scope of its ecological function, phase 2” Delft Hydraulic report H1300, Delft, The Netherlands.

Fitzgerald, D. M. 1988. “Shoreline erosional-depositional processes associated with tidal inlets” Hydrodynamics and sediment dynamics of tidal inlets, Lecture Notes on Coastal and Estuarine Studies 29, Aubrey and D. G. weishar, eds., Springer-Verlag, New York, 186-225.

Fitzgerald, D. M. 1996. “Geomorphic variability and morphologic and sedimentologic controls on tidal inlets” Journal of Coastal Research, 23, 47-71.

Fitzgerald, D. M., Kraus, N. C. and Hands, E. B. 2000. “Natural mechanisms of sediment bypassing at tidal inlets” Report ERDC/CHL CHETN-IV-30, US Army Corps of Engineers.

Friedrichs, C. and Aubrey, D. G. 1988. “Non-linear tidal distortion in shallow well-mixed estuaries: a synthesis” Estuarine, Coastal and Shelf Sciences, 27, 521-545.

Gerritsen, F. 1990. “Morphological stability of Inlets and channels of the Western Wadden Sea”, Report GWAO-90.019. Rijkswaterstaat RIKZ, The Hague.

Hayes, M. O. 1975. “Morphology of sand accumulation in estuaries.”, Estuarine Research, L. E. Cronin, ed., Academic Press, New York, 3-22.

Hayes, M. O. 1979. “Barrier Island morphology as a function of tidal and wave regime”, Barrier Islands: From the Gulf of St Lawerence to the Gulf of Mexico, S. P. Leatherman, ed., Academic Press, New York, 1-27.

Hibma, A., De Vriend, H. J. and Stive, M. J. F. 2003. “Numerical modeling of shoal pattern formation in well-mixed elongated estuaries” Estuarine, Coastal and Shelf Science, 57, 981-991.

Hibma, A. 2004. “Morphodynamic modeling of channel-shoal systems” Communications on Hydraulic and Geotechnical Engineering, vol. 04-3, Delft University of Technology, Delft, 122p.

Hubbard, D. K., Barwis, J. H. and Nummendal, D. 1979. “The role of waves and tidal currents in the development of tidal inlet sedimentary structures and sand body geometry: examples from the North Carolina, South Carolina and Georgia.” Journal of Sedimentary Petrology, 49, 1073-1092.

Lesser, G. R., Roelvink, J. A., Van Kester, J. A. T. M. and Stelling, G. S. 2004. “Development and validation of a three-dimensional model” Coastal Engineering, 51, 883-915.

Lesser, G.R., De Vroeg, J.H., Roelvink, J.A., De Gerloni, M. and Ardone, V. 2003. “Modeling the morphological impact of submerged offshore Breakwaters” Proc.Coastal Sediments V03.

Louters, T. and Gerritsen, F. 1994. “The Riddle of the Sands. A Tidal System's Answer to a Rising Sea Level.” Report RIKZ-94.040. Rijkswaterstaat RIKZ, The Hague

O'Brien, M. P. 1931. “Estuary tidal prisms related to entrance areas” Civil Engineering, 1, 738-739.

O'Brien, M. P. 1969. “Equilibrium flow areas of inlets and sandy coasts” Journal of Waterways, Harbors, and Coastal Engineering, 95, 43-55.

Oertel, G. F. 1975. “Ebb-tidal deltas of Georgia Estuaries” Estuarine research, L. E. CRONIN, ed., Academic press, New York, 267-276.

Oertel, G. F. 1988. “Processes of sediment exchange between tidal inlets, ebb deltas and barrier islands”, lecture notes on coastal and estuarine studies, Vol. 29; Hydrodynamics and sediment dynamics of tidal inlets, L. W. D.G. Aubrey and L. Weishar, eds., Springer-Verlag, New York.

Renger, E. and Partenscky, H. W. 1974. “Stability criteria for tidal basins”, proceedings 14th Coastal Engineering Conference, ASCE, Vol2, ch. 93,1974 pp. 1605-1618.

Rinaldo, A., Lanzoni, S. and Marani, M. 2001. “River and tidal networks” In: Seminara, G., Blondeaux, P. (Eds.), River, Coastal and Estuarine Morphodynamics. Springer-Verlag, Berlin.

Roelvink, J.A. 2006. “Coastal morphodynamic evolution techniques”, Coastal Engineering 53, pp. 277-287.

Roelvink, J.A., Walstra, D.J.R. and Chen, Z., 1994. “Morphological modelling of Keta lagoon case” Proc.24th Int. Conf. on Coastal Engineering. ASCE, Kobe, Japan.

Roelvink, J.A.., Boutmy, A. and Stam, J. M. 1998. "A simple method to predict long-term morphological changes" Proc.26th Int. Conf. on Coastal Engineering, Copenhagen. ASCE, New York, pp. 3224–3237.

Roelvink, J.A., Jeuken, M.C.J.L., van Holland, G., Aarninkhof, S.G.L. and Stam, J.M.T., 2001. "Long-term, process-based modelling of complex areas" Proc.4th Coastal Dynamics Conference, Lund, Sweden.

Roelvink, J.A., Van Kessel, T., Alfageme, S. and Canizares, R. 2003. "Modelling of barrier island response to storms" Proc. Coastal Sediments V03.

Sha, L. P. 1990. "Sedimentological studies of the ebb-tidal deltas along the West Frisian Islands, the Netherlands" Geologia Ultaiectina, Mededelingen van de Faculteit Aardwetenschappen no. 64, University Utrecht, p 159.

Sha, L.P. and Van der Berg, J.H. , 1993. "Variation in ebb-tidal delta geometry along the coast of Yhe Netherlands and German Bight" Journal of Coastal Research , 9(3), pp.730-746.

Speer, P. E., Aubrey, D. and Friedrichs, C. 1991. "Nonlinear hydrodynamics of shallow tidal inlet / bay systems" Tidal Hydrodynamics, B. B. Parker, ed., John Wiley, New York, 321-339.

Steijn, R., Roelvink, J.A., Rakhorst, D., Ribberink, J. and Van Overeem, J. 1998. "North –Coast of Texel:A comparison between Reality and Prediction" Coastal Engineering, pp: 2281 – 2 2293.

Stive, M. J. F., M., C., Wang, Z. B., Ruol, P. and Buijsman, M. C. 1998. "Morphodynamics of a tidal lagoon and adjacent coast." 8th International Biennial Conference on Physics of Estuaries and Coastal Seas, The Hague, 397-407.

Thanh, D. Q. 2006. "Bank erosion and long-term morphodynamic equilibrium in alluvial estuaries" MSc Thesis WSE-CEPD-06.07, UNESCO-IHE, Delft, The Netherlands.

Ubbink, M. J. 2004. "Morphological development of the Western Wadden Sea after human intervention near the Afsluitdijk" MSc Thesis, Delft University of Technology, Delft, The Netherlands.

Van der Wegen, M. 2005. "Long-term estuarine morphodynamics evolution of a tidal embayment using a 2 dimensional process based model" submitted to Journal of Geophysical Research, private communication.

Van Geer, P. 2007. "Long-term modeling of western part of Dutch Wadden Sea" Parallel study, private communication, to be published as Delft Hydraulic report in 2007.

Van Goor, M. A. 2001. "Influence of relative sea level Rice on the coastal inlets and tidal basins" Delft Hydraulic report Z2822, Delft, The Netherlands.

Van Veen, J. 2002. "Ebb and Flood channel system in the Netherlands tidal waters" English translation of original Dutch text, Delft University Press, Delft, the Netherlands (original Dutch text: Van Veen, J., 1950. Eb en vloed scharen in de Nederlandsche getij wateren. Journal of the Royal Dutch Geographical Society (KNAG), 67, 303-325).

Walton, T. L. and Adams, W. D. 1976. "Capacity of inlet outer bars to store Sand" Proc. 15th International Conference on Coastal Engineering, Honolulu, 303-325.

Wang, Z. B., Louters, T. and De Vriend, H. J. 1995. "Morphodynamic modeling for a tidal inlet in the Wadden Sea." Marine Geology, 126, 289-300.

Wang, Z. B., Elias E., Van Koningsveld M. and Tonnon P.K., 2006 ."Sediment budget analysis and testing hypotheses for the Dutch coastal system" Delft Hydraulic report Z1400, Delft, The Netherlands.

Appendix A

In order to show the difference in the calculated parameter of Marsdiep basin with the tidal level in the last year of simulation and the temporal and spatial varying tide, one of the simulations with schematized bathymetry (L02) is analyzed with temporal and spatial varying tide. The results are given in the following figures.

As it is clear, although the tidal range increasing in during the simulation (Figure A-1), the development of Marsdiep basin on Friedrichs and Aubrey graph and development of flat characteristics of Marsdiep does not change that much , the main difference is in changes of the tidal prism during the simulation which is shown in the figure A-3. This can have some effects on the comparing the result of the model with the relation between tidal prism and channel volume.

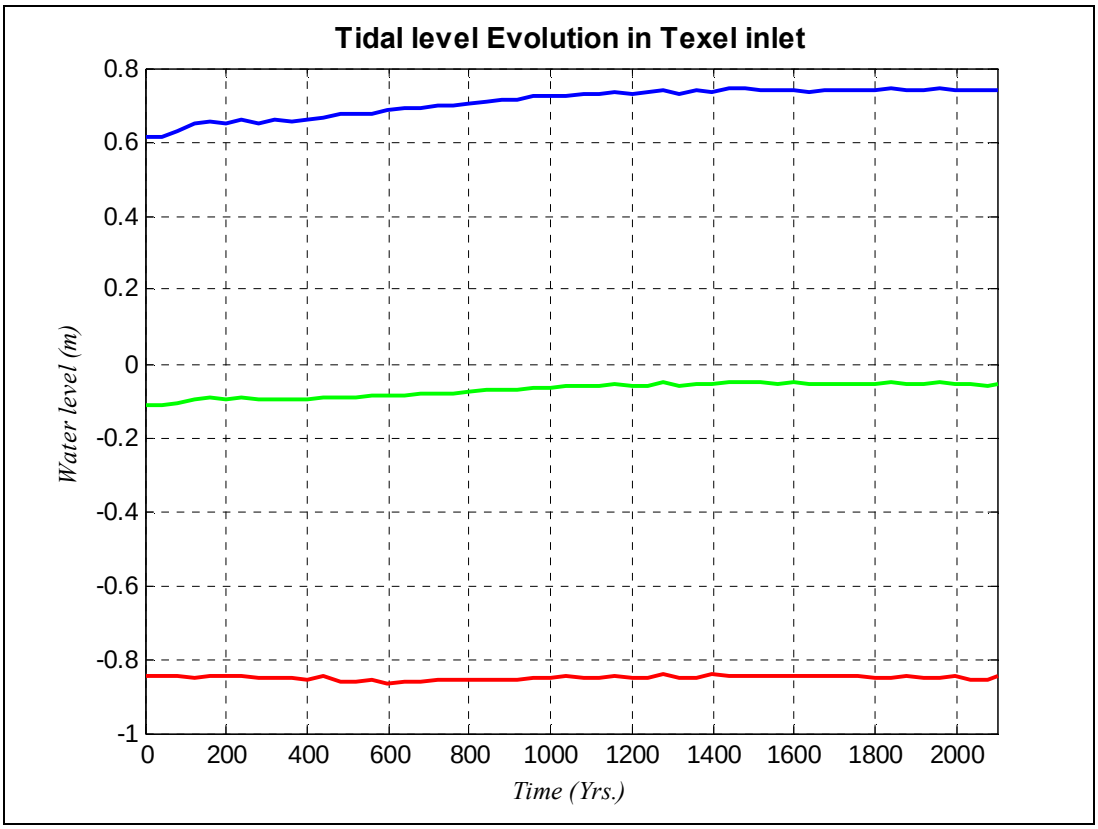

Figure A- 1: Changes in tidal elevation in front of Texel inlet during the morphological simulation.

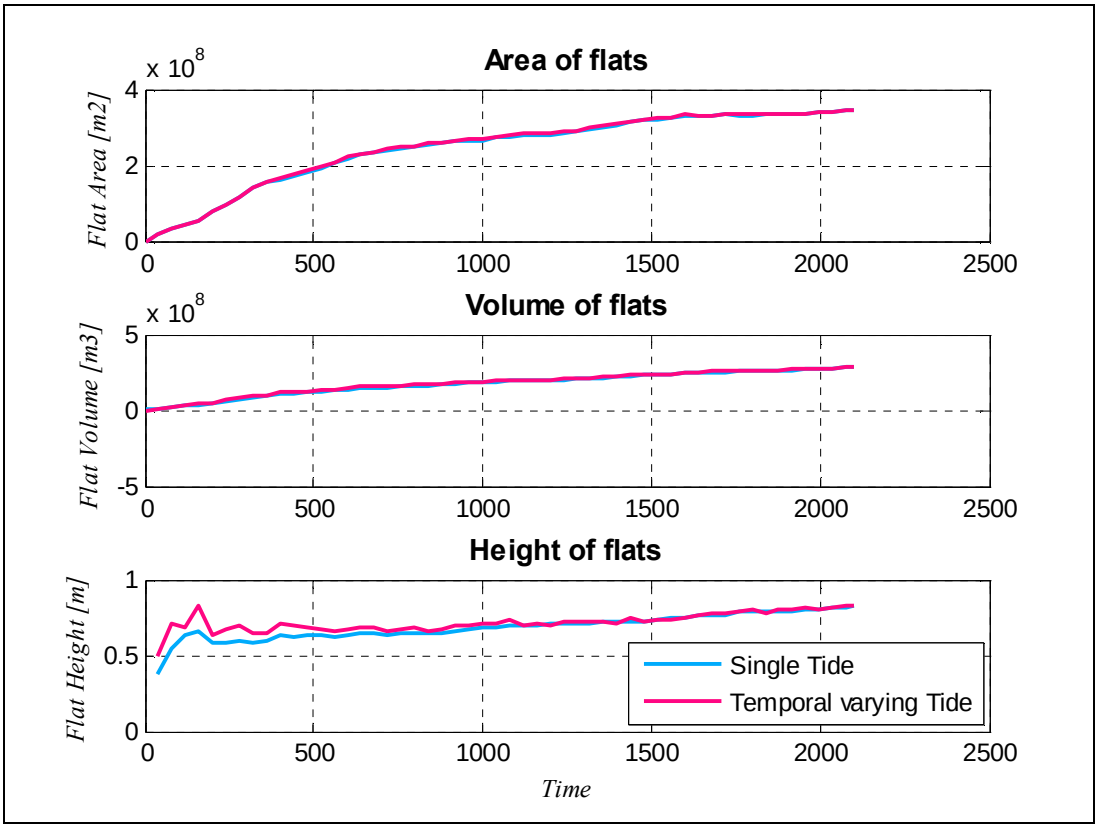

Figure A- 2: Development of flat characteristics in Marsdiep, calculated with different tides

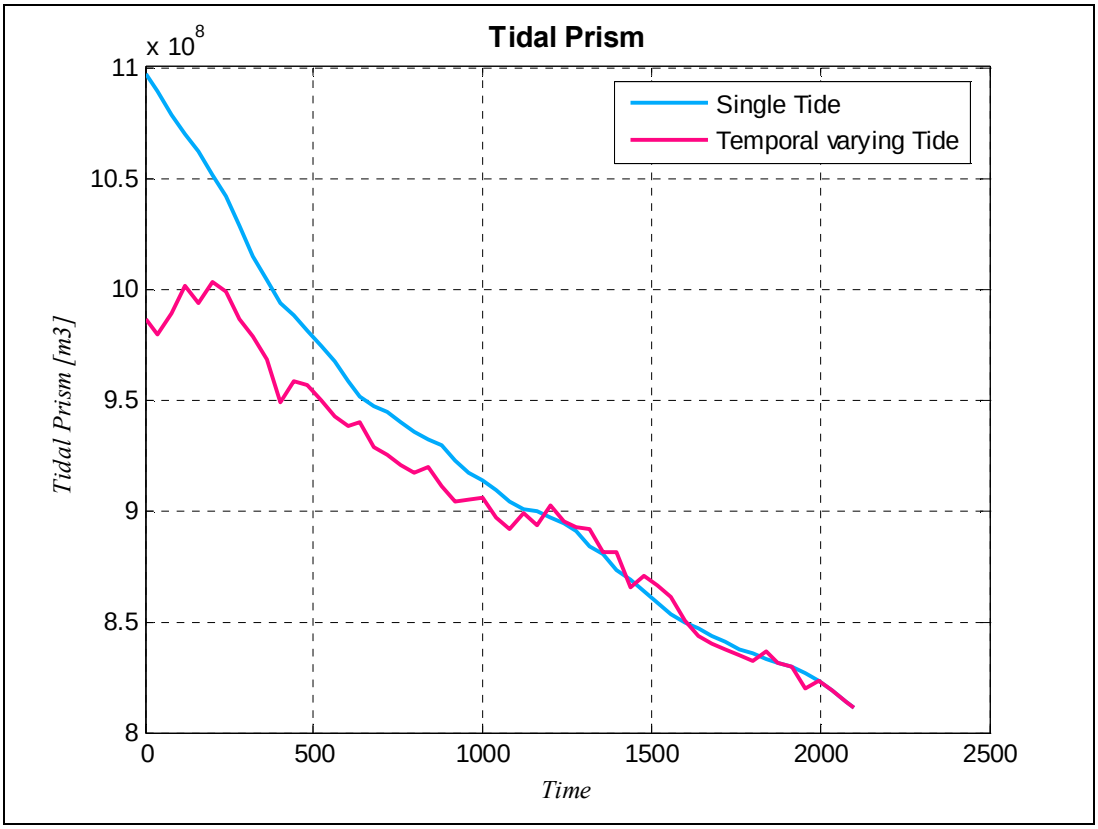

Figure A- 3: Changes in tidal prism in Marsdiep, calculated with different tides

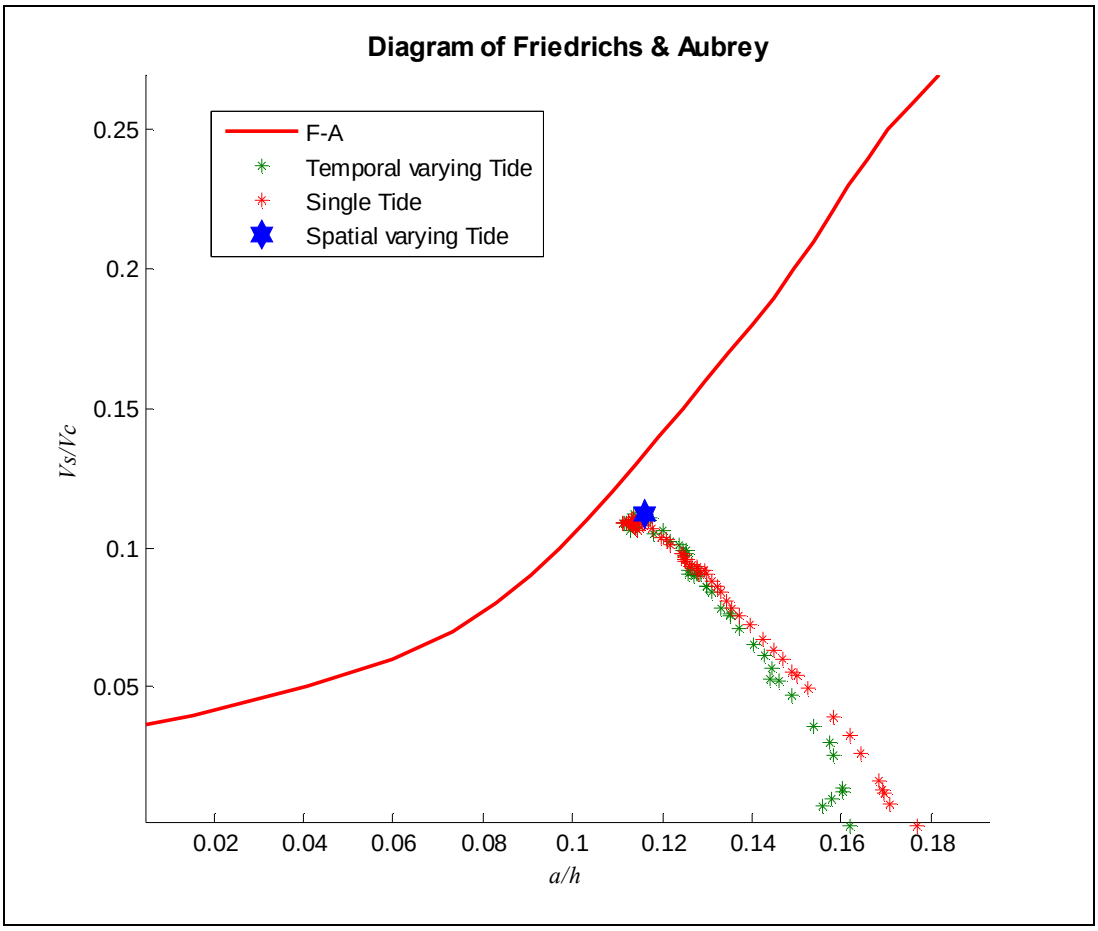

Figure A- 4: Development of Marsdiep characteristics on Friedrichs and Aubrey graph calculated with different tides

Appendix B

In the Analyzer, which is written in MATLAB® environment to analyze the tidal basin parameters, the following parameters are determined directly from the hypsometry of volume or area.

Area of Basin : A_b
Area of Channels : A_C
Volume of water in the basin
when the water level is at MHW : V_{HW}
Volume of Channels : V_C

Other parameters are calculated using the following relations :

$$A_f = A_b - A_c$$

$$P = V_{HW} - V_C$$

$$V_{c-F,A} = V_c + A_c.a$$

$$V_s = P - A_c.2a$$

$$h = \frac{V_c}{A_c} + a$$

$$V_f = A_f.2a - V_s$$

$$h_f = \frac{V_f}{A_f}$$